OFFICE COPY NTIS No. PB87-216107

$18.95

BRIDGE WATERWAYS ANALYSIS MODEL: RESEARCH REPORT

Research, Development, and Technology
Turner-Fairbank Highway Research Center
6300 Georgetown Pike
McLean, Virginia 22101-2296

Report No.
FHWA/RD-86/108

Final Report
July 1986

U.S. Department of Transportation

Federal Highway Administration

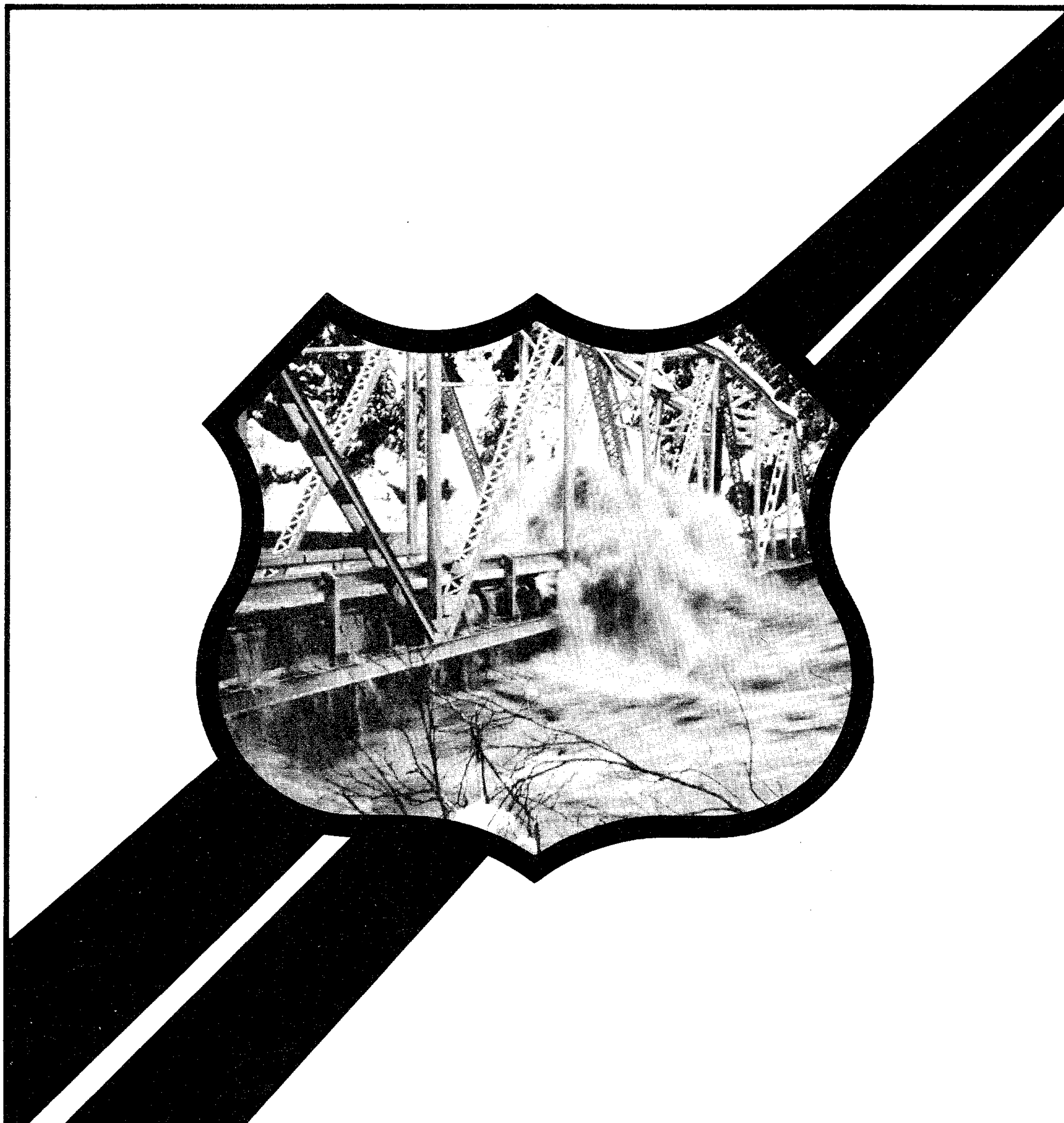

FOREWORD

This report describes a computer model for water surface profile computations for stream segments with or without highway crossings. The model was developed for the Federal Highway Administration, Offices of Research, Development, and Technology, by the United States Geological Survey. It will be of interest to hydraulic engineers for State and Federal agencies, local governments and consultants.

The report and the computer model are used for National Highway Institute workshops which are nationwide. The computer model has already been tested by a select group of State highway agencies and has been presented at several pilot workshops.

Sufficient copies of the report are being distributed to provide a minimum of ten copies to each FHWA Regional office, one copy to each FHWA Division office and one copy to each State highway office. Direct distribution is being made to the Division offices.

Richard E. Hay

Richard E. Hay, Director
Office of Engineering and
Highway Operations
Research and Development
Federal Highway Administration

NOTICE

Technical Report Documentation Page

1. Report No.: FHWA/RD-86/108

2. Government Accession No.:

3. Recipient's Catalog No.:

4. Title and Subtitle: BRIDGE WATERWAYS ANALYSIS MODEL: RESEARCH REPORT

5. Report Date: July 1986

6. Performing Organization Code:

7. Author(s): J. O. Shearman, W. H. Kirby, V. R. Schneider, and H. N. Flippo

8. Performing Organization Report No.:

9. Performing Organization Name and Address:
U.S. Geological Survey, WRD
415 National Center
12202 Sunrise Valley Drive
Reston, VA 22092

10. Work Unit No. (TRAIS): FCP 35H4-162

11. Contract or Grant No.: P.O. 9-3-0189

12. Sponsoring Agency Name and Address:
Office of Engineering & Highway Operations R&D
Federal Highway Administration
6300 Georgetown Pike
McLean, VA 22101-2296

13. Type of Report and Period Covered: Final Report, Oct. 1979 - Sept. 1985

14. Sponsoring Agency Code:

15. Supplementary Notes:
FHWA Contract Managers (COTRs): J. Sterling Jones (HNR-10)
John Kurdziel (HRT-10)
Philip Thompson (HNG-31)

16. Abstract

This report describes WSPRO which is a digital model for water-surface profile computations. Profile computations for open-channel flow are compatible with conventional techniques used in existing step-backwater analysis models. WSPRO incorporates several desirable features from existing models. Profile computations for free-surface flow through bridges are based on relatively recent developments in bridge backwater analysis and recognize the influence of bridge geometry variations. Pressure flow situations (girders partially or fully inundated) are computed using existing Federal Highway Administration techniques. Embankment overtopping flows, in conjunction with either free-surface or pressure flow through the bridge, can be computed. WSPRO is also capable of computing profiles at stream crossings with multiple openings (including culverts).

Although specifically oriented towards hydraulic design of stream highway crossings using risk analysis, WSPRO is equally suitable for water-surface profile computations unrelated to highway design. The report provides a detailed discussion of the theory and computational techniques used in the model. Model capabilities and data requirements are described in more general terms. Specific data coding instructions and examples of model applications are to be published in a users manual. Results of model application to five field-verification sites are discussed, along with a comparison of WSPRO results with results obtained from two existing models. Also presented is a discussion of the applicability of WSPRO to design of bridges with risk analysis.

17. Key Words: Bridge backwater, Open-channel flow, Water-surface profiles, Road overflow, Bridges, Risk analysis, Hydraulic design, Multiple openings

18. Distribution Statement: No restrictions. This document is available to the public through the National Technical Information Service, Springfield, VA 22161.

19. Security Classif. (of this report)	20. Security Classif. (of this page)	21. No. of Pages	22. Price
Unclassified	Unclassified	126	

Form DOT F 1700.7 (8-72)   Reproduction of completed page authorized

TABLE OF CONTENTS

Chapter		Page
I	INTRODUCTION	1
II	CAPABILITIES OF THE MODEL	3
III	WATER-SURFACE PROFILE COMPUTATION THEORY	6
	Step-backwater Computations	6
	Single-opening Bridge Hydraulics	13
	Free-surface Flow	17
	Effective Flow Length	20
	Coefficient of Discharge	26
	Pressure Flow	28
	Orifice Flow	29
	Submerged Orifice Flow	31
	Profile Computations	33
	Road Overflow	33
	Profile Computations for Combined Flow	36
IV	MULTIPLE WATERWAY OPENING COMPUTATION THEORY	41
V	CULVERT ANALYSIS	47
VI	MODEL COMPARISONS AND RESULTS	54
VII	APPLICABILITY TO RISK ANALYSIS	71
VIII	SUMMARY AND CONCLUSIONS	79
	APPENDIX Coefficient of Discharge for Bridges	81
	REFERENCES	110

LIST OF FIGURES

Figure		Page
1.	Sketch of subreach for standard step-backwater computations	7
2.	Cross-section locations for stream crossing with a single waterway opening	14
3.	Definition sketch of assumed streamlines for relatively low degrees of contraction	23
4.	Definition sketch of assumed streamlines for relatively high degrees of contraction	25
5.	Assumed flow pattern for a nonsymmetric constriction with nonhomogeneous roughness distribution	27
6.	Definition sketch for orifice flow computations	30
7.	Discharge coefficient for orifice flow	31
8.	Definition sketch for submerged orifice flow computations	32
9.	Definition sketch for road overflow computations	35
10.	Coefficients for road overflow	37
11.	Cross-section locations for step-backwater computations in lieu of weir flow computations for combined flow situations	40
12.	Sketch of typical multiple bridge opening situation illustrating valley strips and cross-section locations	42
13-17.	Water-surface profiles for:	
	13. Buckhorn Creek near Shiloh, Alabama	66
	14. Cypress Creek near Downsville, Louisiana	67
	15. Okatoma Creek near Magee, Mississippi	68
	16. Okatoma Creek East of Magee, Mississippi	69
	17. Poley Creek near Sanford, Alabama	70
18.	Typical elevation-damage-discharge relation upstream from a bridge site	75
19.	Typical relation between minimum embankment elevation, design discharge, and bridge opening design alternative	77

LIST OF FIGURES (continued)

Figure | Page

20. Definition sketch of type 1 opening, vertical embankments embankments and vertical abutments, with or without wingwalls 83
21. Definition sketch of type 2 opening, sloping embankments without wingwalls 84
22. Definition sketch of type 3 opening, sloping embankments and sloping abutments (spillthrough) 85
23. Definition sketch of type 4 opening, sloping embankments and vertical abutments with wingwalls 86
24. Coefficients for type 1 openings 88
25. Wingwall of adjustment factors for type 1 openings 89
26. Coefficients for type 2 openings, embankment slope 1 to 1 90
27. Coefficients for type 2 openings, embankment slope 2 to 1 91
28. Coefficients for type 3 openings, embankment slope 1 to 1 92
29. Coefficients for type 3 openings, embankment slope 1 1/2 to 1 93
30. Coefficients for type 3 openings, embankment slope 2 to 1 94
31. Coefficients for type 4 openings, embankment slope 1 to 1 95
32. Coefficients for type 4 openings, embankment slope 2 to 1 96
33. Adjustment factors for piers or piles 97
34. Adjustment factors for spur dikes 98

LIST OF TABLES

Table		Page
1.	Summary of flow classes for a single bridge opening	16
2-7.	Observed and computed water-surface elevations for:	
	2. Buckhorn Creek near Shiloh, Alabama	60
	3. Cypress Creek near Downsville, Louisiana	61
	4. Okatoma Creek near Magee, Mississippi	62
	5. Okatoma Creek East of Magee, Mississippi	63
	6. 1,900 cfs for Poley Creek near Sanford, Alabama	64
	7. 4,600 cfs for Poley Creek near Sanford, Alabama	65
8.	Cross-reference of figures and tables pertaining to the base coefficient of discharge	87
9.	Cross-reference of figures and tables pertaining to adjustment factors	87
10.	Base coefficient of discharge, C', for type 1 opening, with or without wingwalls	99
11.	Variation of adjustment factor, k_r, for type 1 opening with entrance rounding	99
12.	Variation of adjustment factor, k_θ, for type 1 opening with wingwalls	100
13.	Base coefficient of discharge, C', for type 2 opening, embankment slope 1 to 1	101
14.	Variation of adjustment factor k_y, for type 2 opening, embankment slope 1 to 1	101
15.	Base coefficient of discharge, C', for type 2 opening, embankment slope 2 to 1	102
16.	Variation of adjustment factor, k_y, for type 2 opening, embankment slope 2 to 1	102
17.	Base coefficient of discharge, C', for type 3 opening, embankment slope 1 to 1	103
18.	Variation of adjustment factor, k_x, for type 3 opening, embankment slope 1 to 1	103

LIST OF TABLES (continued)

Table Page

19. Base coefficient of discharge, C', for type 3 opening, embankment slope 1 1/2 to 1 104
20. Variation of adjustment factor, k_x, for type 3 opening, embankment slope 1 1/2 to 1 104
21. Base coefficient of discharge, C', for type 3 opening, embankment slope 2 to 1 105
22. Base coefficient of discharge, C', for type 4 opening, embankment slope 1 to 1 105
23. Slopes of family of curves for determining adjustment factor, k_θ, for wingwall angle for type 4 openings, embankment slope 1 to 1 106
24. Base coefficient of discharge, C', for type 4 opening, embankment slope 2 to 1 106
25. Slopes of family of curves for determining adjustment factor, k_θ, for wingwall angle for type 4 openings, embankment slope 2 to 1 107
26. Adjustment factor, k_j, for piers 107
27. Adjustment factor, k_j, for piles 108
28. Adjustment factors for spur dikes 109

SYMBOLS AND UNITS

Symbol(s)	Definition	Units
a, a_i	Subsection flow area. Subscripted when referring to subsection i.	ft^2
A, A_i	Total flow area of a cross section. Subscripted when referring to cross section i.	ft^2
A_1	In single-opening bridge situations, the total area of the approach cross section. In multiple opening analyses, the total area of the upstream match cross section.	ft^2
A_3, A_{3j}	Gross flow area (ignoring piers/piles) in a bridge opening. Subscripted with j when referring to the gross area of the jth opening of a multiple opening analysis.	ft^2
A_j	In reference to piers/piles, the submerged area (normal to the flow) of the piers/piles.	ft^2
A_j	In reference to multiple opening analysis, the flow area of the approach cross section for the valley strip of the jth opening.	ft^2
b	Length of the bridge opening (span between abutments)	ft
b_d	Offset distance from the abutment to straight dikes.	ft
b_t	Length between abutments at the elevation of the water surface in the bridge opening.	ft
B	In reference to bridges, total valley width in the approach reach at a bridge.	ft
B	In reference to culverts, the span (width) of the culvert barrel.	ft
B_W	The incremental weir length between adjacent pairs of coordinates defining a road grade section.	ft
C	Coefficient of discharge for a bridge opening.	
C'	Base coefficient of discharge for a bridge opening (unadjusted for parameter variation from index values).	

LIST OF SYMBOLS (continued)

Symbol(s)	Definition	Units
C_D	Discharge coefficient for pressure (orifice flow through a bridge opening.	
C_e	Slope correction factor for culvert computations.	
C_f	Coefficient of discharge for free flow (no tailwater submergence) over a weir used in embankment overtopping computations.	
C_j	Coefficient of discharge for the $j\underline{th}$ opening in a multiple opening analysis.	
d	A subscript indicating spur dike parameter.	
d, d_i	Depth of flow in a culvert barrel. Subscripted when referring to culvert section i.	ft
d_c	Critical flow depth in a culvert barrel.	ft
d_n	Normal flow depth in a culvert barrel.	
D	Height of a culvert barrel.	ft
F	Froude number.	
g	Gravitational acceleration.	ft/s^2
h, h_i, h_{in}	Static head (water-surface elevation) above an arbitrary datum. Subscripted with i when referring to cross section i. n is included in the subscript when referring to natural (unconstricted) water-surface elevations in bridge analyses.	ft
h_{ds}	Water-surface elevation immediately downstream from a bridge opening.	ft
h_e	Expansion loss in a subreach for open-channel and bridge computations.	ft
h_e	Entrance loss in culvert computations.	ft
h_f, $h_{f(i-j)}$	Friction loss in a subreach. (i-j) is included in the subscript when referring to the subreach between cross sections i and j.	ft

Symbol(s)	Definition	Units
h_{min}, h_{max}	Minimum and maximum water-surface elevations (limits) of various iterative solutions for water-surface elevation.	ft
h_R	Static head upstream from an embankment; referenced to the datum common to all cross sections.	ft
h_s	Static head on the embankment from upstream water-surface elevation; using the road grade as the datum.	ft
h_t	Static head on the embankment from downstream water-surface elevation; using the road grade as the datum.	ft
h_{us}	Water-surface elevation immediately upstream from a bridge opening.	ft
h_v, h_{vi}, h_{vin}	Velocity head. Subscripted when referring to cross section i. n included in subscript when referring to natural (unconstricted) conditions.	ft
Δh	Head differential used to compute submerged orifice flow through a bridge opening.	ft
H	Total head used to compute weir flow for embankment overtopping; datum is the road grade.	ft
H_R	Total head immediately upstream from an embankment; referenced to datum common to all cross sections.	ft
HW	Headwater elevation in culvert computations.	ft
ΔH	Difference in total head between adjacent sections during energy balance trials.	ft
i	Subscript used to denote i^{th} cross section or i^{th} subsection.	
(i-j)	Compound subscript used to denote subreach between cross sections i and j.	
j	Subscript used to denote j^{th} opening and the associated valley strip in a multiple opening analysis.	
j	Ratio of pier area to gross area in a bridge opening (A_j/A_3).	

LIST OF SYMBOLS (continued)

Symbol(s)	Definition	Units
k, k_i	Subsection conveyance. Subscripted when referring to subsection i.	ft^3/s
k_c	Coefficient used to compute contraction loss in a subreach.	
k_e	Coefficient used to compute expansion loss in a subreach.	
k_e	Coefficient used to compute entrance loss for a culvert.	
k_t	Factor for adjusting discharge for submerged weir flow conditions.	
$k_?$	Factor for adjusting the base coefficient of discharge for different parameters. The ? is replaced by subscripts to indicate various adjustments as follows: a for skewed elliptical dikes; b for offset straight dikes; d for length of dikes; F for Froude number; j for piers or piles; r for entrance rounding; w for wingwall width; x for wetted abutment length; y for average depth at abutments; and θ for wingwall angle.	
K, K_i	Total conveyance of a cross section. Subscripted when referring to cross section i.	ft^3/s
K_1	In single-opening bridge situations, the total conveyance of the approach cross section. In multiple opening analyses, the total conveyance of the upstream match cross section.	ft^3/s
K_c	Controlling conveyance in some friction loss computations for bridge backwater analysis.	ft^3/s
K_d	Conveyance of the spur dike section.	ft^3/s
K_j	Total conveyance of the approach cross section for the valley strip of the jth opening.	ft^3/s
K_{mxr}	Conveyance of the horizontal slice of the approach section between the water-surface and minimum road grade elevation.	ft^3/s
K_q	Portion of the approach section conveyance corresponding to projection of the bridge length, b.	ft^3/s

LIST OF SYMBOLS (continued)

Symbol(s)	Definition	Units
K*	Total bridge backwater coefficient for FHWA method (Bradley, 1970).	
L, $L_{(i-j)}$	Flow length in a subreach. Subscripted with (i-j) when referring to the subreach between sections i and j.	ft
L	Flow length through a bridge opening.	ft
L	Length of a culvert barrel.	ft
L_{av}	Effective flow length in the approach reach to a bridge.	ft
L_{opt}	Distance between a bridge and the optimum location location for the approach section.	ft
L_R	Width of top of embankment (effective crest length) in the direction of flow.	ft
m	Flow contraction ratio, $1 - Kq/K_1$.	
m′	Geometric channel contraction ratio, $1 - {}^b/B$.	
n	Manning's roughness coefficient.	$ft^{1/6}$
N	Number of openings in multiple opening analysis and number of barrels for multiple barrel culverts.	
P, P_i	Wetted perimeter of a cross section. Subscripted when referring to cross section i.	ft
q_j	Portion of total discharge apportioned to the $j\underline{th}$ opening in multiple opening analyses.	ft^3/s
q_j^*	Channel resistance ratio for the valley strip of the j<u>th</u> opening in multiple opening analyses.	
Q, Q_i	Total discharge, subscripted when referring to discharge at section i.	ft^3/s
QBO	Discharge through a bridge opening.	ft^3/s
QRD	Discharge over an embankment.	ft^3/s
r	Subsection hydraulic radius.	ft

LIST OF SYMBOLS (continued)

Symbol(s)	Definition	Units
R	Hydraulic radius.	ft
S	Slope of a culvert barrel.	ft/ft
s, s_i	Streamline length between approach and bridge sections. Subscripted when referring to a specific streamline.	ft
S_f	Mean (or average) friction slope of a subreach.	ft/ft
S_{fi}	Friction slope at cross section i.	ft/ft
T	Top width of cross section.	ft
V	Mean velocity in a cross section.	ft/s
WS	Trial water-surface elevation in many iterative solutions.	ft
x, y	Transverse and longtitudinal coordinates for computing streamline length.	ft
Y_{bed}	Average streambed elevation for pressure flow computations.	ft
Y_{ls}	Low-steel elevation of a bridge.	ft
Y_R	Elevation on a road grade section.	ft
Y_u	Average depth of flow at upstream side of bridge for pressure flow computations.	ft
Z	Hydraulic depth of flow in bridge opening.	ft
α, α_i	Kinetic energy correction factor for nonuniform velocity distribution, subscripted when referring to cross section i.	
β, β_i	Momentum correction factor for nonuniform velocity distribution, subscripted when referring to cross section i.	
δ	Variable defined by equation 31b.	
ε	Variable defined by equation 31a.	
π	A constant (3.1416).	

LIST OF SYMBOLS (continued)

Symbol(s)	Definition	Units
Φ	Variable defined by equation 30.	

FACTORS FOR CONVERTING INCH-POUND UNITS TO
INTERNATIONAL SYSTEM OF UNITS (SI)

Multiply	By	To obtain
cubic foot per second ft^3/s	0.02832	cubic meter per second (m^3/s)
foot (ft)	0.3048	meter (m)
foot per second (ft/s)	0.3048	meter per second (m/s)
foot per second squared (ft/s^2)	0.3048	meter per second squared (m/s^2)
inch (in)	25.40	millimeter (mm)
square foot (ft^2)	0.0929	square meter (m^2)
pounds per square foot (lb/ft^2)	4.882	kilograms per square meter (km/m^2)

Chapter I

INTRODUCTION

Federal Highway Administration (FHWA) policy on design of flood plain encroachments is to consider the impact of encroachment alternatives on the flood plain rather than to size bridge openings for an arbitrary design discharge. To comply with this policy, designers are often required to make repetitive water-surface profile computations for several alternatives and for a wide range of floods, including floods which will overtop the road.

FHWA assessed existing computer models for water-surface profile computations to determine their applicability and adaptability to hydraulic design of bridges in accordance with this policy. Each of the existing models had some good features but also had limitations that restricted their applicability. Some details of the assessment are discussed in chapter VI. As a result of their assessment, FHWA concluded that the best solution was to develop a comprehensive, design-oriented model that could be readily applied in conjunction with their design policy. Therefore, FHWA initiated a contract with the U.S. Geological Survey (USGS) to develop an improved water-surface profile computation program. FHWA wanted a model that would be compatible with conventional step-backwater analyses, but would be easy to use, would have improved computations for flow through bridge openings, would handle combined road overflow and bridge-opening flow, would handle multiple waterway openings in a logical manner, and would have the capability to selectively output summary tables to enhance later analyses.

WSPRO, a digital model for water-surface profile computations, was developed to meet these needs. This report describes WSPRO in terms of its capabilities, data requirements, and the theory and computational techniques incorporated into the model. Also presented are (1) a comparison of computed results from WSPRO with results from two existing models for five field-verification sites, and (2) a discussion of the applicability of WSPRO when designing bridges using risk analysis concepts.

Data requirements are described in very general terms. Explicit instructions for input data coding, interpretation of results, and applications of the model will be published in a users manual. A rough draft users manual currently exists (1986). Suggestions from current users is expected to result in substantial improvement of this draft document.

Chapter II

CAPABILITIES OF THE MODEL

A primary objective of this model development was to provide a water-surface profile computational tool specifically applicable to bridge waterway design using risk analysis concepts. Provisions have thus been made for data input flexibility to permit easy modification of bridge-opening and embankment characteristics so that several alternative designs may be analyzed in a single job submission. Also, output capabilities have been structured to permit various summaries of these analyses for application to risk analysis. However, the model is also well suited and easily used for analyzing water-surface profiles for nondesign situations. In addition to eliminating limitations of existing computer models, an attempt was also made to incorporate many positive features from existing models into this comprehensive model. This chapter outlines the capabilities of the model with more detailed discussion presented as appropriate in the following chapters.

Capabilities related to input and output are:

- Most of the input data are coded in free format which provides much greater flexibility in data coding and greatly reduces the need to consult a user instruction manual, especially for an infrequent user.
- Many coefficients and computational control parameters are assigned reasonable default values by the model and generally need not be specified.
- Generally, the model assumes that data not coded for a particular cross section are identical to the data of the previous cross section. Missing data are propagated from the previous section, thus eliminating the need for repetitive coding of those data that remain constant from section to section.
- It is possible to fabricate valley cross sections from a template cross section when two or more cross sections are very similar in shape.
- Bridge openings may be defined either (1) entirely by horizontal-station and ground-elevation coordinates (for existing bridges or fixed-geometry design conditions), or (2) in terms of geometric

parameters of bridge components which are combined with valley cross-section data to "build" the bridge cross section.

- Spur dikes, in a manner similar to bridge openings, may be defined in entirety by the user or "built" by the model.
- Road grade data may be defined in terms of either (1) horizontal-station and ground-elevation coordinates, or (2) vertical-curve data.
- When nonstandard conditions are encountered, many of the variable coefficients and parameters which would normally be computed by the model can be "overridden" with user-specified values.
- Users can control both the amount of output and the type of information that is output and even design their own output tables.
- Output is stored in data files on magnetic storage devices. These files may be retained to obtain additional output without re-executing the job.
- Printer plots of cross-section data may be obtained.

Capabilities related to general computational procedures are:

- Water-surface profile computations in the absence of bridges are generally consistent with the methods used in existing models.
- Any combination of subcritical, critical, and supercritical flow profiles may be analyzed for one-dimensional, gradually varied, steady flow.
- Discharge may be varied from cross section to cross section to account for tributary and lateral flow gains or losses.
- Up to 20 profiles for different discharges and/or initial water-surface elevations may be computed at one time.
- Initial water-surface elevations for each profile may be specified by the user or computed by the model. If a slope (energy gradient) is specified the model will use the normal water-surface elevation which is computed by slope-conveyance. If neither an elevation nor a slope is specified, the model will use the critical water-surface elevation computed on the basis of minimum specific energy.
- Variable Manning's roughness coefficients may be specified for any cross section to reflect roughness changes both horizontally and vertically in the cross section.
- Up to three different flow lengths for left, central, and right portions of the valley may be specified between any two valley

cross sections. A conveyance-weighted average of these lengths is used to compute friction loss.

- o Users may select the friction-slope averaging technique to be used in the friction loss computations.

- o Users may specify the coefficients used to compute energy losses associated with expansion or contraction of flow.

Capabilities related to water-surface profile computations for a single-opening bridge are:

- o The length used to compute friction loss immediately upstream from the opening is an average length of the approximate streamlines that the flow must follow to get through the bridge opening.

- o Friction losses for flow through the bridge are computed assuming that the cross section having the minimum conveyance has some control over the flow in all of the subreaches affected by the bridge.

- o The model will compute backwater for both free-surface and pressure flow situations at a bridge.

- o The model can compute water-surface profiles through bridges for cases where road overflow occurs in conjunction with flow through the bridge opening.

- o The effect of spur dikes on the water-surface profile is estimated when spur dike data are coded.

Capabilities related to analysis of multiple waterway openings are:

- o An iterative procedure is used to apportion the flow among the individual openings and compute a water-surface profile for each individual opening using a representative strip of the valley. Iterations continue until both the flow apportionment and a conveyance-weighted average water-surface elevation at a common upstream cross section do not change significantly on successive iterations.

- o The valley is divided into strips on the basis of stagnation points which are computed from the relative flow areas of adjacent openings.

- o Discharge is apportioned on the basis of flow area of the openings and conveyance of the flood plain.

- o Culverts can be included in multiple opening analyses. FHWA culvert algorithms are incorporated in the model. Many of the culvert coefficients are stored internally, thus greatly simplifying culvert input.

Chapter III

WATER-SURFACE PROFILE COMPUTATION THEORY

Bridge waterway design usually requires determination of the amount of backwater caused by the encroachment of the flood plain and how far upstream the bridge-affected water-surface elevations will be higher than water-surface elevations for unconstricted flow (natural profile). Thus, the model must be capable of computing water-surface profiles through unconstricted valley reaches in addition to computing water-surface profiles through bridges.

STEP-BACKWATER COMPUTATIONS

The model uses a standard step method similar to that described by Chow to compute backwater in the unconstricted valley reaches.[4] This method requires description of a series of cross sections which segment the valley reach into relatively short subreaches. Subreaches should be sufficiently short so that the assumption of gradually varied, steady flow is valid within each subreach.

The model requires definition of the geometry and roughness of each cross section. Cross-sectional geometry is described by a series of coordinates which define the horizontal station and the ground elevation of each ground point. Horizontal stationing is measured from any arbitrary datum on the left bank (except at bridges where certain cross sections must be referenced to a common horizontal datum). The model uses left to right as a positive direction and assumes that left and right are defined by looking downstream. Ground elevations at all cross sections must be referenced to a common datum. Roughness is defined by Manning's n-values. Variable roughness coefficients may be specified to reflect roughness changes both horizontally and vertically at any cross section. The user must specify a skew angle for cross sections which are not surveyed on a line normal to the flow. Also, expansion and contraction coefficients, friction loss computation equations, and variable flow lengths for overbank and main channel subareas may be specified for each subreach.

The standard step method is based upon the principle of conservation of energy, i.e., the total energy head at an upstream section must be equal to the total energy head at the downstream section plus any energy losses that occur between the two sections. Thus, the energy equation between two adjacent cross sections (fig. 1) may be written

$$h_1 + hv_1 = h_0 + hv_0 + h_f + h_e \qquad (1)$$

where the subscripts o and 1 indicate the downstream and upstream cross sections, respectively; h_1 and h_0 are water-surface elevations; hv_1 and h_{vo} are velocity heads; and h_f and h_e are, respectively, the friction loss and the expansion/contraction loss in the subreach. Each of these terms has units of feet.

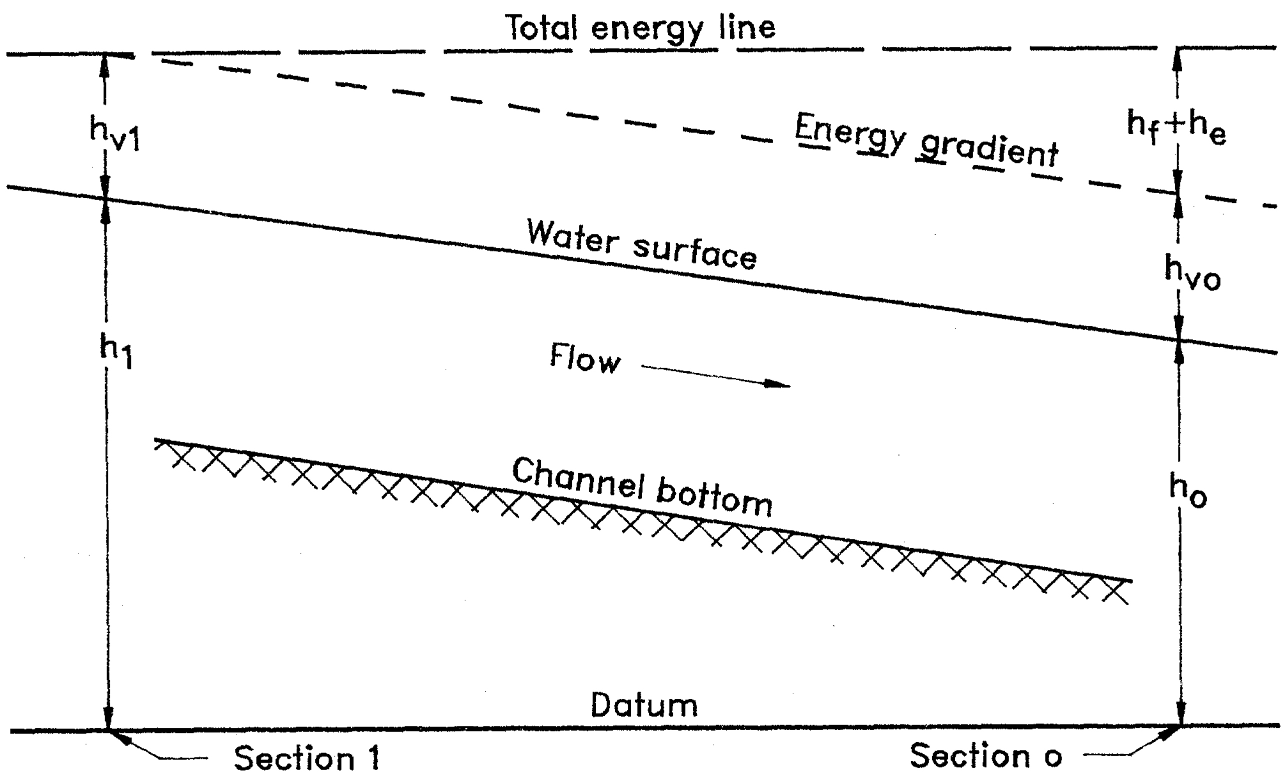

Figure 1. Sketch of subreach for standard step-backwater computations.

The velocity head terms are computed by

$$h_v = \frac{\alpha Q^2}{2g A^2} \tag{2}$$

where Q is the discharge at the section in ft^3/s (cubic feet per second), A is total cross-sectional flow area in ft^2, g is gravitational acceleration in ft/s^2, and α is the kinetic energy correction factor for nonuniform velocity distribution. The correction factor, α , is computed as

$$\alpha = \frac{\Sigma (k^3/a^2)}{K^3/A^2} \tag{3}$$

where k and a are subsection conveyance and flow area, respectively, and K is total cross-sectional conveyance. Conveyance is computed for each subsection by

$$k = \frac{1.49}{n} ar^{2/3} \tag{4}$$

where n is Manning's roughness coefficient and r is the subsection hydraulic radius.

Friction loss in a subreach is computed as

$$h_f = L S_f \tag{5}$$

where L is the flow length and S_f is the average friction slope in the subreach. Flow length may be either (1) a single user-specified subreach length, or (2) a conveyance-weighted length computed by the model on the basis of up to three user-specified subreach lengths. This latter option was adapted from the HEC-2 model.[20] Another HEC-2 capability incorporated into this model provides the user with the option to select the method of computing the average friction slope. The default option in WSPRO is the geometric mean slope, computed as

$$S_f = \frac{[(Q_o + Q_1)/2]^2}{K_o K_1} \tag{6}$$

The other options are the average conveyance method

$$S_f = \left(\frac{Q_o + Q_1}{K_o + K_1}\right)^2 \tag{7}$$

the average friction slope method

$$S_f = 1/2 \left[\left(\frac{Q_o}{K_o}\right)^2 + \left(\frac{Q_1}{K_1}\right)^2\right] \tag{8}$$

and the harmonic mean friction slope

$$S_f = \frac{2\ S_{fo}\ S_{f1}}{S_{fo} + S_{f1}} \tag{9}$$

with S_{fo} and S_{f1} computed by $\left(\frac{Q}{K}\right)^2$ at their respective sections.

The expansion/contraction loss in a subreach is computed by

$$h_e = k_e\ (h_{v1} - h_{vo}) \tag{10}$$

for expanding flow (i.e., $h_{v1} > h_{vo}$), and

$$h_e = k_c\ (h_{vo} - h_{v1}) \tag{11}$$

for contracting flow (i.e., $h_{vo} > h_{v1}$). The user may specify the expansion (k_e) and contraction (k_c) coefficients to be used in each subreach. The model will default to values of 0.5 and 0.0 for the expansion and contraction loss coefficients, respectively. The range of these coefficients, from ideal transitions to abrupt changes, are 0.0 to 1.0 for k_e and 0.0 to 0.5 for k_c.

A direct solution of equation 1 is not possible when either h_0 or h_1 is unknown, since the associated velocity head and the energy loss terms are then also unknown. Therefore, an iterative procedure must be used to determine the unknown elevation. This model computes the difference in total energy between two sections, ΔH, as

$$\Delta H = (h_1 + h_{v1}) - (h_0 + h_{v0} + h_f + h_e) \tag{12}$$

Successive estimates of the unknown elevation are used to compute the unknown velocity head and loss terms until equation 12 yields an absolute value of ΔH that is within an acceptable tolerance. Generally, a user-specified tolerance on the order of 0.01 to 0.05 ft will be sufficient to obtain satisfactory results from automated computation of water-surface profiles. Slightly higher tolerances may need to be specified for some high-velocity situations. However, if a specified tolerance exceeding 0.1 ft is required to obtain a solution there would be reason to suspect data inadequacies (e.g., insufficient number of cross sections).

There may be two water-surface elevations in a cross section which yield an acceptable ΔH from equation 12; one in the subcritical-flow regime and one in the supercritical-flow regime. This model does not provide the capability to obtain a direct solution for a water-surface profile that represents any combination of supercritical flow and subcritical flow at adjacent cross sections. The step-backwater computational procedure does not include provisions to evaluate the additional energy losses that occur in such flow transitions. Therefore, although it is possible that a subcritical water-surface elevation at one cross section and a supercritical water-surface elevation at an adjacent cross section will satisfy equation 1, such a solution is not truly correct and should be regarded as unacceptable. It is also possible that a critical water-surface elevation at one cross section and either a subcritical or supercritical water-surface elevation at an adjacent cross section will satisfy equation 1. Assuming that (1) appropriate control parameters and cross section data have been specified, and (2) computations have proceeded in the appropriate direction, such a combination represents a correct, acceptable solution for a water-surface profile.

This model is designed, to the greatest extent possible, to reject computed water-surface elevations which are in the incorrect flow regime. Subcritical flow at any point is affected (controlled) by downstream flow conditions. Conversely, supercritical flow is affected (controlled) by upstream flow conditions. Therefore, subcritical profile computations should be performed from downstream to upstream and supercritical profile computations should be performed from upstream to downstream. It is possible for an energy balance to be obtained when not following the above convention. However, it is quite common, when computing in the wrong direction, for the computed profile to diverge from the true profile.

This model requires the user to adhere to the following convention for computational direction: (1) upstream for subcritical flow; and (2) downstream for supercritical flow. This practice eliminates the problem of divergence between computed and true profiles. It also provides a relatively firm basis for evaluating the hydraulic validity of computed profiles. The model simply does not accept computed water-surface elevations in the wrong flow regime as valid solutions.

Assurance of the appropriate flow regime for downstream (supercritical) computations is quite straightforward in the model. The water-surface elevation for critical flow is computed on the basis of minimum specific energy for each and every cross section during downstream computations. Each and every trial water-surface elevation is constrained to be greater than minimum ground elevation and less than or equal to the critical water-surface elevation. Thus, any trial value satisfying the energy balance of equation 12 is automatically in the correct flow regime.

The vast majority of upstream (subcritical) profile computations are for flow conditions significantly higher than critical flow. Determination of the elevation of minimum specific energy is a time-consuming (expensive) iterative process. Therefore, an attempt is made to avoid computation of critical water-surface elevation for a cross section unless the flow is near critical flow. A Froude number test is a good alternative method of assuring that a trial elevation that satisfies the energy balance criteria is also in the subcritical flow range. A Froude number is computed by

$$F = Q/(A \sqrt{gA/\alpha T}) \tag{13}$$

where T is the cross section top width, in ft, and the other symbols are as previously defined. This computed Froude number is usually an approximation because equation 13 is derived using the assumption that α remains constant at all flow depths. If the computed Froude number is less than a user-specified Froude number test value the trial water-surface elevation will be accepted as a valid subcritical solution.

At a cross section where flow is nearly critical, it is possible that every trial water-surface elevation that satisfies equation 12 within an acceptable tolerance will be rejected because the computed Froude number is greater than the Froude number test value. Since the computed Froude number is only an approximation, the possibility exists that a valid solution will be rejected. Therefore, the model determines the critical water-surface elevation to establish the actual lower boundary of the subcritical flow regime. Another attempt is made to balance the energy equation using only trial water-surface elevations at or higher than the critical elevation. Any of these trial elevations that satisfy the tolerance are considered acceptable regardless of the computed Froude number because the computed critical water-surface elevation is based on minimum specific energy.

It is possible that, during upstream computations, no energy balance will be found between the initial trial water-surface elevation and the maximum elevation in the cross section. In such a case, it is assumed that either (1) the elevation increment was too large, allowing a valid solution to be skipped, or (2) the initial trial water-surface evaluation was so high that a valid solution was missed. To cover both of these possibilities, the elevation increment is halved and critical water-surface elevation is computed to establish the absolute minimum elevation for valid solutions. Another attempt is made to find a valid solution using the halved elevation increment and trial water-surface elevations in the subcritical flow regime. Since the subcritical flow regime has been defined the Froude number test is not exercised during this search.

At any cross section where an acceptable solution is not found, in both upstream and downstream computations, the model assumes critical flow exists at that cross section. The model then uses the critical water-surface elevation at that cross section as the "known" elevation for computing the water-surface profile through the next subreach. It is the user's responsibility to apply the necessary engineering judgement to determine the acceptability of these critical-flow assumptions. When such assumptions are judged to be unacceptable the user must adjust and/or add to the input data to obtain acceptable water-surface profile computations or perform appropriate alternate hydraulic analyses that will provide acceptable results.

SINGLE-OPENING BRIDGE HYDRAULICS

Computation of the water-surface profile through a stream crossing having a single waterway opening requires definition of a minimum of four cross sections. In situations where uniformity of channel shape and valley slope permit, it is possible to provide this definition on the basis of a single surveyed cross section because the model provides fairly flexible data propagation capabilities.

The cross sections numbered 4, 3F, and 1 (fig. 2) are unconstricted valley sections and will be referenced throughout this report as exit, full-valley, and approach sections, respectively. These three sections, along with the bridge-opening section (section 3, fig. 2), represent the minimum definition of a stream crossing. The bridge-opening section is located at the downstream face of the bridge. Another location (section 2, fig. 2) at

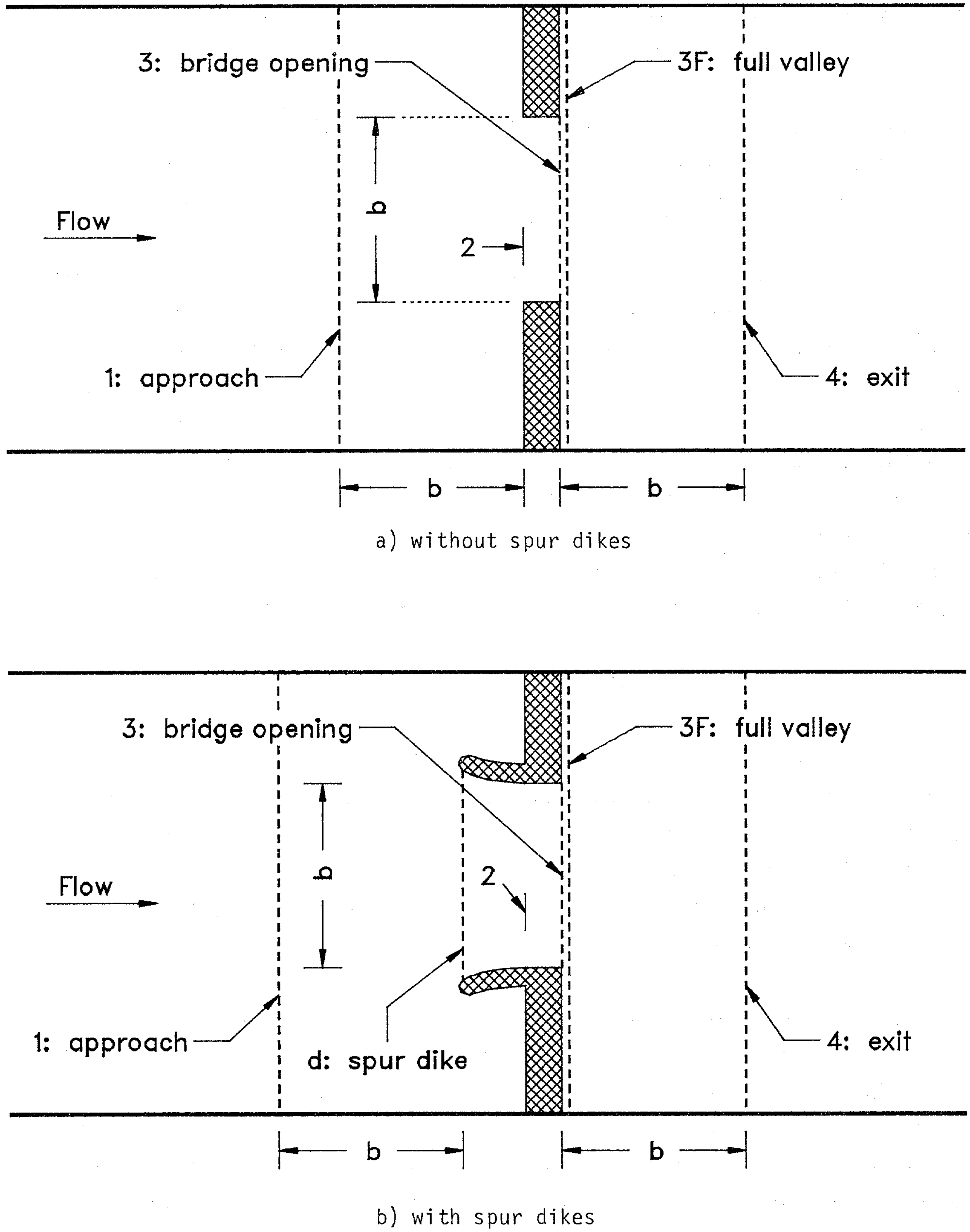

Figure 2. Cross-section locations for stream crossing with a single waterway opening.

the upstream face of the bridge is a control point in some of the computations but requires no input data. If spur dikes are present, a dike section located at the toe of the dikes must be defined (section d, fig. 2b). Also, if flow over the embankment might occur, a road-grade section (not shown on fig. 2) is required to define the top of the embankment, which would serve as the crest of a weir. Computations within the model require that the bridge-opening, road-grade (if any), and approach sections be referenced to a common horizontal datum. An option exists for implicit definition of this common horizontal datum when existing data do not conform to this requirement.

The flow situation that exists at a single bridge opening depends upon the relative elevations of the water surface both upstream and downstream of the bridge with respect to the elevations of the top of the bridge opening (hereafter referred to as low steel) and the top of the road grade. Free-surface flow exists when there is no contact or insignificant contact of water surface and low steel. Pressure flow through the bridge opening occurs as either (1) submerged orifice flow (when the water surface is in contact with low steel for the full flow length through the bridge) or (2) orifice flow (when only the upstream water surface is in contact with low steel). Any of the above flows through the bridge opening can occur in conjunction with road overflow. Numerical values are assigned to each flow class to provide a convenient means of directing computational sequences within the model and identifying the flow class on output. The flow class depends upon the elevation of the water surface relative to (1) the elevation of low steel in the bridge, which determines whether there will be free surface or pressure flow through the opening, and (2) the minimum elevation along the top of the embankment, which determines whether or not there will be road overflow. Table 1 summarizes the flow classes along with the governing elevation relationships. The symbols used are defined as follows: h_{ds} and h_{us} are the water-surface elevations immediately downstream and immediately upstream of the bridge, respectively; Y_{ls} is the low-steel elevation; and Y_{min} is the minimum embankment elevation.

Table 1. Summary of flow classes for a single bridge opening.

Class No.	Flow Class	Relative Elevations		
1	free-surface	$h_{ds}<Y_{1s}$	$h_{us}<Y_{1s}$	$h_{us}<Y_{min}$
2	orifice	$h_{ds}<Y_{1s}$	$h_{us}>Y_{1s}$	$h_{us}<Y_{min}$
3	submerged orifice	$h_{ds}>Y_{1s}$	$h_{us}>Y_{1s}$	$h_{us}<Y_{min}$

a) Flow only through the bridge opening.

Class No.	Flow Class	Relative Elevations		
4	free-surface	$h_{ds}<Y_{1s}$	$h_{us}<Y_{1s}$	$h_{us}>Y_{min}$
5	orifice	$h_{ds}<Y_{1s}$	$h_{us}>Y_{1s}$	$h_{us}>Y_{min}$
6	submerged orifice	$h_{ds}>Y_{1s}$	$h_{us}>Y_{1s}$	$h_{us}>Y_{min}$

b) Combination of flow through the bridge opening and weir flow over the road grade.

The model precedes each single-opening bridge analysis with computation of the natural profile from the exit section to the full-valley and approach sections. Natural profile elevations are hereafter subscripted as h_{in} where i is the section number. These data permit determination of the amount of backwater caused by the constriction and also are used as the initial trial elevations in the iterative solution for the water-surface profile through the bridge.

Free-Surface Flow

Water-surface profile computations for free-surface bridge flow situations are performed in accordance with the methods outlined by Schneider et al.[18] These methods were shown to produce significantly better results when compared with the FHWA and USGS methods. Improved computed results are attributed primarily to revisions in the computation of friction losses in the vicinity of the bridge. As discussed below, these revisions include use of an effective flow length from the approach section to the bridge-opening section and use of a selected minimum conveyance as a representative conveyance for the subreaches both upstream and downstream of the bridge opening. Another minor improvement is attributed to the use of an expansion loss between the bridge-opening section and exit section.

The total energy equation between the exit and approach sections (sections 4 and 1), assuming natural profile elevation at section 4, can be written as

$$h_1 + h_{v1} = h_{4n} + h_{v4n} + \text{Losses}_{(1-4)} \tag{14}$$

where $\text{Losses}_{(1-4)}$ equals the summation of friction losses in the subreaches between sections 1 and 4 plus an expansion loss between sections 3 and 4.

All of the friction-loss computations in this phase of the analysis use the geometric mean conveyance. The total discharge, Q, is assumed to be constant between sections 1 and 4. The number of subreaches used by the model to compute friction losses depends upon whether or not spur dikes are present. Without spur dikes, the friction losses between the approach section and the upstream face of the bridge (sections 1 and 2, fig. 2a) are

$$h_{f(1-2)} = \frac{L_{av}\ Q^2}{K_1 K_c} \tag{15}$$

When spur dikes are present, friction losses upstream from the bridge are computed separately for the two subreaches (sections 1 to d and d to 2, fig. 2b) upstream from the bridge by

$$h_{f(1-d)} = \frac{L_{av}\ Q^2}{K_1 K_c} \tag{16}$$

and

$$h_{f(d-2)} = \frac{L_{(d-2)}\ Q^2}{K_d K_c} \tag{17}$$

In equations 15 through 17, L_{av} is the effective flow length in the approach reach, K_1 and K_3 are total conveyances for sections 1 and 3, K_c is a control conveyance described below, and $L_{(d-2)}$ is the straight-line flow distance from d to 2. The theory and computation of L_{av} is discussed in more detail below under "Effective Flow Length." The value used for K_c is the minimum of the following conveyances; K_3, K_d (if dikes exist)+2nd K_q. K_q is the conveyance of the K_q section, which is defined as that segment of the approach section that conveys discharge that can flow through the bridge opening without contraction.[15] The horizontal limits of the K_q section are determined by projecting the bridge opening to the approach section with the projection lines oriented parallel to the general direction of flow. Schneider et al. found that use of the minimum control conveyance, K_c, contributed towards improved comparisons of computed versus observed water-surface profiles through bridges. The friction loss through the bridge is

$$h_{f(2-3)} = L_{(2-3)}\left(\frac{Q}{K_3}\right)^2 \tag{18}$$

where $L_{(2-3)}$ is the straight-line flow distance between sections 2 and 3. The friction loss in the flow expansion reach is computed as

$$h_{f(3-4)} = \frac{b\ Q^2}{K_c\ K_{4n}} \tag{19}$$

The expansion loss from section 3 to 4 is computed by

$$h_e = \frac{Q^2}{2g\ A_4{}^2} \left[2\beta_4 - \alpha_4 - 2\beta_3\left(\frac{A_4}{A_3}\right) + \alpha_3\left(\frac{A_4}{A_3}\right)^2\right] \tag{20}$$

where β is a momentum correction factor for nonuniform flow distribution. α_4 is computed by equation 3 and β_4 is computed as

$$\beta_4 = \frac{\Sigma\ (k^2/a)}{K^2/A} \tag{21}$$

where lower case and upper case indicate subsection and total section properties. α_3 and β_3 are related to bridge geometry and are computed by

$$\alpha_3 = \frac{1}{C^2} \tag{22}$$

and

$$\beta_3 = \frac{1}{C} \tag{23}$$

where C is the coefficient of discharge for the bridge, which is estimated in accordance with procedures outlined by Matthai.[15] A summary of these procedures is presented below under "Coefficient of Discharge."

The model uses an iterative procedure to determine h_3, h_d (if spur dikes exist), and h_1. It is necessary to simultaneously balance the energy equation for the two subreaches (without dikes) or for the three subreaches (with dikes). Regardless of the dike situation, the energy equation for the subreach between sections 3 and 4 is

$$h_3 = h_{4n} + h_{v4n} + h_{f(3-4)} + h_e - h_{v3} \tag{24}$$

where equations 19 and 20 are used to compute $h_{f(3-4)}$ and h_e. Without spur dikes, h_1 is determined by

$$h_1 = h_3 + h_{v3} + h_{f(2-3)} + h_{f(1-2)} - h_{v1} \tag{25}$$

where the friction losses are computed using equations 18 and 15. With spur dikes, two subreaches are used between sections 3 and 1. At the dike section

$$h_d = h_3 + h_{v3} + h_{f(2-3)} + h_{f(d-2)} - h_{vd} \tag{26}$$

with equations 18 and 17 used to compute friction losses, and at the approach section

$$h_1 = h_d + h_{vd} + h_{f(1-d)} - h_{v1} \tag{27}$$

where the friction loss is computed by equation 16. The solution is accomplished in the following steps:

(1) Compute L_{av} based on natural profile elevations.

(2) Assign initial trial values at the bridge-opening and approach sections of $h_3 = h_{3n}$ and $h_1 = h_{1n}$. If dikes are present, assign $h_d = h_{dn}$ where h_{dn} is determined by interpolation between h_{3n} and h_{1n}.

(3) Compute section properties for the current trial elevations at sections 3, d (if any), and 1; determine K_c; determine C; and compute energy losses and velocity heads.

(4) Compute h_3 (eq. 24); h_d if necessary (eq. 26); and h_1 (eq. 25 or 27, as appropriate).

(5) Compare each of the computed elevations with the current trial elevation for that section. If each and every one of these elevation differences is within an acceptable tolerance the solution is complete. Otherwise, assign new trial elevations equal to the last computed elevation and return to step 3.

Effective Flow Length

Since friction losses are directly proportional to flow length, it becomes imperative to obtain the best possible estimate of flow length, especially for those cases where the friction loss is a significant component of the energy balance between two sections. Previous computational methods that did compute separate friction loss components estimated the approach reach friction loss on the basis of the straight-line distance between sections 1 and 2 (or d if dikes existed). For minor degrees of constriction, this was usually adequate. However, for more significant constrictions, this straight-line distance is representative of only that portion of the flow that is generally in direct line with the opening. Flow further away from the opening must flow not only downstream, but also across the valley to get to the opening, thus traveling much farther than the straight-line distance.

Schneider et al. tabulated average streamline lengths for various approach section locations and various degrees of constriction.(18) These results are not directly applicable in this model because they are derived for symmetric constrictions in channel reaches having uniform, homogeneous flow conveyance characteristics. Even if the exact-solution algorithms were developed for nonsymmetric, nonhomogeneous conditions, the computer resource requirements for an exact solution are too great to warrant inclusion in this model. Therefore, a simplified computational technique was developed and incorporated into this model to compute average streamline length.

Schneider et al. defined the optimum location of the approach section as

$$L_{opt} = \frac{b}{\pi\,(1-m')}\quad\Phi \tag{28}$$

where L_{opt} is the distance, in ft, between the approach section and the upstream face of the bridge opening, b is the bridge-opening length, and m' is the geometric contraction ratio computed by

$$m' = 1 - b/B \tag{29}$$

where B is the top width, in ft, of the approach section flow area. The Φ term in equation 28 is computed by

$$\Phi = \frac{1}{2} \ln \left[\left(\sqrt{\frac{8}{\varepsilon^2} + 8} - \frac{3}{\varepsilon} - \varepsilon \right) \left(- \sqrt{8 + 8\varepsilon^2} - 3\varepsilon - \frac{1}{\varepsilon} \right) \right] - \ln \left(\varepsilon - \frac{1}{\varepsilon} \right) \quad (30)$$

where ε is computed by

$$\varepsilon = 1 + \delta + \sqrt{\delta^2 + 2\delta} \quad (31a)$$

with δ computed as

$$\delta = \frac{2}{\tan^2 \left[1 - \left(\frac{b}{2B} \right) \pi \right]} \quad (31b)$$

L_{opt} is located in a zone of nearly one-dimensional flow, thus satisfying the basic requirements of the one-dimensional energy equation. However, it was also determined in that study that the approach section could be placed almost anywhere, with reasonable values for friction loss computed so long as the average streamline length is used in the computations. Therefore, it was decided to retain the past convention of placing the approach section one bridge-opening length upstream from the bridge opening and to use the average streamline length in the friction loss computations.

The simplified computational technique varies depending upon the relative magnitudes of L_{opt} and b. To introduce the technique, discussion is limited to the ideal situation of a symmetric constriction with uniform, homogeneous conveyance. For such conditions only one-half of the valley cross section is required. This one-half section is divided into ten equal-convenyance streamtubes between edge of water and the centerline at both the L_{opt} location and the upstream face of the bridge. Equal-conveyance streamtubes are equivalent to equal-flow streamtubes for one-dimensional flow. Figure 3 illustrates a case with a small geometric contraction ratio. L_{opt} is less than b for lesser degrees of constriction. Since L_{opt} is located in a zone of nearly one-dimensional flow, the streamlines are essentially parallel between the approach section and the L_{opt} location. Between L_{opt} and the bridge opening the corresponding flow division points are connected

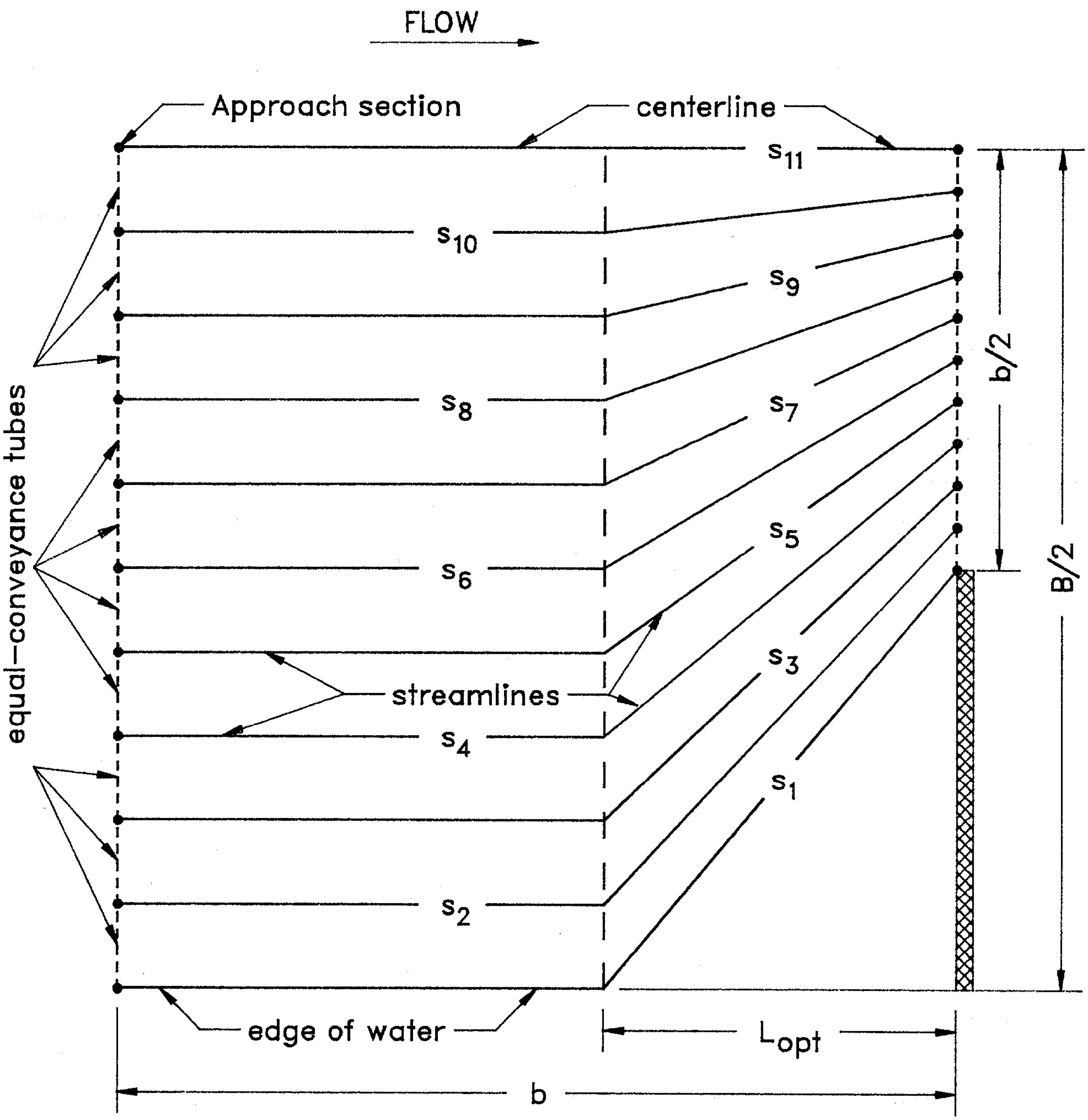

Figure 3. Definition sketch of assumed streamlines for relatively low degrees of contraction.

with straight lines. The effective flow length used by the model is the average length of the ten equal-flow streamtubes computed by

$$L_{av} = 1/10 \left[\sum_{i=2}^{10} s_i + (s_1 + s_{11})/2 \right] \tag{32}$$

where i indicates the streamline number and s is the individual streamline length. Although the straight-line pattern is a gross simplification of the actual curvilinear streamlines, the computed L_{av} values are less than 2 percent greater than the exact solution for small geometric contraction ratios.

Figure 4 illustrates a relatively high degree of geometric contraction. Simply connecting the flow division points of the L_{opt} and bridge sections does not result in representative lengths for those streamlines furthest away from the opening. Therefore, a parabola is computed by the equation

$$y^2 = 2b \left(x + \frac{b}{2} \right) \tag{33}$$

This parabola has its focus at the edge of water and its axis in the plane of the upstream face of the bridge. Positive x and y distances are measured from the edge of water towards the stream centerline and upstream from the plane of the bridge, respectively. For portions of the section where L_{opt} is upstream from this parabola, the parallel streamlines are projected to the parabola and then a straight line connects this projected point with the corresponding flow division point in the bridge opening. Flow division points of the L_{opt} section at or downstream from the parabola are connected directly to their corresponding flow division point for the bridge opening. Only the distances between the approach and bridge-opening sections are used to compute L_{av} with equation 32. This process generally produces results that are within 5 percent of the exact solution. For very severe constrictions (i.e., $m' = 0.95$), the differences are closer to 10 percent.

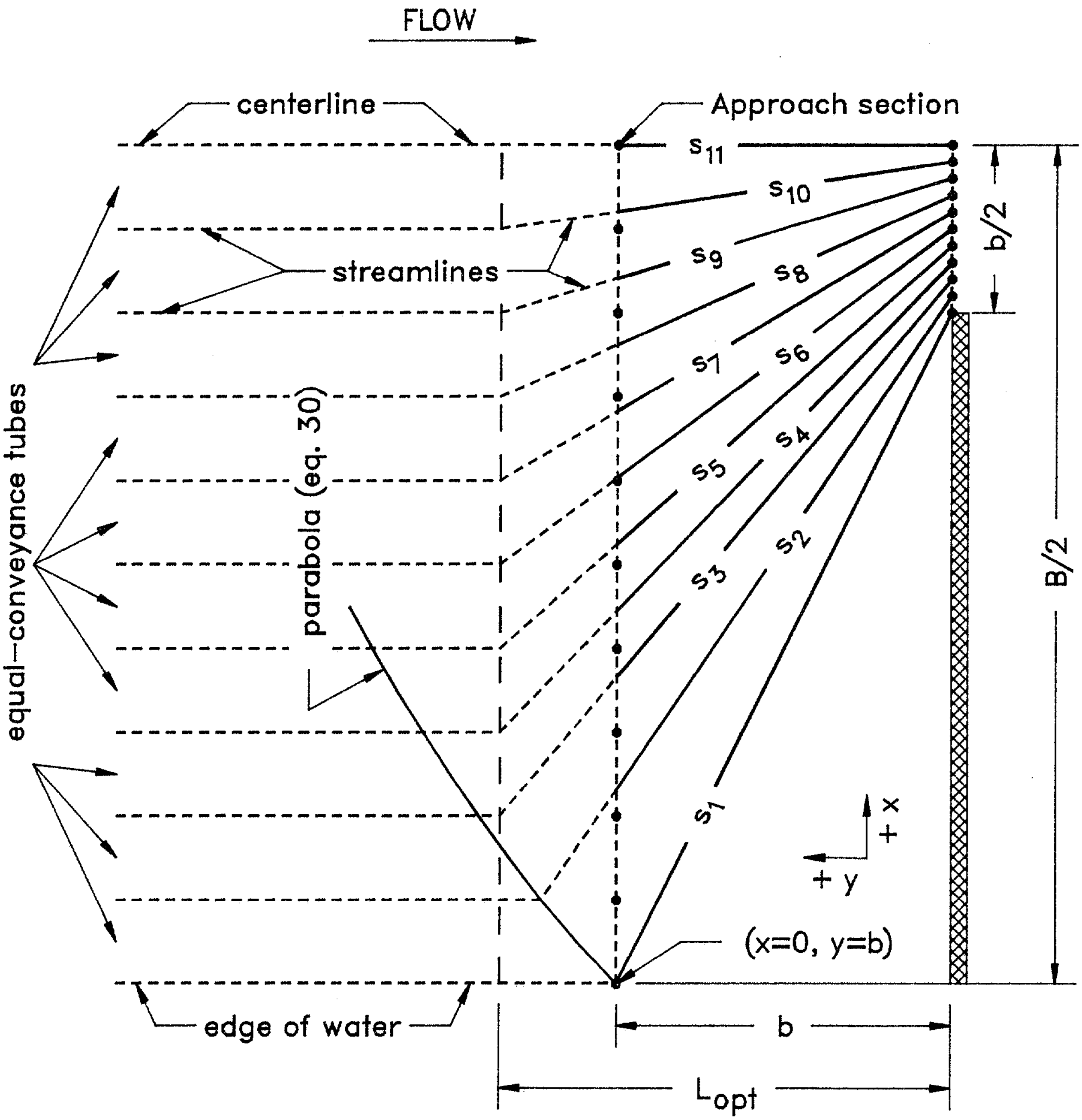

Figure 4. Definition sketch of assumed streamlines for relatively high degrees of contraction.

Nonuniform conveyance distribution in the approach reach is represented by defining the streamtubes on a conveyance basis. The model determines the horizontal stationing of 19 interior flow division points that subdivide both the L_{opt} and bridge sections into 20 tubes of equal conveyance. Asymmetric constrictions with nonuniform conveyances are analyzed by treating each half of the reach on either side of the conveyance midpoints separately, then averaging the results. L_{av} for each side is the conveyance-weighted average streamline length. Figure 5 illustrates a typical asymmetric, nonuniform conveyance situation.

Coefficient of Discharge

The coefficient of discharge, as defined by Matthai and used in this model, is a function of bridge geometry and flow characteristics.[15] Matthai's report presents detailed instructions for computing the coefficient of discharge for the four most common types of bridge openings. It is not practical to reproduce that entire report herein, but the following paragraphs summarize the procedures as adapted to this model. All of the key figures from Matthai's report, the tabular values and equations used in the model to determine the coefficient of discharge, and a discussion of the minor modifications made to Matthai's procedures are presented in the appendix.

Bridge openings are classified as one of four different types depending upon characteristics of embankment and abutment geometry. Regardless of opening type, the first step is to determine a base coefficient of discharge, C', which is a function of (1) a channel contraction ratio and (2) a ratio of flow length through the bridge, L, to the bridge-opening length, b. The channel contraction ratio is

$$m = 1 - \frac{K_q}{K_1} \tag{34}$$

where K_q is the conveyance of part of the approach section as described in the definition of K_c following equation 17, and K_1 is the total conveyance of

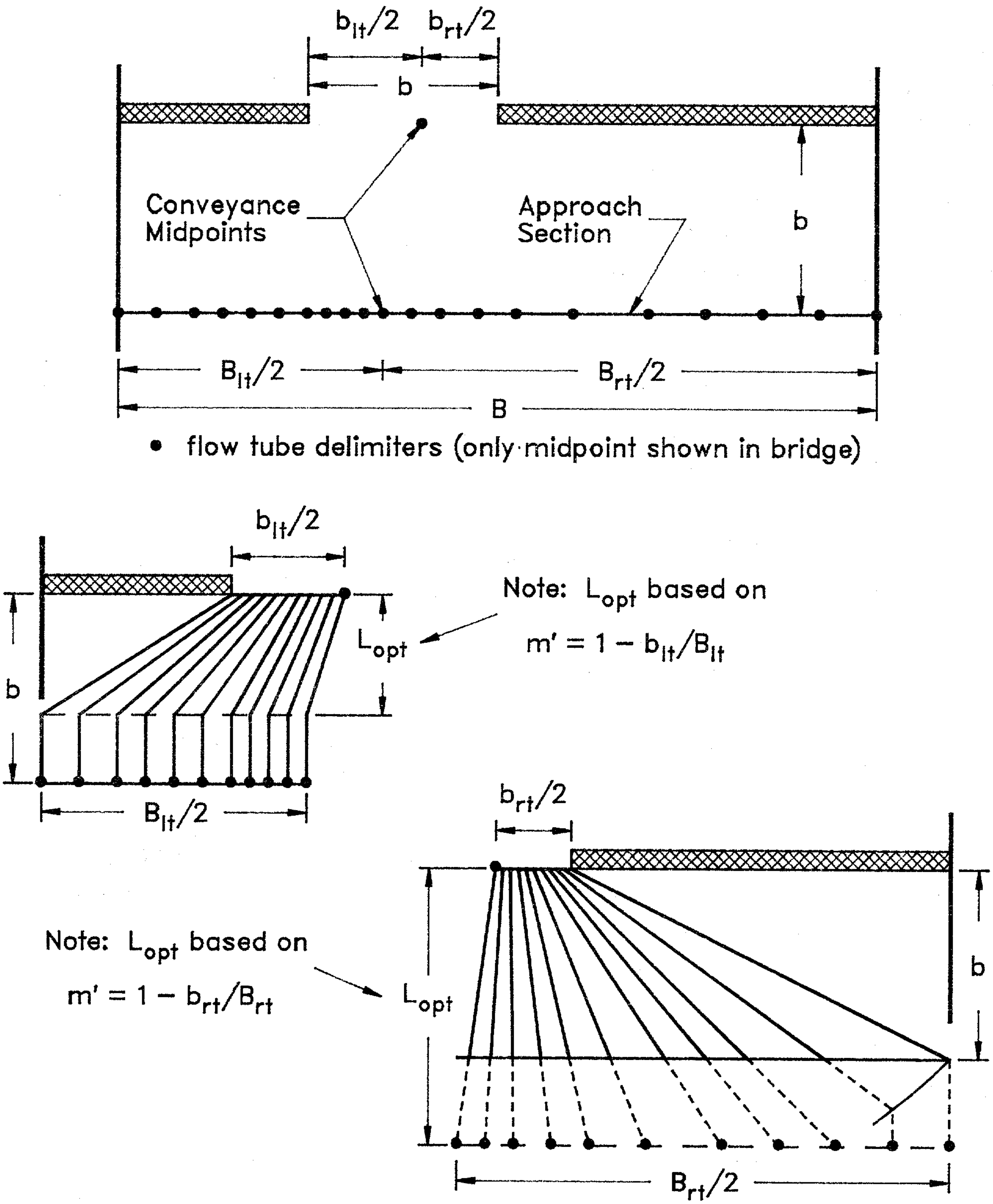

Figure 5. Assumed flow pattern for a nonsymmetric constriction with nonhomogeneous roughness distribution.

the approach section. The definition of the L and b terms for the length ratio depends upon the opening type. The definition sketches in the appendix define these terms for each opening type. The final coefficient of discharge, C, is computed by multiplying C′ by a series of adjustment factors to account for variations in geometry and flow from the base conditions used to derive C′. The number of parameters for which adjustment factors are required depends partially upon the opening type. Following is a summary description of the opening types and the adjustment factors that are unique to each.

- o Type 1 openings have vertical embankments and vertical abutments with or without wingwalls. The discharge coefficient is adjusted for the Froude number (k_F) and also for wingwall width (k_W) if wingwalls are present or for entrance rounding (k_r) if there are no wingwalls.

- o Type 2 openings have sloping embankments and vertical abutments and do not have wingwalls. The discharge coefficient is adjusted on the basis of the average depth of flow at the abutments (k_y).

- o Type 3 openings have sloping embankments with spillthrough abutments. The discharge coefficient is adjusted on the basis of entrance geometry (k_x).

- o Type 4 openings have sloping embankments, vertical abutments, and wingwalls. The discharge coefficient is adjusted depending upon the wingwall angle (k_Θ).

In addition to the above adjustment factors, which are dependent upon opening type, there are adjustment factors for piers or piles (k_j) and spur dikes (k_a, k_b, k_d) that may be applied to all opening types. The relationships used to compute all of the above adjustment factors are shown in the appendix.

Pressure Flow

Free-surface flow cannot exist if there is significant contact of the water surface with the bridge superstructure. Instead, pressure flow, which is proportional to the square root of the head differential, is established. This model analyzes pressure flow situations as either orifice flow or submerged orifice flow depending upon the degree of contact between the water surface and the superstructure.

Orifice Flow

If the water surface is in contact only with the upstream girders, the water-surface profile through the bridge can be determined by use of an orifice flow equation. According to Bradley, discharge through the opening, QBO, may be computed as

$$QBO = C_D\, A_{3net} \sqrt{2g\,(Y_u - Z/2 + h_{v1})} \tag{35}$$

where C_D is a discharge coefficient, A_{3net} is the net area (gross area less area of piers or piles) in the bridge opening for an elevation of h_{us}, and the parenthetical expression beneath the radical is the effective head.(3) Figure 6 illustrates the definition of the variables involved in this computation. The water-surface elevation immediately upstream from the bridge, h_{us}, is computed by

$$h_{us} = h_1 - h_{f(1-2)} \tag{36}$$

where h_1 is the water-surface elevation at the approach section and $h_{f(1-2)}$ is an estimate of the friction loss in the approach reach. This friction-loss term is computed using equation 15 with K_c set to equal to the bridge-opening conveyance, K_3. The velocity head at the approach section, h_{v1}, is assumed to be applicable throughout the approach reach. The submergence elevation, Y_{1s}, is either computed from input data defining bridge deck elevation and girder depth or specified by the user. The hydraulic depth, Z, within the bridge opening is

$$Z = A_{3net}/b \tag{37}$$

and the reference bed elevation (Y_{bed}) is estimated as

$$Y_{bed} = Y_{ls} - Z \tag{38}$$

and the average upstream depth is

$$Y_u = h_{us} - Y_{bed} \tag{39}$$

A relationship between Y_u/Z and C_D determined in the laboratory is shown in figure 7.[3] The dashed portion of the relationship indicates a transition zone of poorly defined flow regime. The model uses an arbitrary value of 1.1 for the Y_u/Z ratio as the breakpoint between free-surface and orifice flow.

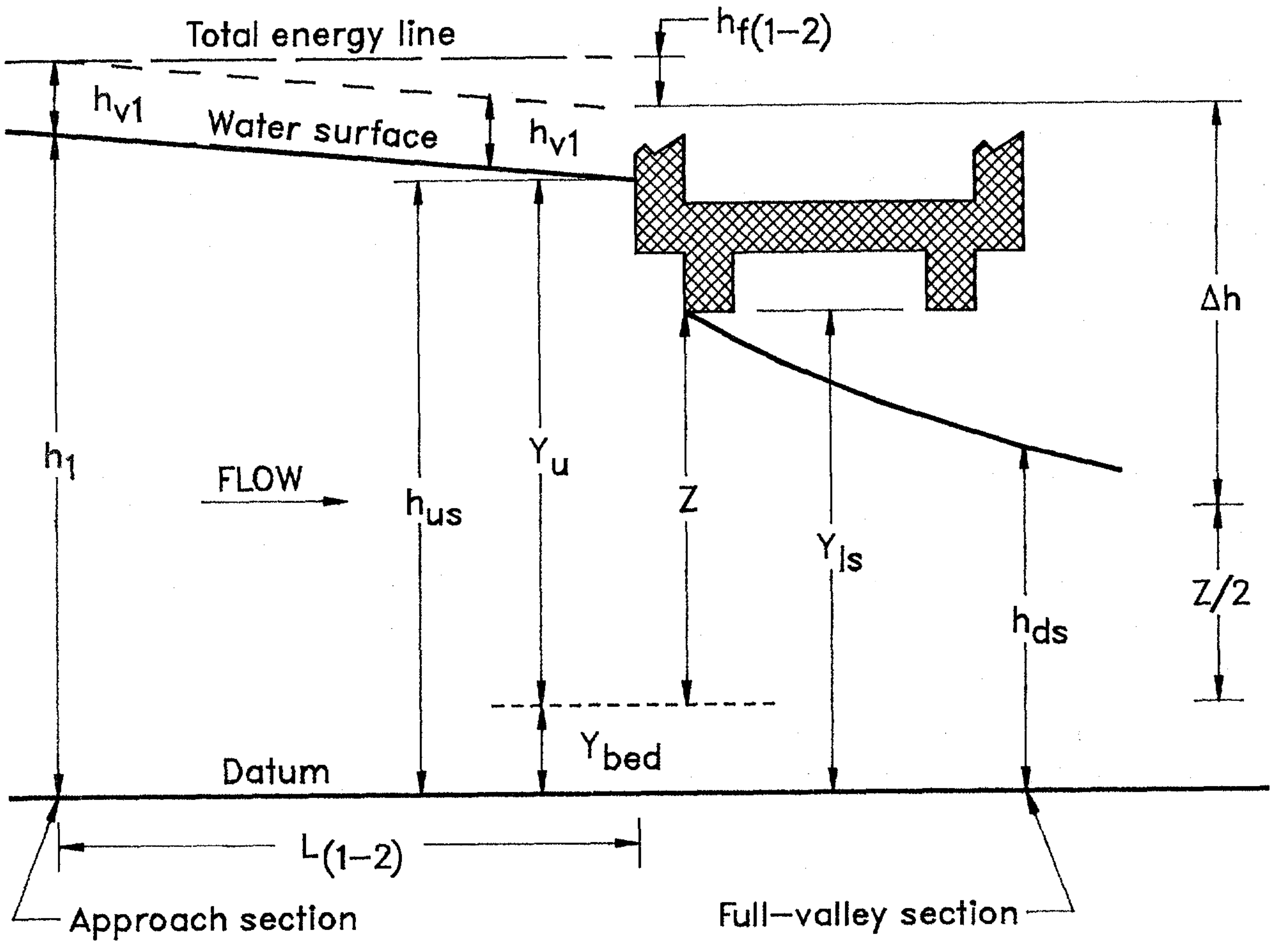

Figure 6. Definition sketch for orifice flow computations.

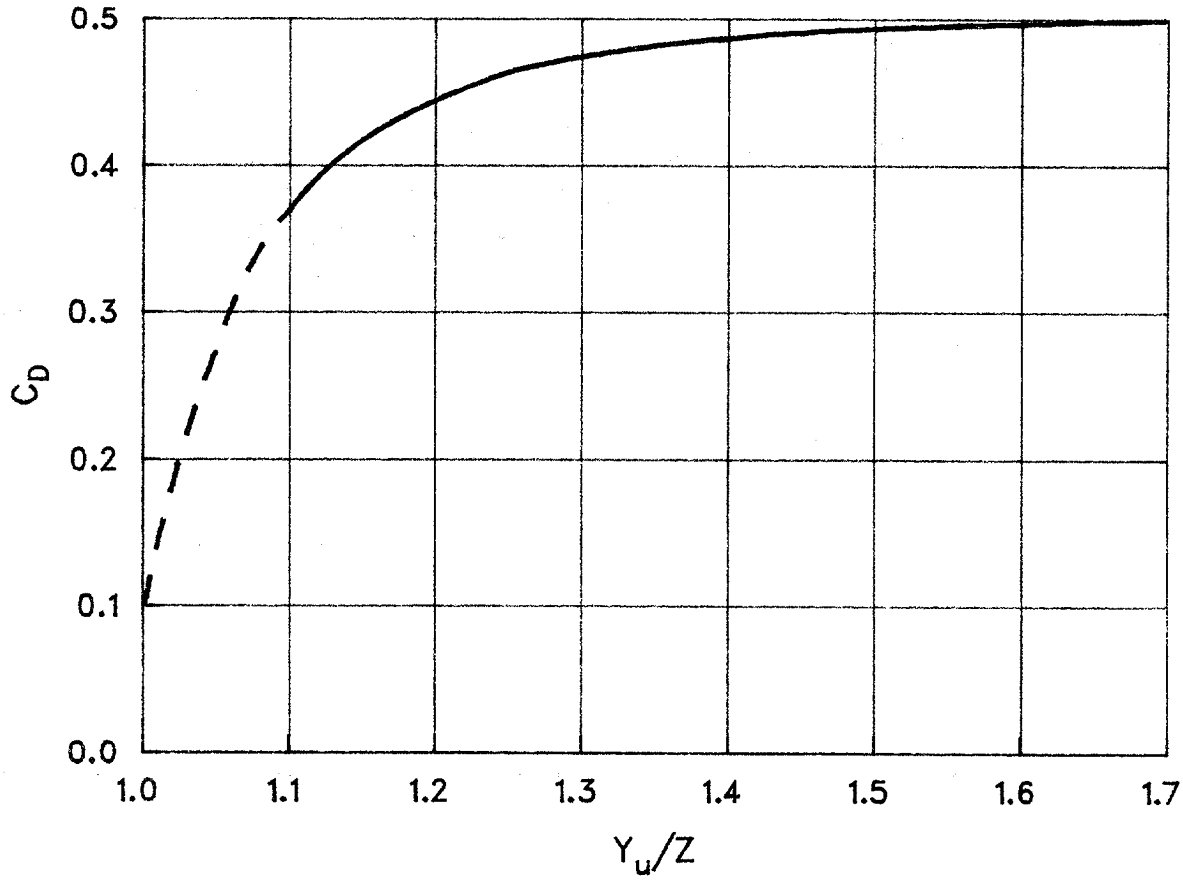

Figure 7. Discharge coefficient for orifice flow.

An iterative procedure is used to determine the value of h_1 that will produce the correct discharge from equation 35. The same procedure is used for submerged orifice flow and is described below under "Profile Computations."

Submerged Orifice Flow

Flow through the bridge is handled as submerged orifice flow when the water surface is in contact with the girders for the entire flow length through the bridge (fig. 8). Discharge through the opening for such a case is computed as

$$QBO = C_D \, A_{3net} \sqrt{2g\Delta h} \qquad (40)$$

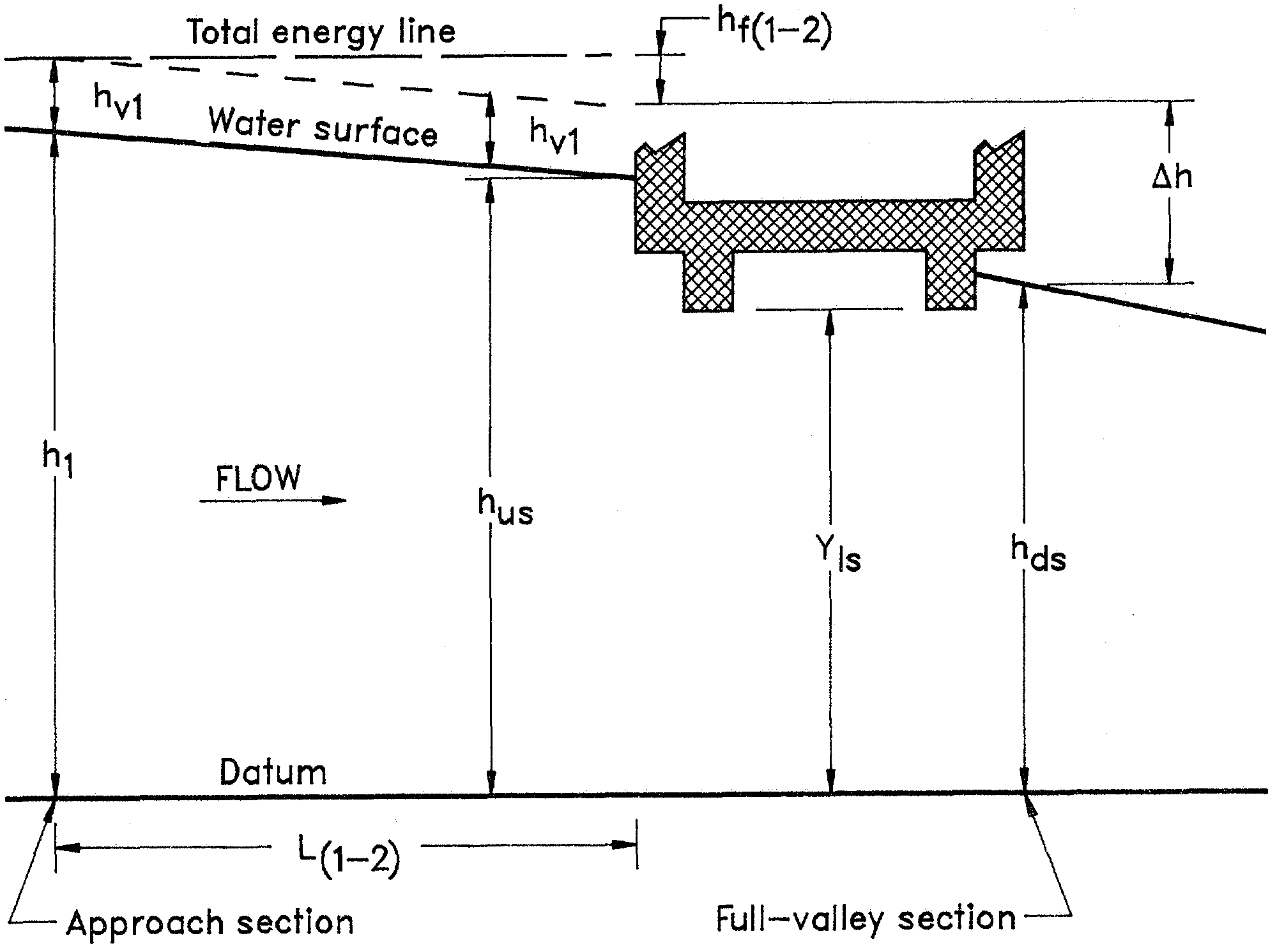

Figure 8. Definition sketch for submerged orifice flow computations.

where C_D is a coefficient discharge, A_{3net} is the total net flow area in the bridge opening, and the head differential is computed by

$$\Delta h = h_{us} + h_{v1} - h_{3n} \tag{41}$$

with the terms as previously defined. Laboratory investigation demonstrated that a constant value of 0.8 is adequate for C_D.[3] Therefore, submerged orifice flow is computed by

$$QBO = 6.42 \ A_{3net} \sqrt{\Delta h} \tag{42}$$

The iterative procedure used to determine the appropriate h_1 value is discussed in the following section.

Profile Computations

Discharge through the bridge opening is known (equal to total discharge) when there is no flow over the embankment. A direct solution is not possible because h_{v1} is a function of h_1 and, for orifice flow, C_D also can vary with elevation. For either case of pressure flow a half-interval method is used to find the approach section elevation, h_1, at which the difference between QBO and total discharge, Q, is within an acceptable tolerance. Generally, a tolerance equal to 1 or 2 percent of the total discharge is an easily attainable goal in automated computations. A tolerance of 5 percent of total discharge is probably a reasonable maximum tolerance to obtain acceptable results. The steps followed within the model are:

(1) Initialize (1) $h_1 = Y_{1s}$ for orifice flow or (2) $h_1 = h_{3n}$ for submerged orifice flow and compute h_{us}. Compute QBO using either equation 35 or 42. Set $h_{min} = h_1$, since this is the absolute minimum pressure flow that is possible.

(2) Set h_1 = maximum ground elevation in the approach section, compute h_{us}, and compute QBO using either equation 35 or 42. Set $h_{max} = h_1$, since this is the maximum pressure flow the model can compute for the opening.

(3) Set $h_1 = (h_{min} + h_{max})/2$, compute h_{us}, and compute QBO using either equation 35 or 42.

(4) Compare QBO and Q and

  (a) if the absolute value of (QBO - Q)/Q is within an acceptable tolerance, the profile computations are adequate and the current value of h_1 may be used to continue computations upstream (assuming that h_1 is not sufficiently high to result in road overflow).

  (b) if QBO > Q, the trial h_1 is too high. Set h_{max} equal to the trial h_1 value and return to step 3.

  (c) if QBO < Q the trial h_1 is too low. Set h_{min} equal to the trial h_1 value and return to step 3.

Road Overflow

When the water-surface elevation immediately upstream from the embankment exceeds the minimum elevation along the top of the embankment, the embankment begins to function as a broad-crested weir. This model applies the methods outlined by Matthai and Hulsing, with some modifications, to determine the water-surface profile for these combined flow situations (i.e., road overflow in conjunction with flow through the bridge opening).[15,12]

Figure 9 illustrates the parameters involved in the weir-flow computations. It is assumed that the approach section is representative of the subreach between the approach section and the embankment. Therefore, the only difference in total energy is some energy loss due to friction. This friction loss is estimated by

$$h_{f(1-R)} = L_{(1-R)} \frac{Q^2}{K_1^{\,2}} \tag{43}$$

The water-surface elevation at the embankment can thus be estimated by

$$h_R = h_1 - h_{f(1-R)} \tag{44}$$

and the associated total energy line elevation is

$$H_R = h_R + h_{v1} \tag{45}$$

If h_R is lower than the lowest embankment elevation, obviously there is no weir flow to be computed. Weir discharges are computed incrementally between the coordinate points defining the top of the embankment. These coordinate points are either input directly by the user or computed from vertical curve control points input by the user. For each incremental length of embankment, B_W, the total head available to produce weir flow is

$$H = H_R - Y_R \tag{46}$$

where Y_R is the average elevation of the incremental length. The static head, h_s, which is required for determining weir coefficients, is

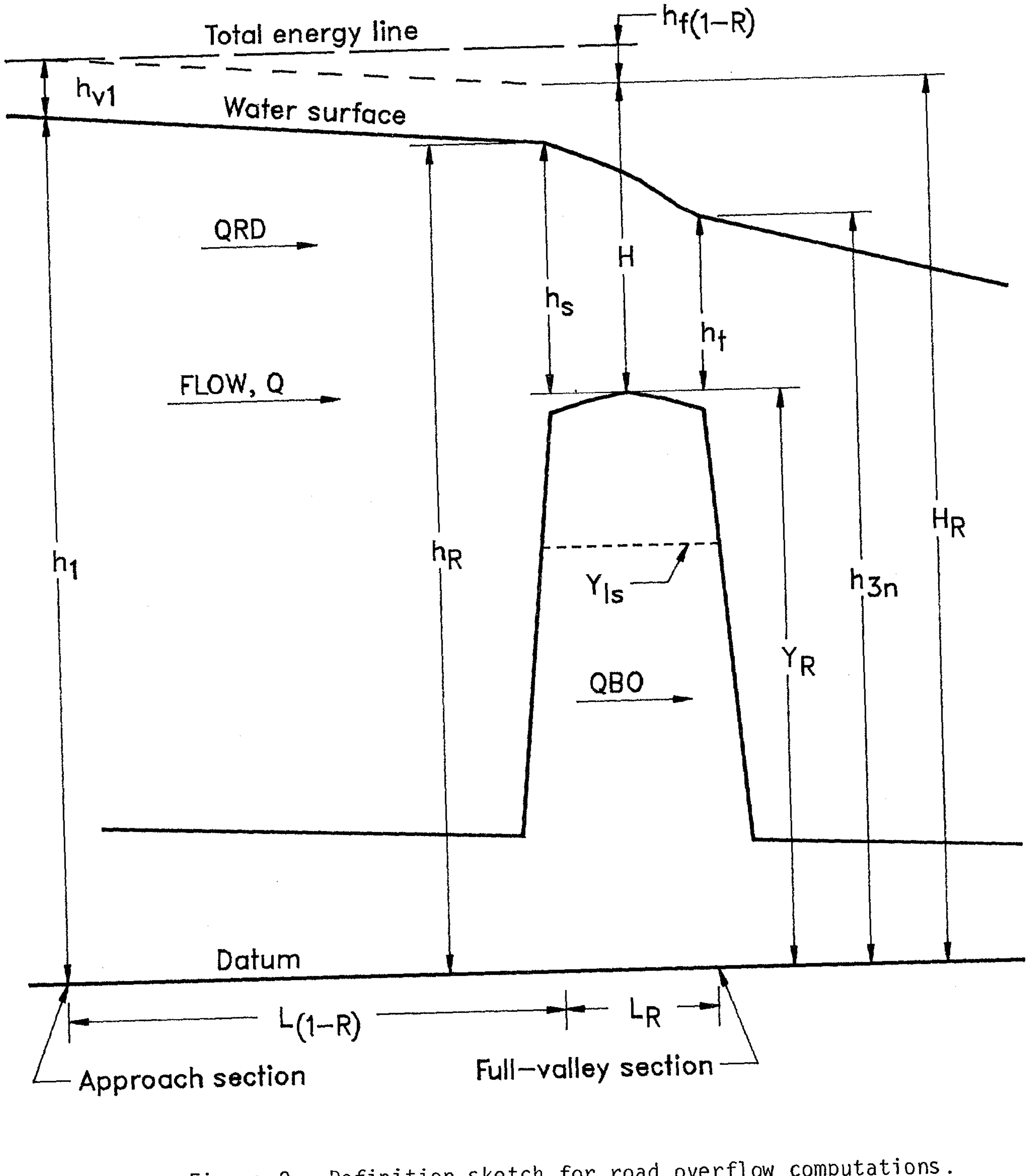

Figure 9. Definition sketch for road overflow computations.

$$h_s = H - h_{v1} \tag{47}$$

The discharge over the incremental length is computed by

$$q = k_t \; C_f \; B_W \; H^{3/2} \tag{48}$$

where C_f is a coefficient of free discharge and k_t is an adjustment factor for submerged weir flow (i.e., h_{3n} higher than embankment elevation).

Figures 10a and 10b are the relationships used for the coefficient of free discharge, and figure 10c is the relationship for the submergence factor. Road overflow is actually computed separately for the portions of the embankment to the left and right of the bridge opening centerline. This permits output of velocities, depths, and widths of road overflow pertinent to embankment design and for potential damage assessment. However, only the total flow over the road, QRD, is required for the profile computations discussed below.

Profile Computations for Combined Flow

The iterative procedure for profile computations for combined flow site depends upon whether the discharge through the bridge opening is free-surface flow or pressure flow. The steps followed for free-surface flow conditions are:

(1) Set h_{max} equal to the h_1 value computed for the entire discharge passing through the opening. Set h_{min} equal to the minimum road grade elevation.

(2) Compute assumed approach elevation WS = $(h_{max} + h_{min})/2$.

(3) Compute flow over road, QRD, for WS. Compute flow through bridge as QBO = Q - QRD. If QBO is positive proceed to next step. Otherwise set h_{max} = WS and repeat previous step.

(4) Compute h_1 for QBO using single-opening computational procedure.

(5) Compare h_1 and WS.

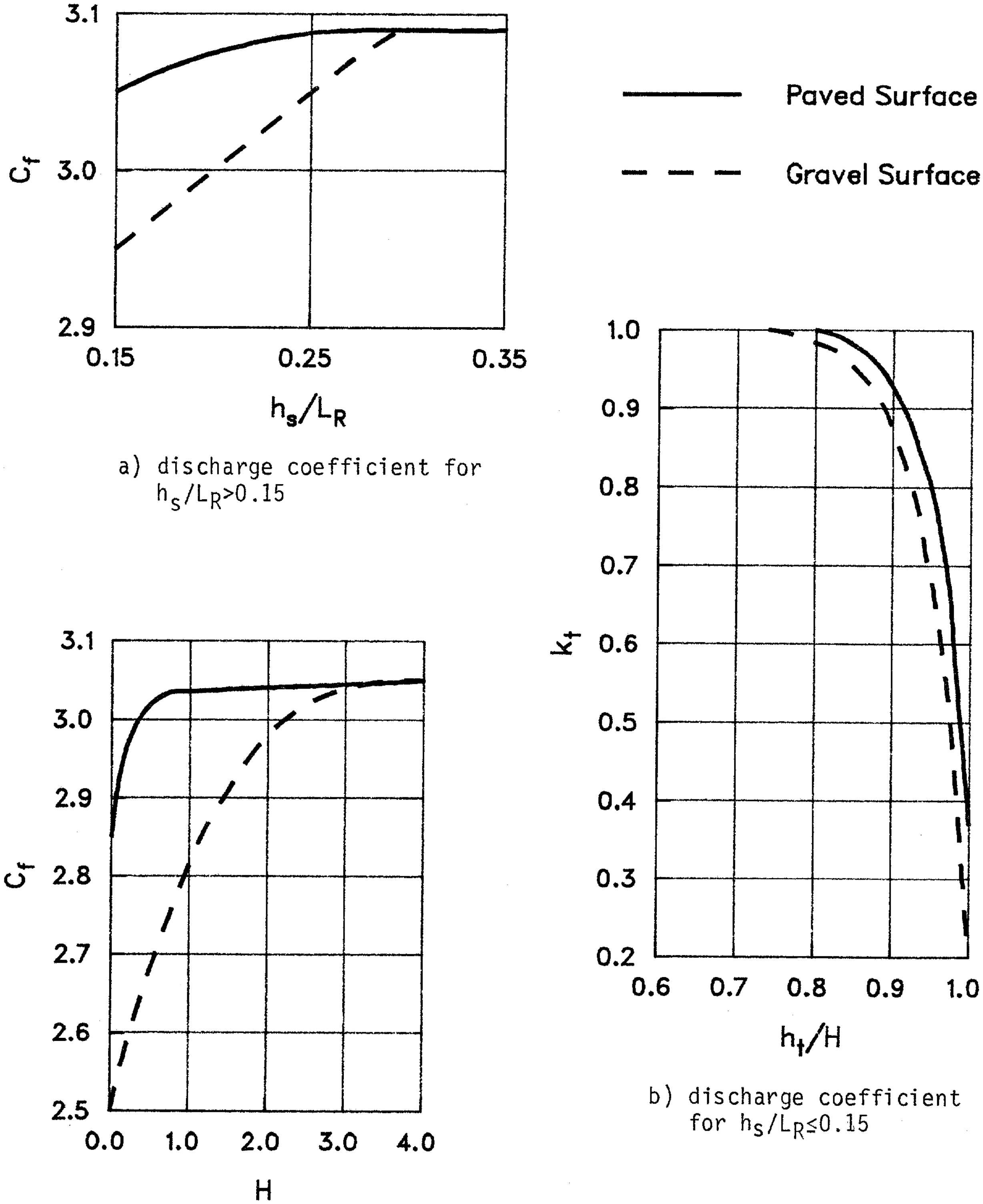

a) discharge coefficient for $h_s/L_R > 0.15$

b) discharge coefficient for $h_s/L_R \leq 0.15$

c) submergence factor

Figure 10. Coefficients for road overflow.

(a) If the absolute value of the difference is within an acceptable tolerance, then compare h_{us} and low steel elevation. If h_{us} is less than low steel, computations may proceed upstream. Otherwise check for possibility of orifice flow. If $Y_u/Z > 1.1$, pressure flow most likely exists and the computational procedure for pressure flow (discussed later) is used.

(b) If $h_1 > WS$ more flow over road is required; therefore, set $h_{min} = WS$ and return to step 2.

(c) If $h_1 < WS$ more flow through the bridge opening is required; therefore, set $h_{max} = WS$ and return to step 2.

When pressure flow through the bridge opening exists, the following steps are followed:

(1) Set h_{max} equal to maximum ground elevation in the approach section. Set h_{min} equal to h_{3n}.

(2) Compute assumed approach section elevation $WS = (h_{max} + h_{min})/2$.

(3) Compute QRD and QBO (using the appropriate equation for free or submerged orifice flow) for the assumed WS.

(4) Compute the error between the total discharge and the sum of computed discharges, $QERR = [Q - (QBO + QRD)]/Q$.

(5) Check the value of QERR.

(a) If the absolute value of QERR is within an acceptable tolerance

-- for submerged orifice flow computations may proceed upstream.

-- for free orifice flow an additional check is made on Y_u/Z. If $Y_u/Z < 1.1$ the assumption is made that pressure flow cannot exist, and free-surface flow results are used.

(b) If QERR is positive the assumed water surface is too high, set $h_{max} = WS$ and return to step 2.

(c) If QERR is negative the assumed water surface is too low, set $h_{min} = WS$ and return to step 2.

Additional checks are performed at the beginning of the profile computations for both free-surface and pressure flow. The total computed flows at both the initial minimum and initial maximum elevations are compared to the actual total discharge. If the total computed discharge at the maximum elevation condition is less than the actual total discharge, the computations are aborted and appropriate error messages are printed. Generally, this would indicate a data coding problem, although this could also occur for a vastly underdesigned bridge opening. If the total computed discharge at the minimum elevation condition is greater than the actual total discharge, there is either a data coding problem or a flow situation that cannot be adequately analyzed using the weir-flow concepts. The model assumes the latter and fabricates a composite cross section from the bridge-opening and embankment sections. The computed properties of the composite section are a summation of (1) the flow area(s) of the segment(s) of the bridge and embankment that are overtopped and (2) the flow area through the bridge opening. This composite section (C, fig. 11) is used, along with the full-valley (3F, fig. 11) and approach (1, fig. 11) sections and a relocated approach section (1R, fig. 11), to compute a water-surface profile using step-backwater computations. The rationale for such an analysis is that the embankment is probably inundated to the extent that the assumption that weir flow exists is no longer valid. Sections 3F and 1 remain at their original locations. Section C is located at the embankment centerline and section 1R is located at the upstream face of the bridge. Section 1R ground elevations are adjusted for the valley slope between the bridge and the approach section. Step-backwater computations are made through the three subreaches defined by these four cross sections. The model assumes that the water-surface elevation for unconstricted flow conditions, h_{3n}, would exist at section 3F. Use of the relocated approach section to define the short subreach from C to 1R is considered essential. Drastic variation of conveyance at adjacent cross-sections (which is likely to exist between sections C and 1) inherently results in unreliable estimates of friction losses. Minimizing the length of this subreach reduces the probable error in the friction-loss computations.

This model also places a constraint on the computation of flow over the road. A primary shortcoming of the road overflow algorithm in other models is that no check is made regarding physical limitations for road overflow. This model incorporates the intuitively obvious logic that only that portion

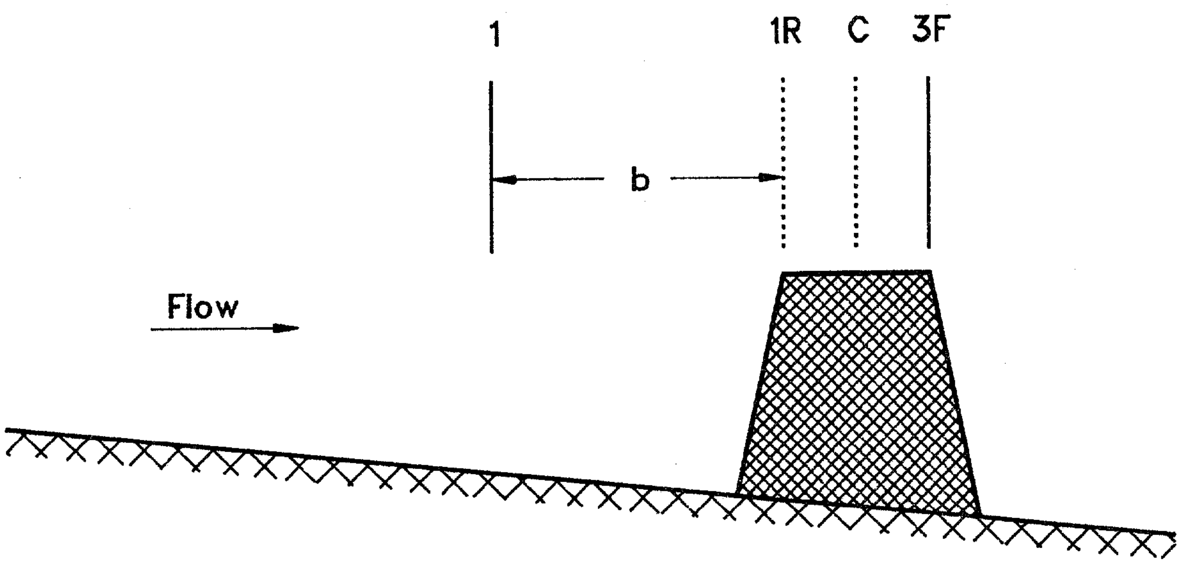

Figure 11. Cross-section locations for step-backwater computations in lieu of weir flow computations for combined flow situtations

of flow at elevations greater than the minimum embankment elevation can flow over the road. The constraint imposed limits the ratio of road overflow to total flow to the ratio of K_{mxr}/K_{tr} where K_{tr} is the total approach section conveyance at elevation h_R and K_{mxr} is the maximum conveyance that can contribute to road overflow. K_{mxr} is the conveyance of the horizontal slice of the approach section between the minimum embankment elevation and h_R. A message is printed to alert the user whenever this constraint is imposed. A user should strongly consider subsequent analysis of such cases using a composite section of the road grade and bridge opening inasmuch as there should be serious doubt as to the existence of true weir flow at such sites.

Chapter IV

MULTIPLE WATERWAY OPENING COMPUTATION THEORY

At some stream crossings, especially those across very wide flood plains, waterway openings in addition to the bridge spanning the main flow channel may be either economically and/or hydraulically justified, or both. Various combinations of culverts and/or bridges may be used. Frequently the additional openings are relatively small and are placed in swales, minor secondary channels, or simply along the flood plain, and are primarily designed to hasten low-water drainage from slack-water areas. Such openings may be ignored when analyzing water-surface profiles for the higher discharges of interest in waterway opening design. Prejudgment of the possible impact of an individual opening is often difficult. As a general rule, it is probably prudent to include "borderline" cases in initial analyses and delete them from further consideration if they have insignificant impact.

Data requirements for multiple opening situations are similar but more extensive than those for the single opening case. One of the basic assumptions in the multiple opening analysis is that the valley can be rationally divided into strips, one strip for each opening, in proportion to the distribution of discharge through the openings and across the valley. Figure 12 represents a typical situation with a centrally located main-channel opening and relief openings on both the left and right flood plains. Unconstricted valley cross sections are required at the locations indicated by D and U on figure 12, as well as immediately downstream of the openings (3F, fig. 12). Section 3F is totally analogous to the full-valley section of the single-opening case. Section D serves as the starting point for analysis of each of the individual openings with a common water-surface elevation of h_{4n} (natural profile elevation) and is referred to as the downstream match section. Section U, referred to as the upstream match section, serves as the termination point for the analysis of each individual opening. These match sections (D and U) must be located such that they satisfy the maximum

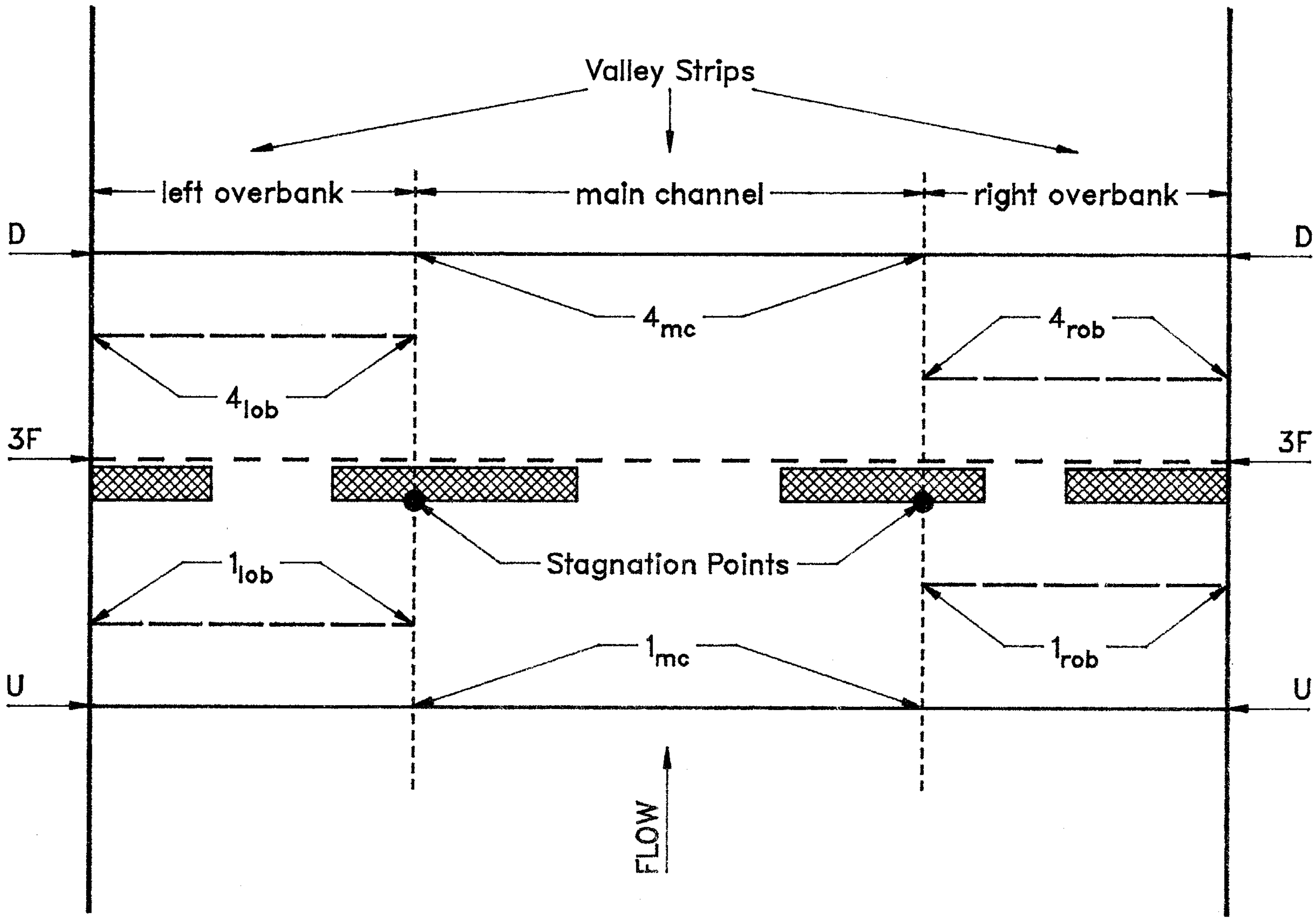

Figure 12. Sketch of typical multiple bridge opening situation illustrating valley strips and cross-section locations.

distance requirements of exit and approach section location for single-opening analysis of each individual opening. Generally, the largest bridge opening will control the location of the match sections. However, an opening with spur dikes could require a greater approach length than a larger opening without spur dikes. Also, for a skewed stream crossing, a smaller opening close to the edge of the flood plain could require an approach section further upstream or an exit section further downstream than would a more centrally located larger opening.

The unconstricted cross sections required for the analysis of each individual opening are derived from sections D, 3F, and U. The assumed valley strip for each opening defines the segments of sections D, 3F, and U that are assigned to each opening (fig. 12). The main-channel opening, in this case, will be assigned the appropriate segment of sections D and U for the exit section (4_{mc}, fig. 12) and approach section (1_{mc}, fig. 12), respectively. For bridge openings requiring an exit section upstream from the downstream match section, the model fabricates exit sections (4_{lob} and 4_{rob}, fig. 12) using the appropriate segment at the full-valley section with elevations adjusted for valley slope. For bridge openings requiring an approach section downstream from the upstream match section, the model fabricates approach sections (1_{lob} and 1_{rob}, fig. 12) using the appropriate segment of the upstream match section with elevations adjusted for valley slope. Full-valley section requirements for each valley strip are satisfied by using the appropriate segment of section 3F.

Definition of each opening is also required. Each bridge opening is described as discussed for single-opening situations; that is, with a bridge-opening section and (when necessary) a dike section. Each culvert opening must be defined in terms of its location, geometry, and hydraulic coefficients.

An approach section located immediately upstream of each culvert opening is fabricated internally using valley slope and the upstream match section. Chapter V describes the culvert hydraulics computations. A road grade section need be defined only if road overflow is possible.

The portion of the total discharge that will flow through each individual opening is dependent on both (1) relative size of each opening and (2) flow distribution in the approach reach. Laboratory investigations by Davidian and others resulted in methods for estimating the location of flow division (stagnation points) along the interior embankments between adjacent openings and for apportioning the total discharge among the individual openings.[10] These methods have been fairly well substantiated using actual field data and have been incorporated into this model.[7,13]

Stagnation points are located in direct proportion to the total flow area of adjacent openings. That is, the distance between the right edge of the left opening and the stagnation point is computed by multiplying the length of embankment between two adjacent openings by the ratio of the left opening flow area to the total flow area of both openings. Boundaries parallel to the flow extended from the stagnation points to both upstream and downstream match sections define the valley strips for each of the individual openings.

Discharge apportionment uses a channel resistance ratio, q^*, to define the flow capabilities of each valley strip. This ratio is computed by

$$q_j^* = \log\left[10\left(\frac{K_j/A_j}{K_1/A_1}\right)^{0.46}\right] \tag{49}$$

where the subscript j indicates the number of the valley strip, and the subscript 1 indicates properties for the entire upstream match section. This ratio, combined with characteristics of the opening, determines the portion of discharge, q_j, through each opening as

$$q_j = q_j^* \left[C_j A_{3j} \Big/ \sum_{j=1}^{N} (C_j A_{3j})\right] Q \tag{50}$$

where Q is the total discharge, C_j and A_{3j} are the discharge coefficient and flow area of the individual opening, N is the number of openings, and the bracketed term is the ratio of the individual opening live flow area to total live flow area at the site.

A common problem in multiple-opening situations is that the size and spacing of the openings does not conform to the conveyance (therefore discharge) distribution in the approach reach. This creates a two-dimensional flow situation with transverse flow away from the smaller openings to the larger openings. In such cases, the above procedures for discharge apportionment and separation of the valley into strips will generally result in valley strips having conveyances greatly out of proportion to the discharge apportioned to them. In an attempt to improve the results of one-dimensional analyses for such cases, this study introduces a conveyance distribution factor, CDF. Used only in the computation of friction losses, this factor essentially diverts conveyance from conveyance-rich strips into conveyance-deficient strips such that the ratio of valley strip conveyance to total conveyance is equal to the ratio of individual opening discharge to total discharge, as would be the case for one-dimensional flow. It is computed by

$$CDF_j = \frac{q_j}{Q} \left(\frac{K_1}{K_j}\right) \tag{51}$$

Each valley strip is treated either as an equivalent single-opening bridge situation by the processes described in the previous chapter or as an individual culvert analysis as outlined in the next chapter. Natural profile elevations at exit sections not located on the downstream match section are estimated by interpolation between the natural profile elevations of the downstream match section and the full-valley section. When an approach section is not located at the upstream match section, the resultant elevation at the upstream match section is determined by standard step backwater computations.

The upstream match section elevations and the associated conveyances of the individual valley strips are used to compute a conveyance-weighted average elevation at the upstream match section. This elevation is used to reestimate stagnation points and apportioned discharges. Water-surface profiles are computed using the revised valley strips and apportioned discharges. This process is repeated until both the apportioned discharges and the conveyance-weighted elevation at the upstream match section agree within acceptable tolerances on two successive trials. The final conveyance-weighted elevation is used as the basis for continuation of profile computations to additional upstream cross sections.

Chapter V

CULVERT ANALYSIS

At many bridge sites, culverts are used to carry the flow of secondary stream channels and drainage swales through the roadway embankment. These culvert openings usually are designed to pass only low-water flows and, therefore, usually have negligible effect on the overall pattern of flow and backwater at the flood flows considered in most bridge waterway analyses. In some cases, however, small bridges in submerged flow under wide roadways may become hydraulically more like culverts than like bridges. In other cases, large culverts may carry significant fractions of the total flow and may have significant effects on the backwater pattern. For the analysis of such situations, culvert computations have been included in the multiple opening analysis.

Culvert computations in this study follow the standard FHWA design procedure for conventional culverts, as described in Hydraulic Engineering Circular No. 5 (HEC-5).[23] That document contains the complete and definitive description of the culvert computation procedure. This section is provided to document the application of those procedures in this study.

In this report, culverts are considered only in the context of multiple-opening bridge situations. The general plan of the culvert computation is to compute the headwater elevation corresponding to a given discharge and given tailwater elevation for a culvert of given dimensions and material. The culvert dimensions and material are specified by the user. The tailwater elevation is the result of step-backwater computations in the reach downstream from the culvert. The portion of the total discharge that is to be conveyed by the culvert is computed by a flow-apportionment procedure described in the previous chapter. The headwater elevation is computed as explained in the following paragraphs. The water-surface elevation at the upstream match section for the culvert valley strip corresponding to the computed headwater elevation is determined by step-backwater computations.

This process is continued until the conveyance-weighted average elevation of all the valley strips meets conditions discussed in the previous chapter.

Culverts exhibit a bewildering variety of flow patterns under varying discharges and tailwater elevations. Although detailed hydraulic calculations can be used to classify these patterns, such classification is not always necessary in the context of culvert design. A simpler approach, appropriate for design use, yields essentially the same results. The wide range of flow patterns is divided into two broad flow types, inlet control and outlet control. For each type of control, the headwater elevation is computed independently, using different hydraulic principles and coefficients. The higher of these headwater elevations is adopted as the answer. This procedure "is accurate, except for a few cases where the headwater is approximately the same for both types of control."(23)

Under inlet control, the flow through the culvert is controlled by conditions at the inlet: the shape and cross-sectional area of the culvert barrel, the beveling or rounding of the inlet edge, the degree of projection of the barrel from the embankment, and the headwater depth. Barrel slope also has a minor effect on the culvert capacity. Barrel roughness and length and tailwater depth, however, have no effect on inlet-controlled flow. Inlet control typically governs when the culvert barrel is short, steep, and smooth, and when there are good getaway conditions at the outlet.

The relationships between inlet conditions and culvert capacity have been established by laboratory tests.(23) The experimental results have been summarized by mathematical formulas, as follows:

$$\frac{HW}{D} = f_e \left(\frac{Q/N}{BD^{3/2}}\right) - C_e S \qquad (52)$$

where HW is headwater depth; D is the height of one culvert barrel; B is the span or width of one culvert barrel; Q is the total discharge; N is the number of barrels; and S is the slope of the culvert barrel. The symbol f_e

represents a fifth-degree polynomial function, $f_e(x) = A + Bx + Cx^2 + Dx^3 + Ex^4 + Fx^5$, where x is the value of the parenthetical expression in equation 52 and the coefficients depend upon the entrance conditions and culvert material. C_e is a slope correction coefficient, which is a function of entrance conditions and barrel slope. The polynomial coefficients (A, B, C, D, E, and F for f_e) and slope correction coefficients used in the model were obtained from FHWA publications.[21,24]

The headwater depth in the above equation, strictly speaking, is the distance between the energy grade line and the inlet invert. That is, it includes the contribution of velocity head at the headwater section. In culvert design practice, however, the velocity head usually is such a small component of the total head that separating velocity head from the total head is not justified. Thus, the headwater usually is assumed to be ponded with zero velocity head, and the headwater depth computed from the inlet-control equation is taken as the height of the water surface above the inlet invert. This practice is followed in this model.

Before performing the outlet-control calculations, it is convenient to perform one simple check on the state of the flow in the culvert: if the normal depth of flow is less than the critical depth, then inlet control governs, and there is no need to do the outlet-control calculations. The normal depth, d_n, is found using the following form of the Manning equation:

$$\frac{n\ (Q/N)}{1.49\ S^{1/2}} = AR^{2/3} \qquad (53)$$

where R is the hydraulic radius and the remaining terms are as previously defined. The depth that satisfies equation 53 is found by trial and error and is the normal depth.

The critical depth in the culvert barrel, d_c, is characterized by the condition that the velocity head equals half the mean depth. This condition can be expressed by:

$$\frac{\alpha\,(Q/N)^2}{g} = \frac{A^3}{T} \tag{54}$$

where T is the top width of flow of one culvert barrel; α is the velocity-head coefficient, tabulated for specified barrel shape and material; and the other terms are as previously defined. The depth that satisfies equation 54 can be found by trial and error and is the critical depth. Note that, because the top width goes to zero as the depth approaches the height of the culvert barrel, D, this equation always will have a solution with d_c less than D.

Under outlet control, the flow through the culvert is controlled by conditions in the culvert barrel and at the outlet, as well as by conditions at the inlet. Thus, barrel roughness, length, and slope, and headwater and tailwater elevations become the primary determinants of the flow through the culvert. Outlet control typically governs long, flat, rough-barreled culverts with high tailwater and obstructed getaway conditions at the outlet.

Under the usual conditions of culvert design, the outlet-controlled culvert barrel flows full or nearly full most or all of its length. Under these conditions, outlet-controlled flow is analyzed by means of the energy equation, as follows:

$$HW + S(L) = h_o + h_v + h_f + h_e \tag{55}$$

where HW is the headwater depth; S is the slope of the culvert barrel; L is the length of the culvert barrel; h_o is the effective tailwater depth; h_v is the velocity head in the culvert barrel at the outlet; h_f is the friction loss in the culvert barrel; and h_e is the entrance loss. In this equation, as in the inlet-control equation, the velocity head has been neglected at the headwater section.

The effective tailwater depth, h_o, is taken as the maximum of the actual tailwater depth, TW, or the depth halfway between critical depth and the top of the barrel, $(d_c + D)/2$. The last three terms on the right-hand side of the energy equation are easy to evaluate when the culvert barrel is flowing completely full. Then the cross-sectional area and, hence, the velocity, is known, and the following formulas may be evaluated directly:

$$V = Q/NA \tag{56}$$

$$h_v = V^2/2g \tag{57}$$

$$h_e = k_e V^2/2g \tag{58}$$

$$h_f = L \left[\frac{n\ V}{1.49\ (R)^{2/3}} \right]^2 \tag{59}$$

where V is the mean velocity for full flow in culvert barrel; k_e is the entrance-loss coefficient, dependent upon entrance conditions; and other symbols are as previously defined. These formulas are considered sufficiently accurate as long as the culvert barrel does flow full for at least part of its length.

The full-flow condition is checked by computing the hydraulic grade line (HGL) and noting whether it intersects the top of the culvert barrel. The height of the HGL at the inlet is HGL = $h_o + h_f$, and the height of the top of the barrel at the inlet is S(L) + D. Both of these heights are measured relative to the outlet invert. Thus, the test for full flow is

$$h_f > S(L) + D - h_o \tag{60}$$

where all symbols are as previously defined. If this condition is not satisfied, backwater calculations have to be used to define the water-surface profile through the culvert barrel. Supercritical flow need not be considered because the inlet will control when supercritical flow occurs in the barrel.

Backwater calculations in prismatic channels such as culvert barrels are conveniently performed by the direct step method.[4] In this method, the energy equation is written in the form

$$d_1 + S(X_1) + \alpha \frac{V_1^2}{2g} = d_o + \alpha \frac{V_o^2}{2g} + S_f X_1 \tag{61}$$

where d_i is the flow depth at section i; V_i is the mean velocity at section i; S_f is the average friction slope between sections o and 1, computed as explained below; X_1 is the distance in feet from downstream section o to upstream section 1; and the other symbols are as previously defined. Starting with known conditions at section o, a direct solution for conditions at section 1 is made possible by defining section 1 to be the upstream point at which a specified depth d_1 occurs. This technique is feasible only in prismatic channels, where the cross-sectional geometry does not vary longitudinally. For given values of d_o and d_1, the cross-sectional geometry can be computed and thus, for given discharge, the following direct solution for X_1 can be computed:

$$X_1 = \frac{(d_o + \alpha V_o^2/2g) - (d_1 + \alpha V_1^2/2g)}{(S - S_f)} \tag{62}$$

in which S_f is computed from the Manning formula using averaged cross sectional properties, as follows:

$$S_f = \left[\frac{n V}{1.49 R^{2/3}}\right]^2 \tag{63}$$

where

$$V = (V_o + V_1)/2 \tag{64}$$

and R, the mean hydraulic radius is computed by

$$R = (A_o/P_o + A_1/P_1)/2 \tag{65}$$

where A_i and P_i are cross-sectional flow areas and wetted perimeters at depth d_i at section i (i = o,1). The profile is advanced through the culvert barrel by choosing an appropriate value for the upstream depth, d_1, for the next step. The depth is decremented if the current depth is greater than the normal depth; otherwise, it is incremented. When the upstream end of the culvert is reached, the entrance loss, $k_e V^2/2g$, described above, is added to the computed depth to yield the headwater depth.

The final step in the culvert analysis is to compare the headwater elevations obtained from inlet-control and outlet-control calculations. The higher headwater elevation is adopted.

The hydraulic calculations just described require specification of the cross-sectional geometry and hydraulic properties of the culvert barrel. The properties of box culverts, circular pipes, and pipe arches are described in detail in FHWA publications.[21,24] The tables of pipe-arch dimensions have been summarized by linear regression formulas that express the top, bottom, and corner radii in terms of the culvert height, span, and material.[21] These formulas have been incorporated into the culvert routines.

Chapter VI

MODEL COMPARISONS AND RESULTS

The primary purpose of this chapter is to compare water-surface profiles computed using WSPRO to known water-surface profiles at several existing bridge sites. In addition, this chapter (1) briefly summarizes the findings of FHWA's assessment of existing computer models and bridge-backwater computational procedures and (2) provides a very limited comparison of results obtained from WSPRO, HEC-2, and E431.

After assessing existing computer models, FHWA recognized the need for a comprehensive, design-oriented model that could readily be applied in conjunction with current policy. Each of the existing models had some good features but also had limitations that restricted applicability for current policies.

FHWA's methodology for bridge backwater analyses can be used for manual solutions.(3) The results are generally adequate in the absence of complexities in physical setting and/or flow conditions. Variations in flow conditions for various bridge geometries are accounted for in the bridge loss coefficients. Major problems arise in the solutions for more complex (nonstandard) conditions. Total losses are based on a K* coefficient which, as derived, includes friction losses. Thus, total computed losses may not reflect actual total losses for nonstandard flow conditions. Also, there is an assumed relationship between the velocity head correction factors for the bridge opening, α_2, and the approach section, α_1. The value of α_2 sometimes becomes very large, thus becoming the predominant factor, and produces questionable computed results.

FHWA's HY-4 is a computer model incorporating part of the above methodology.(25) The program is design oriented in that it is easy to run, it can analyze several bridge lengths with a single job submission, it does not require extensive data coding, and it has convenient output format. HY-4, however, is limited to subcritical free flow through bridge openings, and it cannot handle road overflow which is an important consideration in any rational analysis of the impact of encroachments on the flood plain. The same shortcomings in loss coefficients are present in the computer model.

USGS's E431 is a computer model which uses a modification of the FHWA methodology for bridge backwater computations.[19] The α_2 problem was eliminated by assuming that using a value of 1.0 for α_2 was at least as good as using the assumed relation between α_2 and α_1. However, the friction-loss problem (related to K*) still exists. E431 does have the capability to analyze combined flow (overtopping of embankment). However, the road overflow algorithm seems to overestimate the weir flow, especially when the embankments are relatively low. E431 input and output are not geared to analysis of several alternative designs. Significant recoding of data may be required for each alternative design, and to obtain the pertinent results the user must search through a quite detailed (sometimes voluminous) set of output data. The input/output formats are such that the infrequent user may find it necessary to frequently consult the user's manual.

The USGS also uses techniques reported by Cragwall to compute bridge backwater.[8] The USGS contracted opening method forms the basis for the procedure.[15] This method has been partially computerized, but not formally documented (Vernon Sauer, USGS, personal communication). Successive manual computations of the coefficient of discharge are required for a complete solution.

Schneider et al., in an extensive study of backwater and discharge computations at constrictions of wide, heavily-vegetated flood plains, developed a computational procedure quite superior to the FHWA and USGS procedures.[18] Although basically a one-dimensional flow analysis, it introduces a degree of two-dimensionality by estimating an effective flow length upstream of the bridge which provides improved estimates of friction losses.

HEC-2 is undoubtedly the most widely used computer model for water-surface profile computations.[20] Its bridge routines, however, are judged by FHWA to be deficient for design purposes. They do not reflect any differences due to various bridge geometry (except for piers), and the coefficients do not reflect more recent research, such as that done by Liu and others.[14] Output is relatively convenient for risk analysis in that the user may select output variables. Significant input recoding is required for alternative designs.

The above findings led to the decision to develop a new model with improved computational methods and input/output schemes that better serve the requirements of FHWA design policy. Therefore, FHWA initiated a contract with the USGS for development of such a model. This model would: (1) be compatible with conventional step-backwater analyses; (2) be design oriented; (3) incorporate the latest bridge backwater computational methods; (4) more adequately analyze combined road overflow and bridge flow; (5) provide a state-of-the-art procedure for multiple-opening analyses; and (6) provide selective output capabilities suited to risk analysis procedures.

The USGS has published a series of Hydrologic Investigation Atlases documenting data from actual flood events at bridges in Alabama, Louisiana, and Mississippi. These reports reflect results of studies performed in cooperation with FHWA and the respective States. Data available includes: (1) flood discharge; (2) water-surface profile based on recovered high-water marks; (3) geometry of the bridge and geometry of the valley for a significant distance both upstream and downstream of the bridge; and (4) roughness coefficients determined by water-surface profile computations.

Data from five of these reports were prepared for analysis by WSPRO, E431, and HEC-2.[1,5,6,16,17] At one of the bridge sites (Poley Creek) data are available for two different flood events, thus making six analyses possible. Tables 2 through 7 (at the end of this chapter) are tabulations of the computed results versus observed flood profiles with the resultant differences. Figures 13 through 17 (at the end of this chapter) are plots of the observed and computed water-surface profiles.

The primary objective of these analyses was to determine how well WSPRO could reproduce the observed water-surface profiles. Results for Buckhorn Creek and Cypress Creek are very acceptable with maximum errors of 0.3 feet (tables 2 and 3; figures 13 and 14). Slightly larger maximum errors of 0.4 and 0.6 feet for the higher and lower discharges were obtained on Poley Creek (tables 6 and 7; figure 17). The two Okatoma Creek sites produced the least satisfactory results. The "near Magee" site produced very poor results downstream from the bridge (table 4; figure 15). The geometry as used in the model may incorrectly reflect the effective flow area, and/or, as suggested by the high-water marks, a one-dimensional flow model is not truly applicable in that reach. The maximum error of 0.7 feet for the "East of Magee" site may not be as bad as it appears (table 5; figure 16). There were no high-water marks immediately upstream from the bridge, and those a few hundred feet upstream had considerable scatter (on the order of 0.3 feet). All of these sites exhibited some degree of nonstandard bridge geometry. They also provided significant flow constriction, thus placing some stress on the applicability of one-dimensional flow models. Therefore, although limited in number, these analyses would indicate that WSPRO is a credible model for bridge waterways analyses.

The objective of comparing WSPRO results to results of E431 and HEC-2 was limited to determining only the differences in the water-surface profile computations through bridges. This required some limitations of features used in each model and some tailoring of certain data. The published roughness coefficients generally indicated roughness changing with depth. Since HEC-2 cannot use vertical and horizontal variation of roughness simultaneously, and horizontal variation was considered more important, the vertical variation of roughness feature of E431 and WSPRO was not used. New roughness coefficients for use in this study were obtained by calibrating the models using the portions of water-surface profiles far enough downstream and upstream of the bridge that they could be considered out of the nonuniform flow zones near the bridge. E431 does not accommodate variable flow lengths between sections. However, since this was a very desirable feature for most of these sites, variable flow lengths were used in WSPRO and HEC-2. Section reference distances for E431 were then tailored to reflect the weighted flow distances of the other two models. All models used geometric mean conveyance in computing friction losses. The selection of expansion and contraction coefficients created no problem because of very low velocity heads. Only the surveyed cross sections were used, although some were shifted upstream or downstream in the vicinity of the bridge to meet model requirements. No attempt was made to provide fabricated or interpolated geometry, even when model results and/or error messages suggested that additional data should be used. Spacing and effective area of cross sections in the vicinity of the bridge for HEC-2 analyses were based on the recommended standard expansion and contraction ratios.[20]

Although the number of analyses is very limited, some conclusions seem apparent. E431 rather grossly underestimates upstream water-surface elevations except for Okatoma Creek East of Magee. This problem is directly linked to friction losses being included in the loss coefficient. At these sites, friction losses are a very significant component of the total losses, except for the Okatoma "East" site. The relations used to compute K* are based on more "average" flow situations thereby not accounting for the above "average" friction losses that occur at these sites. HEC-2 and WSPRO results are quite comparable for the entire profile for Cypress Creek. For Buckhorn Creek, Okatoma Creek "near", and the low discharge on Poley Creek, the results are quite comparable at and upstream from the approach section (one bridge length upstream from the bridge). However, in the immediate vicinity of the bridge some of the HEC-2 differences are quite large (e.g., Buckhorn Creek). Thus, even though the upstream results are quite adequate, HEC-2 does not reproduce the observed profile in the vicinity of the bridge very well. It would appear that although the total losses computed by HEC-2 are reasonable, they are not distributed correctly. For Okatoma Creek "East" and the higher discharge on Poley Creek, the errors in the vicinity of the bridge are large enough to carry on upstream somewhat further. Perhaps if additional sections had been used in some of these analyses, the results would have been improved somewhat. Overall, WSPRO appears to give better results and tends to more completely define the profile because of the location of the cross sections used in the model.

Table 2. Observed and computed water-surface elevations for Buckhorn Creek near Shiloh, Alabama

STUDY SITE: Buckhorn Creek near Shiloh, Alabama   DISCHARGE: 4,150 cfs

DATA SOURCE: Ming, Colson, and Arcement (1979)

		COMPUTED RESULTS FROM							
	KNOWN	- HEC2 (N) -		- HEC2 (S) -		--- E431 ---		-- WSPRO ---	
DISTANCE	WSEL	WSEL	ERROR	WSEL	ERROR	WSEL	ERROR	WSEL	ERROR
0	316.0	316.0	0.0	316.0	0.0	316.0	0.0	316.0	0.0
1025	317.5	317.5	0.0	317.5	0.0	317.5	0.0	317.5	0.0
2340	319.0	319.2	+0.2	319.2	+0.2	319.2	+0.2	319.2	+0.2
3030	320.0	320.4	+0.4	320.4	+0.4	320.0	0.0	320.0	0.0
3380	320.5	321.2	+0.7	321.2	+0.7	320.4	-0.1	- -	- -
3445	- -	- -	- -	- -	- -	- -	- -	320.5	(-0.1)
3710	320.8	322.1	+1.3	- -	- -	320.8	0.0	320.8	0.0
[3710]	- -	322.1	- -	322.1	- -	320.8	- -	321.1	- -
[3750]	- -	322.5	- -	322.1	- -	- -	- -	- -	- -
3750	321.6	322.6	+1.0	- -	- -	- -	- -	- -	- -
3940	321.9	322.9	+1.0	322.5	+0.6	- -	- -	- -	- -
*4005	- -	- -	- -	- -	- -	321.3	(-0.7)	322.3	(+0.3)
4990	323.1	323.6	+0.5	323.3	+0.2	322.6	-0.5	323.1	0.0
6240	324.1	324.3	+0.2	324.1	0.0	323.6	-0.5	323.9	-0.2
7400	324.6	324.9	+0.3	324.8	+0.2	324.6	0.0	324.8	+0.2

NOTES:
1) Dashed entries indicate no information available.
2) Error values in parentheses estimated by interpolation.
3) For HEC-2, (N) and (S) indicate normal and special bridge routine, respectively.
4) Bridge-opening sections indicated by brackets; adjacent sections reflect elevations at edge of flooded area.
5) One bridge length upstream from bridge indicated by asterisk (*).

Table 3. Observed and computed water-surface elevations for Cypress Creek near Downsville, Louisiana

STUDY SITE: Cypress Creek near Downsville, Louisiana DISCHARGE: 1,500 cfs

DATA SOURCE: Arcement, Colson, and Ming (1979)

		COMPUTED RESULTS FROM							
	KNOWN	- HEC2 (N) -		- HEC2 (S) -		--- E431 ---		-- WSPRO ---	
DISTANCE	WSEL	WSEL	ERROR	WSEL	ERROR	WSEL	ERROR	WSEL	ERROR
0	112.3	112.3	0.0	112.3	0.0	112.3	0.0	112.3	0.0
1050	112.8	112.8	0.0	112.8	0.0	112.8	0.0	112.8	0.0
1650	113.4	113.4	0.0	113.3	0.0	113.4	0.0	113.4	0.0
2260	114.7	- -	- -	- -	- -	- -	- -	- -	- -
2275	- -	- -	- -	- -	- -	114.6	(-0.1)	114.6	(-0.1)
2390	114.8	115.1	+0.3	- -	- -	114.7	-0.1	114.7	-0.1
[2390]	- -	115.1	- -	115.1	- -	114.7	- -	114.8	- -
[2430]	- -	115.3	- -	115.1	- -	- -	- -	- -	- -
2430	116.0	115.4	-0.6	- -	- -	- -	- -	- -	- -
2520	116.1	- -	- -	- -	- -	- -	- -	- -	- -
*2545	- -	- -	- -	- -	- -	115.2	(-0.9)	115.8	(-0.3)
2890	116.2	116.1	-0.1	115.9	-0.3	115.5	-0.7	116.0	-0.2
3525	116.7	116.5	-0.2	116.4	-0.3	116.2	-0.5	116.5	-0.2
4125	117.2	117.2	0.0	117.1	-0.1	117.1	-0.1	117.2	0.0
4660	119.0	118.9	-0.1	118.9	-0.1	119.0	0.0	119.0	0.0

NOTES:
1) Dashed entries indicate no information available.
2) Error values in parentheses estimated by interpolation.
3) For HEC-2, (N) and (S) indicate normal and special bridge routine, respectively.
4) Bridge-opening sections indicated by brackets; adjacent sections reflect elevations at edge of flooded area.
5) One bridge length upstream from bridge indicated by asterisk (*).

Table 4. Observed and computed water-surface elevations for Okatoma Creek near Magee, Mississippi

STUDY SITE: Okatoma Creek near Magee, Mississippi DISCHARGE: 16,100 cfs

DATA SOURCE: Colson, Ming, and Arcement (1978)

		COMPUTED RESULTS FROM							
	KNOWN	- HEC2 (N) -		- HEC2 (S) -		--- E431 ---		-- WSPRO ---	
DISTANCE	WSEL	WSEL	ERROR	WSEL	ERROR	WSEL	ERROR	WSEL	ERROR
0	355.7	355.7	0.0	355.7	0.0	355.7	0.0	355.7	0.0
2175	358.3	357.9	-0.4	357.9	-0.4	358.1	-0.2	358.1	-0.2
5240	360.0	360.0	0.0	360.0	0.0	360.1	+0.1	360.1	+0.1
6930	363.0	361.9	-1.1	361.9	-1.1	361.5	-1.5	361.5	-1.5
7700	363.7	363.7	0.0	363.7	0.0	362.5	-1.2	362.5	-1.2
8225	- -	- -	- -	- -	- -	- -	- -	363.1	(-0.7)
8445	363.8	365.9	+2.1	- -	- -	363.4	-0.4	363.4	-0.4
[8445]	365.3	365.8	+0.5	365.9	+0.6	363.4	-1.9	363.6	-1.7
[8485]	- -	366.1	- -	366.0	- -	- -	- -	- -	- -
8485	- -	366.5	- -	- -	- -	- -	- -	- -	- -
8630	367.2	- -	- -	- -	- -	- -	- -	- -	- -
*8705	- -	- -	- -	- -	- -	366.3	(-0.9)	367.2	(0.0)
9300	367.4	367.7	+0.3	367.3	-0.1	366.5	-0.9	367.3	-0.1
10700	367.8	367.9	+0.1	367.6	-0.2	366.9	-0.9	367.6	-0.2
12025	368.2	368.3	+0.1	368.1	-0.1	367.6	-0.6	368.1	-0.1
13400	368.8	368.8	0.0	368.7	-0.1	368.3	-0.5	368.7	-0.1

NOTES:
1) Dashed entries indicate no information available.
2) Error values in parentheses estimated by interpolation.
3) For HEC-2, (N) and (S) indicate normal and special bridge routine, respectively.
4) Bridge-opening sections indicated by brackets; adjacent sections reflect elevations at edge of flooded area.
5) One bridge length upstream from bridge indicated by asterisk (*).

Table 5. Observed and computed water-surface elevations for Okatoma Creek east of Magee, Mississippi

STUDY SITE: Okatoma Creek east of Magee, Mississippi DISCHARGE: 12,100 cfs

DATA SOURCE: Colson, Arcement, and Ming (1978)

		COMPUTED RESULTS FROM							
	KNOWN	- HEC2 (N) -		- HEC2 (S) -		--- E431 ---		-- WSPRO ---	
DISTANCE	WSEL	WSEL	ERROR	WSEL	ERROR	WSEL	ERROR	WSEL	ERROR
13400	368.8	368.8	0.0	368.8	0.0	368.8	0.0	368.8	0.0
15450	369.2	369.4	+0.2	369.4	+0.2	369.3	+0.1	369.2	0.0
17115	369.5	370.8	+1.3	370.8	+1.3	369.9	+0.4	369.8	+0.3
17465	- -	- -	- -	- -	- -	- -	- -	370.1	(+0.3)
17625	370.0	372.1	+2.1	- -	- -	370.2	+0.2	370.2	+0.2
[17625]	- -	372.3	- -	372.1	- -	370.2	- -	369.8	- -
[17645]	- -	372.4	- -	372.6	- -	- -	- -	- -	- -
17645	- -	372.4	- -	- -	- -	- -	- -	- -	- -
17765	371.9	- -	- -	- -	- -	- -	- -	- -	- -
*17805	- -	- -	- -	- -	- -	372.7	(+0.8)	372.6	(+0.7)
18175	372.0	374.1	+2.1	374.2	+2.2	372.8	+0.8	372.7	+0.7
19190	372.3	374.2	+1.9	374.3	+2.0	373.0	+0.7	372.9	+0.6
21040	373.7	374.8	+1.1	374.9	+1.2	374.0	+0.3	373.9	+0.2
22090	375.7	375.9	+0.2	375.9	+0.2	375.6	-0.1	375.6	-0.1
23730	377.4	378.1	+0.7	378.1	+0.7	378.1	+0.7	378.0	+0.6

NOTES:
1) Dashed entries indicate no information available.
2) Error values in parentheses estimated by interpolation.
3) For HEC-2, (N) and (S) indicate normal and special bridge routine, respectively.
4) Bridge-opening sections indicated by brackets; adjacent sections reflect elevations at edge of flooded area.
5) One bridge length upstream from bridge indicated by asterisk (*).

Table 6. Observed and computed water-surface elevations for 1,900 cfs for Poley Creek near Sanford, Alabama

STUDY SITE: Poley Creek near Sanford, Alabama DISCHARGE: 1,900 cfs

DATA SOURCE: Ming, Colson, and Arcement (1978)

		COMPUTED RESULTS FROM							
	KNOWN	- HEC2 (N) -		- HEC2 (S) -		--- E431 ---		-- WSPRO ---	
DISTANCE	WSEL	WSEL	ERROR	WSEL	ERROR	WSEL	ERROR	WSEL	ERROR
0	230.2	230.2	0.0	230.2	0.0	230.2	0.0	230.2	0.0
1120	231.2	231.3	+0.1	231.3	+0.1	231.2	0.0	231.2	0.0
1650	232.3	232.8	+0.5	232.8	+0.5	232.3	0.0	232.3	0.0
1980	232.9	234.0	+1.1	234.0	+1.1	233.3	+0.4	- -	- -
1990	- -	- -	- -	- -	- -	- -	- -	233.3	(+0.4)
2190	233.2	234.7	+1.5	- -	- -	233.8	+0.6	233.8	+0.6
[2190]	- -	234.8	- -	234.7	- -	233.8	- -	234.2	- -
[2220]	- -	234.9	- -	234.8	- -	- -	- -	- -	- -
2220	234.6	234.9	+0.3	- -	- -	- -	- -	- -	- -
*2420	- -	- -	- -	- -	- -	234.4	(-0.4)	235.0	(+0.2)
2480	234.8	235.3	+0.5	235.2	+0.4	- -	- -	- -	- -
3500	235.6	235.8	+0.2	235.9	+0.3	235.5	-0.1	235.7	+0.1
4340	236.6	236.9	+0.3	236.9	+0.3	236.8	+0.2	236.8	+0.2

NOTES:
1) Dashed entries indicate no information available.
2) Error values in parentheses estimated by interpolation.
3) For HEC-2, (N) and (S) indicate normal and special bridge routine, respectively.
4) Bridge-opening sections indicated by brackets; adjacent sections reflect elevations at edge of flooded area.
5) One bridge length upstream from bridge indicated by asterisk (*).

Table 7. Observed and computed water-surface elevations for 4,600 cfs for Poley Creek near Sanford, Alabama

STUDY SITE: Poley Creek near Sanford, Alabama DISCHARGE: 4,600 cfs

DATA SOURCE: Ming, Colson, and Arcement (1978)

		COMPUTED RESULTS FROM							
	KNOWN	- HEC2 (N) -		- HEC2 (S) -		--- E431 ---		-- WSPRO ---	
DISTANCE	WSEL	WSEL	ERROR	WSEL	ERROR	WSEL	ERROR	WSEL	ERROR
0	232.2	232.2	0.0	232.2	0.0	232.2	0.0	232.2	0.0
1120	233.3	233.5	+0.2	233.5	+0.2	233.3	0.0	233.3	0.0
1650	234.4	234.8	+0.4	234.8	+0.4	234.1	-0.3	234.1	-0.3
1980	234.9	236.2	+1.3	236.2	+1.3	- -	- -	- -	- -
1990	- -	- -	- -	- -	- -	235.0	(+0.1)	235.0	(+0.1)
2190	235.3	237.4	+2.1	- -	- -	235.5	+0.2	235.5	+0.2
[2190]	- -	237.4	- -	237.4	- -	235.5	- -	236.1	- -
[2220]	- -	237.7	- -	237.4	- -	- -	- -	- -	- -
2220	237.0	237.8	+0.8	- -	- -	- -	- -	- -	- -
*2420	- -	- -	- -	- -	- -	236.6	(-0.6)	237.6	(+0.4)
2480	237.2	238.3	+1.1	238.1	+0.9	- -	- -	- -	- -
3500	238.0	238.7	+0.7	238.8	+0.8	237.7	-0.3	238.3	+0.3
4340	239.0	239.4	+0.4	239.5	+0.5	238.9	-0.1	239.2	+0.2

NOTES:
1) Dashed entries indicate no information available.
2) Error values in parentheses estimated by interpolation.
3) For HEC-2, (N) and (S) indicate normal and special bridge routine, respectively.
4) Bridge-opening sections indicated by brackets; adjacent sections reflect elevations at edge of flooded area.
5) One bridge length upstream from bridge indicated by asterisk (*).

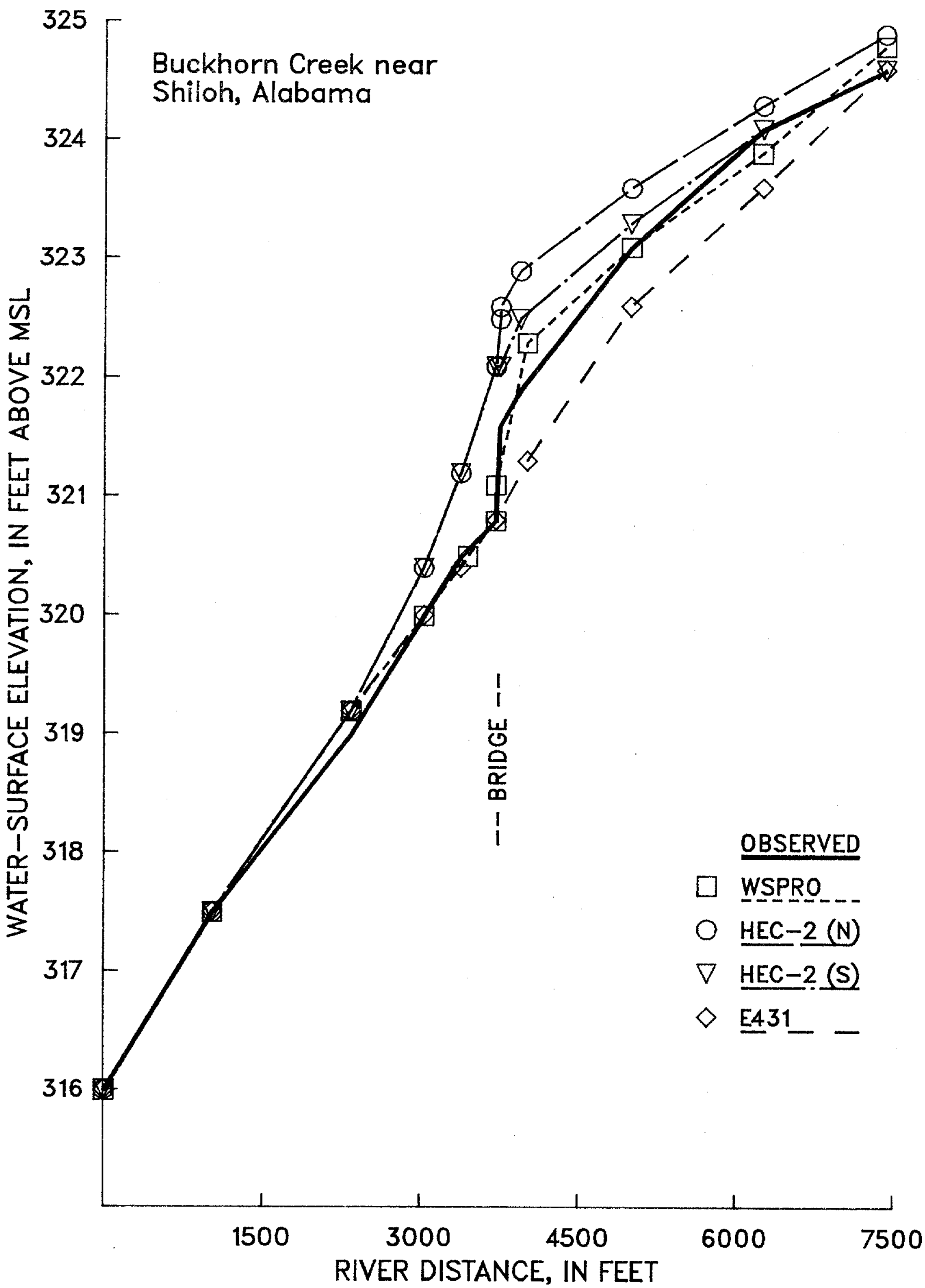

Figure 13. Water-surface profiles for Buckhorn Creek near Shiloh, Alabama.

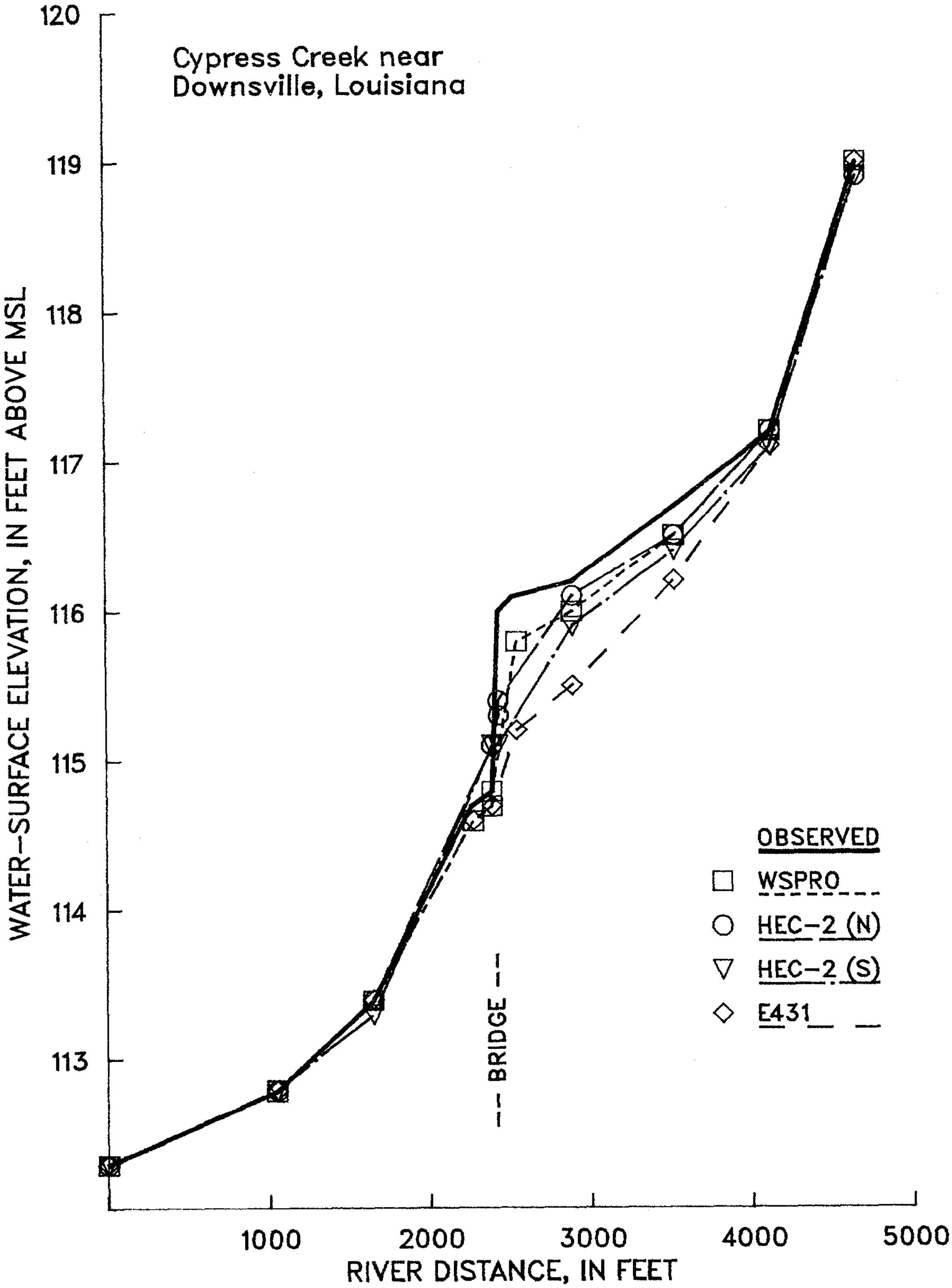

Figure 14. Water-surface profiles for Cypress Creek near Downsville, Louisiana.

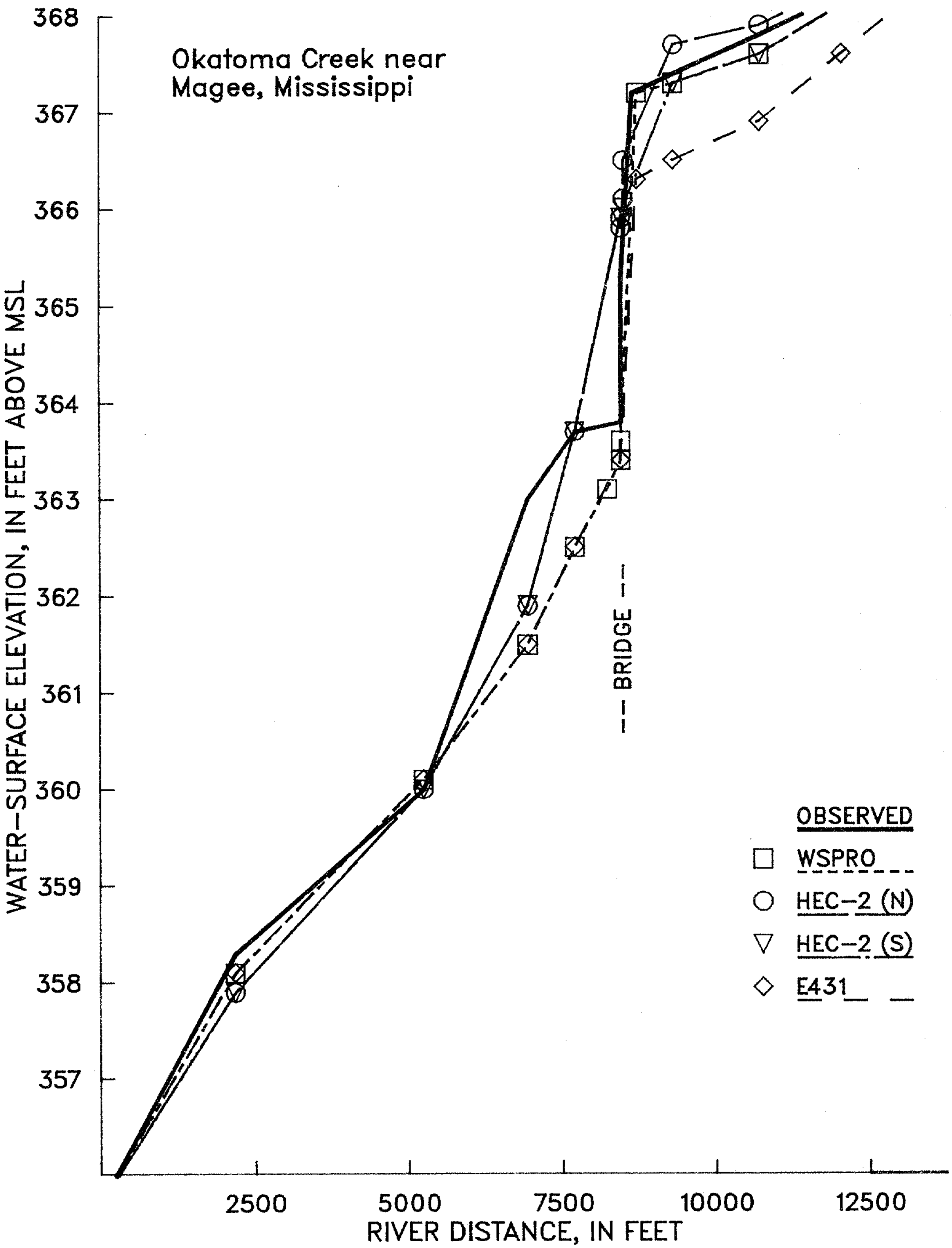

Figure 15. Water-surface profiles for Okatoma Creek near Magee, Mississippi.

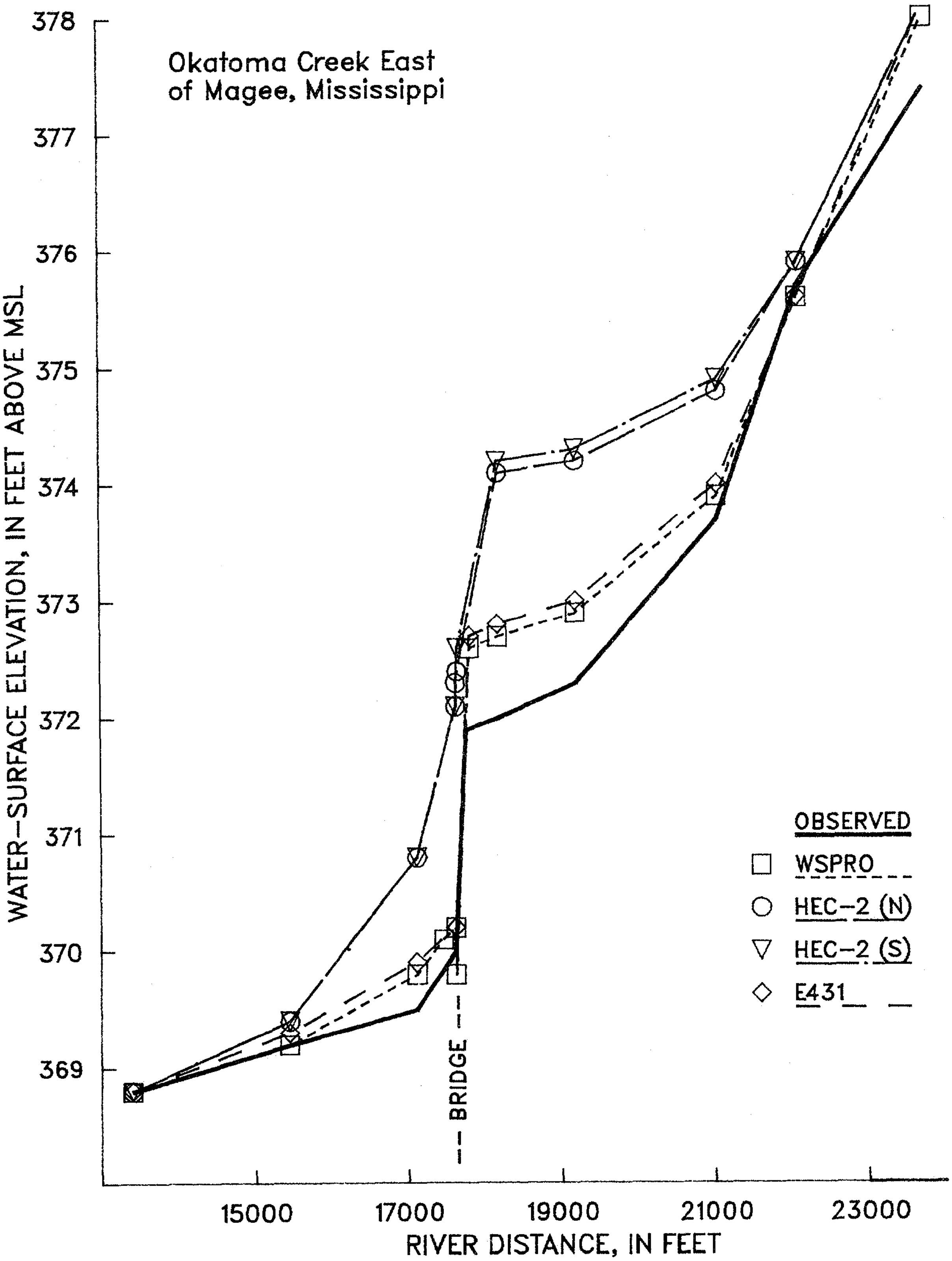

Figure 16. Water-surface profiles for Okatoma Creek East of Magee, Mississippi.

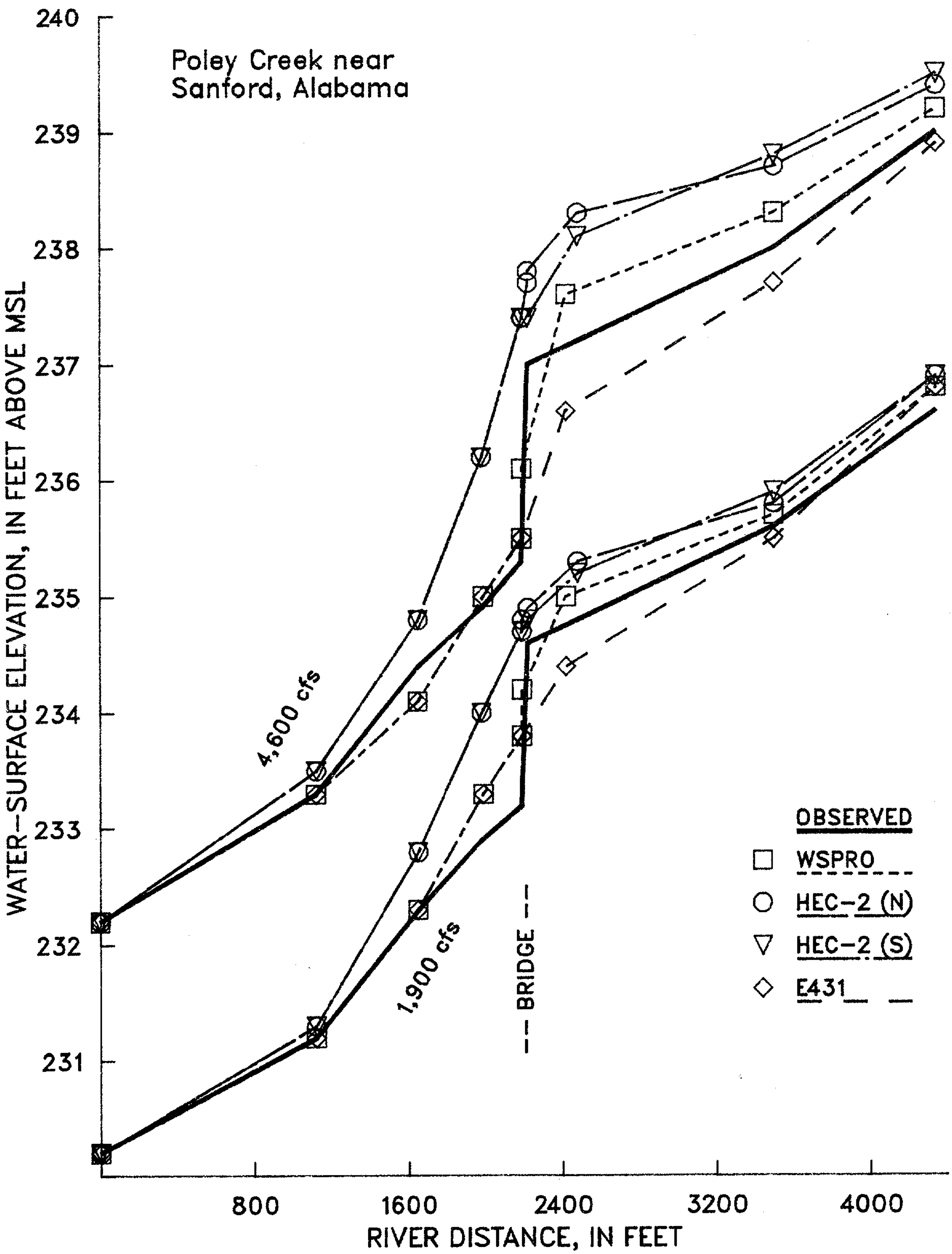

Figure 17. Water-surface profiles for Poley Creek near Sanford, Alabama.

Chapter VII

APPLICABILITY TO RISK ANALYSIS

Risk analysis is a key component in selecting bridges and culverts that have the least total economic cost (LTEC) to society. FHWA has promoted LTEC design through an engineering circular and a series of workshops.[22] FHWA considers LTEC design as not only a logical approach to implementing Executive Order 11988 "Floodplain Management," but also as a rational approach to design of hydraulic structures for highways since it leads to the best expenditure of public funds without penalizing one sector of society for the benefit of others.

LTEC design balances the economics of various factors including: construction costs, traffic losses, highway facility damages, and upstream property damages attributed to backwater. These are four primary cost factors that are common to most sites. Except for construction costs, complete evaluation of each of these factors depends to a varying degree upon bridge-backwater computations.

Traffic losses occur when the crossing itself is impassable due to flooding. Highway facility damages are those damages due to scour within the bridge opening and damage to embankments and pavement surfaces subjected to overtopping during floods. When these damages are substantial, they, in turn, add to the interruption of traffic while repairs are being made. To estimate these damages, one needs to know flow velocity through the bridge opening, depth and velocity over the roadway, length of roadway that is inundated, and duration of inundation.

Construction of bridges and culverts on flood plains most often involves constriction of the natural floodway. This constriction results in a increased water-surface elevation (backwater) upstream which may cause incremental flood damage to property adjacent to the crossing. The highway agency should not be held responsible for flood damage incurred under normal flow conditions before the bridge, embankment, or culvert is in place, regardless of flood magnitude. The highway agency is responsible, however, for the additional (incremental) flood damage which results from backwater associated with the construction of a stream crossing. Incremental flood damage, typically, increases with flood magnitude until overtopping of the roadway occurs. Subsequent to overtopping, incremental flood damages still increase but at a slower rate due to the rapidly increasing flow potential past the constriction with rising stage.

Backwater damages are of two types; namely, those associated with structures on the flood plain and those associated with marginal areas that can no longer be developed because of zoning statutes or no longer be cropped as effectively because the frequency of inundation changes. Damages associated with development potential and crop yields are somewhat related to the lateral extent of flooding on the flood plain. To assess backwater damages, one must compute water-surface profiles and associated damages for normal or natural conditions without the stream crossing and subtract damages under these conditions from the damages associated with the stream crossing in place.

A flexible water-surface profile computation model is a valuable tool for the above analyses. Risks are computed by weighting damages from discrete flood discharges by the probability of occurrence and integrating these damages for enough discharges to adequately represent the full flood-frequency curve. Typically, eight to ten water-surface profiles may be computed for each stream crossing alternative being considered. One important aspect of the WSPRO model is that many of the data needed for risk analyses are stored in machine-readable files and can be readily tabulated for further computations. Some examples of such data are water-surface elevations at each cross section (with and without the stream crossing), left and right edge of water on the flood plain, depths and velocities over the roadway, horizontal limits of inundation of the roadway, and velocities through the bridge opening.

WSPRO is specifically designed to facilitate computation of hydraulic data required to estimate the costs associated with the above damages. One very logical approach to applying the model is to consider the water-surface profile computations being comprised of three separate phases, as discussed below. While other approaches are possible (and maybe sometimes a necessity) the model was tailored to fit this approach. This approach is quite efficient as it eliminates redundant water-surface profile computations and repetitive damage calculations. The phases are: (1) developing rating curves (stage-discharge relations) at the exit and approach cross sections for unconstricted (no bridge) flow conditions; (2) computing water-surface profiles upstream of the bridge for determining incremental flood damages attributable to bridge backwater; and (3) computing water-surface profiles through the bridge for the design alternatives. Factors that may alter this sequence are pointed out in the following discussions of each of these phases.

Rating curves at the exit and approach cross sections provide starting water-surface elevations for the subsequent phases. Thus, they should be developed for the entire range of applicable discharges and in sufficient detail to provide a reliable estimate of elevation (discharge) for any discharge (elevation). Available flow data (from gaging stations and/or historical flood information) in the immediate vicinity of the bridge site may eliminate (or drastically reduce) the need for water-surface profile computations downstream of the bridge. Also, if flow conditions are such that reliable estimates of rating curves can be obtained by alternative methods (e.g., slope-conveyance techniques) such methods should be applied because they are less time-consuming and much cheaper. Unfortunately, lack of resources (e.g., time and/or money) may preclude the data acquisition and thorough analyses required to develop highly reliable rating curves, thereby forcing application of alternative methods. Generally, there will be a much higher degree of uncertainty associated with the results of less-detailed methods. When economically feasible and dictated by lack of available flow information, more-detailed analyses should be considered. Reliable rating curves can be developed using step-backwater analyses. The simplest application involves computation of water-surface profiles from a downstream point at which the rating curve is known (or can be reliably estimated). When no rating curve information is available (or the known information is too far away) the principle of converging backwater curves may be utilized. Simply stated, water-surface profiles computed for a given discharge with different downstream water-surface elevations will converge at some point upstream. For this latter approach the reach downstream of the bridge should be long enough such that convergence occurs at or downstream of the exit section. The most upstream section reuired for either step-backwater application is the approach section. Davidian presents excellent discussion of the data requirements and computational procedures for step-backwater analyses.[10]

The second phase is based upon the assumption that it is possible to develop a relationship between the water-surface elevation at the approach cross section and total flood damages upstream from the bridge site for any given discharge. Figure 18 (limited to four discharges for clarity) illustrates the desired end-product of this phase. The lowest elevation for each discharge curve represents the "natural" (unconstricted) water-surface elevation for that discharge. The corresponding damage amount represents damages that would occur without any constriction in place (hereafter referred to as base damages). The dashed curve connecting the lower ends of each of the discharge curves represents base damages for any approach section elevation. The discharges associated with any elevation can be determined from the approach section rating curve from the first phase. The dashed arrows from a on the abscissa to a' on the ordinate indicate the base damages (a') for the discharge, Q_2. The first bridge design alternative, which results in an elevation of b at the approach section, causes total upstream flood damages equal to b'. The difference between b' and a' is the incremental flood damages that may be attributed to that design alternative. Likewise, a second design alternative results in a water-surface elevation of c with total upstream flood damages of c' and the associated incremental upstream flood damages equal to the difference between c' and a'. Developing the relationship of fig. 18 requires computing several water-surface profiles from the approach cross section to some point upstream. The distance upstream must be sufficient to allow the profile of maximum bridge backwater

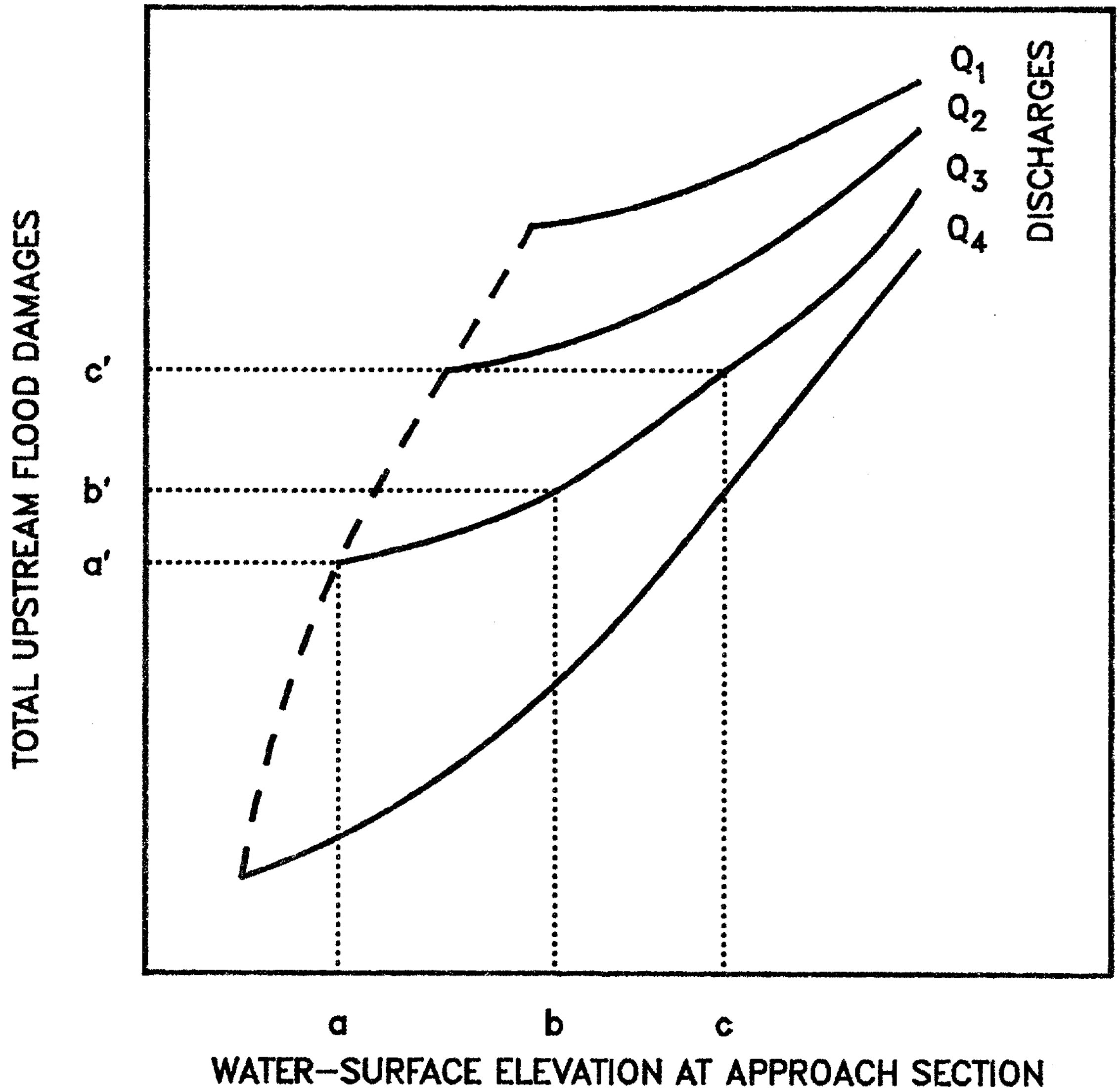

Figure 18. Typical elevation-damage-discharge relation upstream from a bridge site.

to return to the "natural" (unconstricted) profile. For each discharge, the profile for unconstricted flow must be computed to determine the flood damages. In addition to the "natural" profile, several additional profiles should be computed to define the damage curve for that discharge. The total number of discharges to be considered depends upon the variation of damages with discharge. A sufficient number would be as many as is required to permit reliable interpolation between individual discharge curves. The number of profiles for each discharge is governed by how irregularly total damages vary with increased elevation. An optional output table which summarizes profile data is designed to be used as a worksheet for the computation of upstream flood damages for each profile computation. Developing a complete relation such as fig. 18 may not be feasible when very few alternatives are being considered. Also, it may not be possible to do so for extremely complex flood damage relationships. An alternate approach is discussed following the discussion of the third phase.

The third phase is the computation of the water-surface profiles from the exit section through the approach section for the various design alternatives. The exit section rating curve from the first phase provides the starting water-surface elevations. Another optional output table provides a tabulation of elevations and other bridge flow and road overflow results pertinent to computation of the various damage amounts. It can also be used as a worksheet for tabulating and totaling the various cost factors. Upstream flood damages can be computed by entering the relation developed in the second phase with the computed water-surface elevation at the approach cross section. It is recommended that the first analysis of each alternative bridge-opening design be conducted such that no embankment overtopping is permitted. Such analyses for a series of discharges serves two useful functions. First, the maximum bridge backwater is determined which may (1) permit early rejection of totally unacceptable alternatives or (2) provide insight as to the amount of embankment overflow required to make a particular alternative more acceptable. Second, such analyses provide results that can be used for direct determination of the minimum overtopping discharge for each design alternative. This minimum overtopping discharge is the discharge that results in an upstream water-surface elevation which would just begin to cause embankment overflow for a given combination of bridge opening and embankment alternatives and can be useful in the evaluation of alternative designs.[22] The model automatically outputs an overtopping elevation for each bridge analysis when there is no embankment overflow. This elevation represents the minimum road grade elevation at which embankment overflow could occur for the given discharge and given bridge opening. Thus, the specified discharge is the minimum overtopping discharge for the specified bridge opening combined with an embankment having a minimum elevation equal to the computed overtopping elevation. A relationship, such as that shown in fig. 19, can be developed by plotting the computed overtopping elevations versus discharge for each alternative bridge length. Then, for a given bridge length and the minimum embankment elevation of the chosen embankment alternative, such a relationship provides the minimum overtopping discharge for that bridge opening and embankment combination.

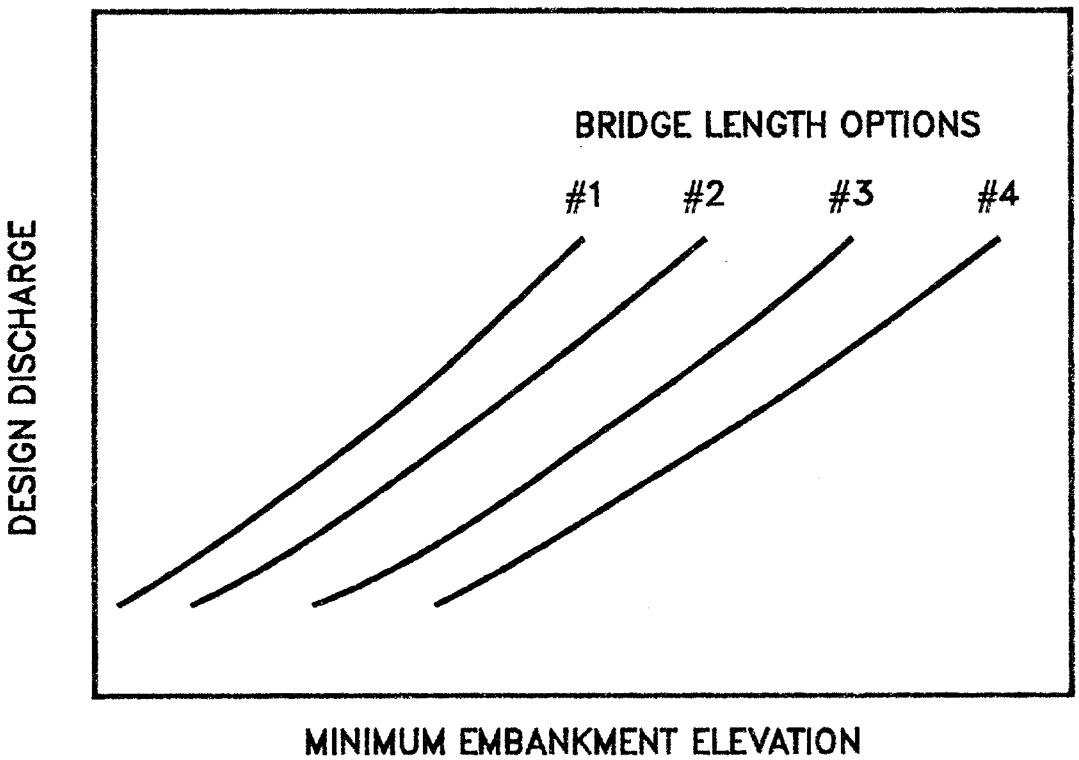

Figure 19. Typical relation between minimum embankment elevation, design discharge, and bridge opening design alternative.

As mentioned previously, there may be cases where an alternate approach for determining upstream flood damages would be preferred or required. Discussion of one possible modified approach follows. The second phase could be limited to computation of the unconstricted profiles from which the base damages for each discharge could be determined. Determination of upstream flood damages (for each discharge for each design alternative) would require:

(1) using the computed approach section water-surface elevation from the third phase to compute the backwater-affected profile upstream from the bridge; (2) determine the total upstream flood damages associated with that profile; and (3) determine the incremental upstream flood damage by subtracting base damages from total damages. Such an approach may be <u>required</u> if a relationship similar to that in fig. 18 is extremely difficult to develop. Also, such an approach may be <u>preferred</u> if the amount of computations to develop the damage relationship approaches the amount of computations for the modified approach (which may be the case when a very limited number of alternatives are being considered).

Chapter VIII

SUMMARY AND CONCLUSIONS

A computer model (WSPRO) was developed for computation of water-surface profiles. WSPRO was developed by the USGS under a contract with the FHWA. It was specifically designed to satisfy FHWA policy which requires consideration of design alternatives in the hydraulic design of bridge waterways.

WSPRO is a comprehensive, design-oriented model very well suited for analyzing alternative designs of bridge openings and their associated approach embankments. Adoption of extensively free-format data input, internal propagation of repetitive data, and a limited degree of cross section fabrication capability generally reduces the input data preparation effort. Also, the user has a great degree of control over selection of model output to suit the analysis.

Computational procedures for water-surface profiles unaffected by bridges are totally compatible with those of existing models. However, water-surface profile computations through bridges are based upon more recent developments than those methods used in existing models. Rather limited testing of WSPRO using data from actual flood events at existing bridges indicate generally acceptable results. All of the test sites involved relatively complex flow situations. WSPRO provided a more complete definition of the water-surface profile, as well as generally improved results when compared to results from other models for these test sites.

WSPRO also has the capability to analyze cases where flow over the approach embankments occurs in conjunction with flow through the bridge opening. The weir-flow computations for the embankment overflow are a slight modification of those in current models. Their total suitability can only be proven after extensive application experience.

An algorithm for an iterative solution for analyzing flow at bridges having multiple waterway openings was also developed. This phase of the model has not been tested beyond verification that the computational procedures work for very simple, hypothetical cases. Assumption of one-dimensional flow at a multiple opening situation can always be questioned (and sometimes totally erroneous). Extensive field application should indicate whether the current algorithm (or modifications thereto) can be used to obtain sufficient estimates of water-surface profiles at such sites (or at least at some such sites). Experience gained by these applications should also be helpful in determining future need for going to two-dimensional modeling techniques.

APPENDIX Coefficient of Discharge for Bridges

Figures 20 through 23 are definition sketches of the four types of openings for which Matthai defined the coefficient of discharge.[15] Figures 24 through 34 are the relationships defining the base coefficient of discharge and the factors used to adjust for nonstandard conditions. Except for type 1 openings, different curves are required for different embankment slopes. Most of these relationships are incorporated into the model in the form of digitized values. The digitized values are shown in tabular form at the end of this appendix. Table 8 cross-references the figures and tables pertaining to the base coefficient of discharge. Table 9 cross-references those figures and tables pertaining to the various adjustment factors.

Generally each of the relationships are incorporated into the model in the form of three arrays. Two one-dimensional arrays contain values of the two independent variables (the abscissa of the relationship and the family of curves), and a two-dimensional array contains the corresponding values of the dependent variable. Exceptions to this form of representation are discussed in the following paragraphs.

The type 1 opening Froude number adjustment (fig. 24) is adequately expressed in equation form as

$$k_F = 0.9 + 0.2F \text{ for } 0.0 \leq F \leq 0.5 \qquad (66)$$

and $$k_F = 0.82 + 0.36F \text{ for } F > 0.5 \qquad (67)$$

where F is the Froude number with an arbitrary upper limit of F = 1.2 for the adjustment.

The average depth adjustment (fig. 30) for a type 3 opening with 2 to 1 embankment slope is determined by the following equations:

$$k_y = 1.00 + 0.3\ y \text{ for } 0.0 \leq y \leq 0.20 \quad (68)$$

$$\text{and} \quad k_y = 1.02 \mp 0.2\ \bar{y} \text{ for } y > 0.2 \quad (69)$$

where $\bar{y} = \dfrac{y_a + y_b}{2b}$ with $\bar{y} = 0.30$ as an upper limit.

The type 4 opening wingwall adjustment factor, k_θ, is computed using slopes of the family of curves (figs. 31 and 32). The equation for specified m-values is

$$k_\theta = 1.0 + (WW - 30)\ Sk_\theta \quad (70)$$

where WW is the wingwall angle and Sk_θ is the appropriate slope from tables 23 or 25. k_θ is obtained by interpolation for intermediate m-values.

Certain adjustments presented by Matthai were not incorporated into WSPRO. The skew adjustment was omitted because WSPRO always computes the flow area normal to the flow for skewed bridge openings. An adjustment for submerged flow was also omitted because the FHWA methodology is used to compute pressure flow when girders are significantly submerger.[3] The Froude number adjustment for type 4 openings with 2 to 1 embankment slope was intentionally omitted for reasons of consistency. There is no similar adjustment for type 4 openings with 1 to 1 embankment slopes, and the adjustment is rather minor. Matthai also applied an adjustment for eccentricity which is a measure of unequal conveyances on left and right overbanks of the approach section. This factor was not included in WSPRO on the bases that (1) it is a very minor adjustment, and (2) the effective flow length accounts for conveyance distribution.

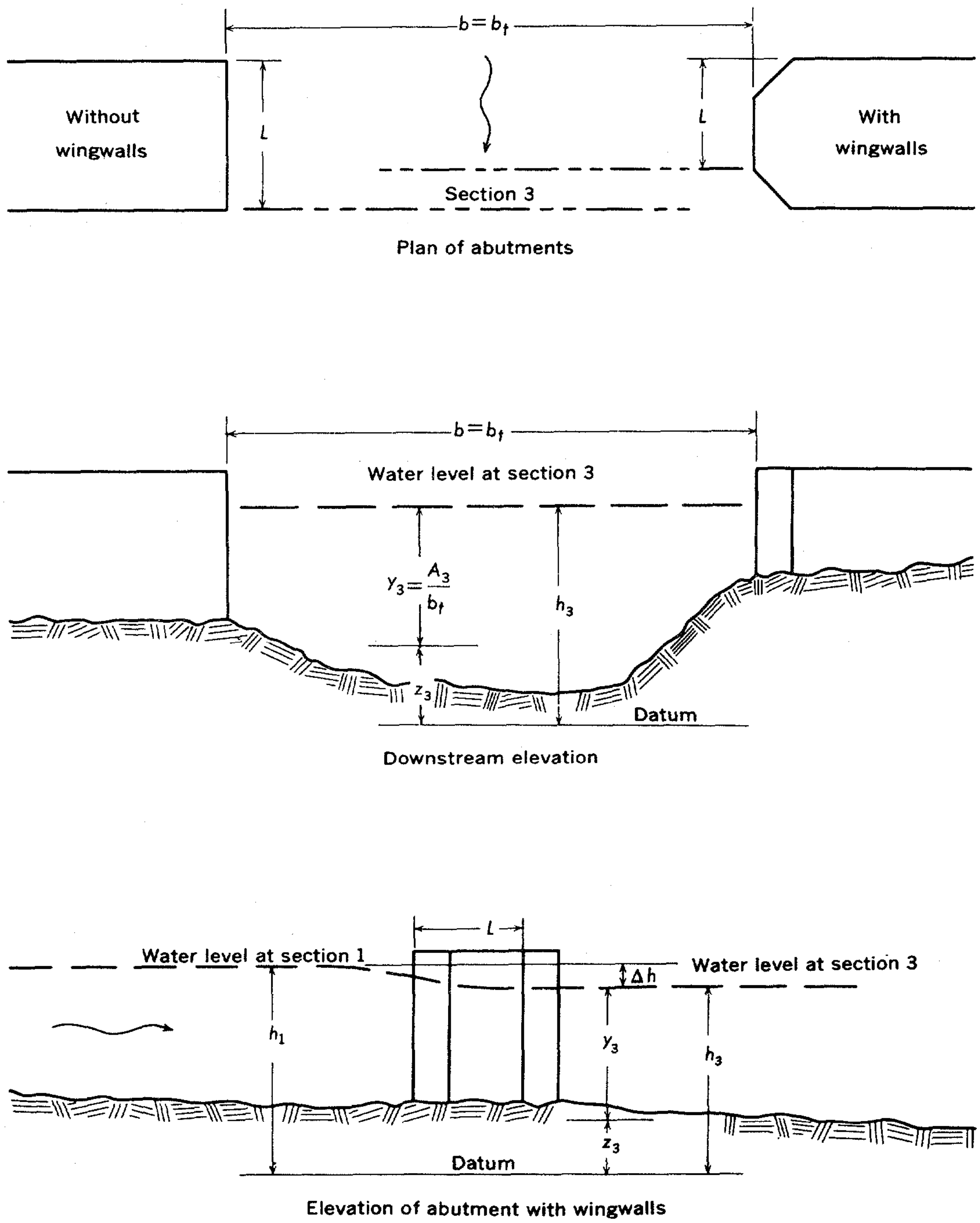

Figure 20. Definition sketch of type 1 opening, vertical embankments and vertical abutments, with or without wingwalls (after Matthai).

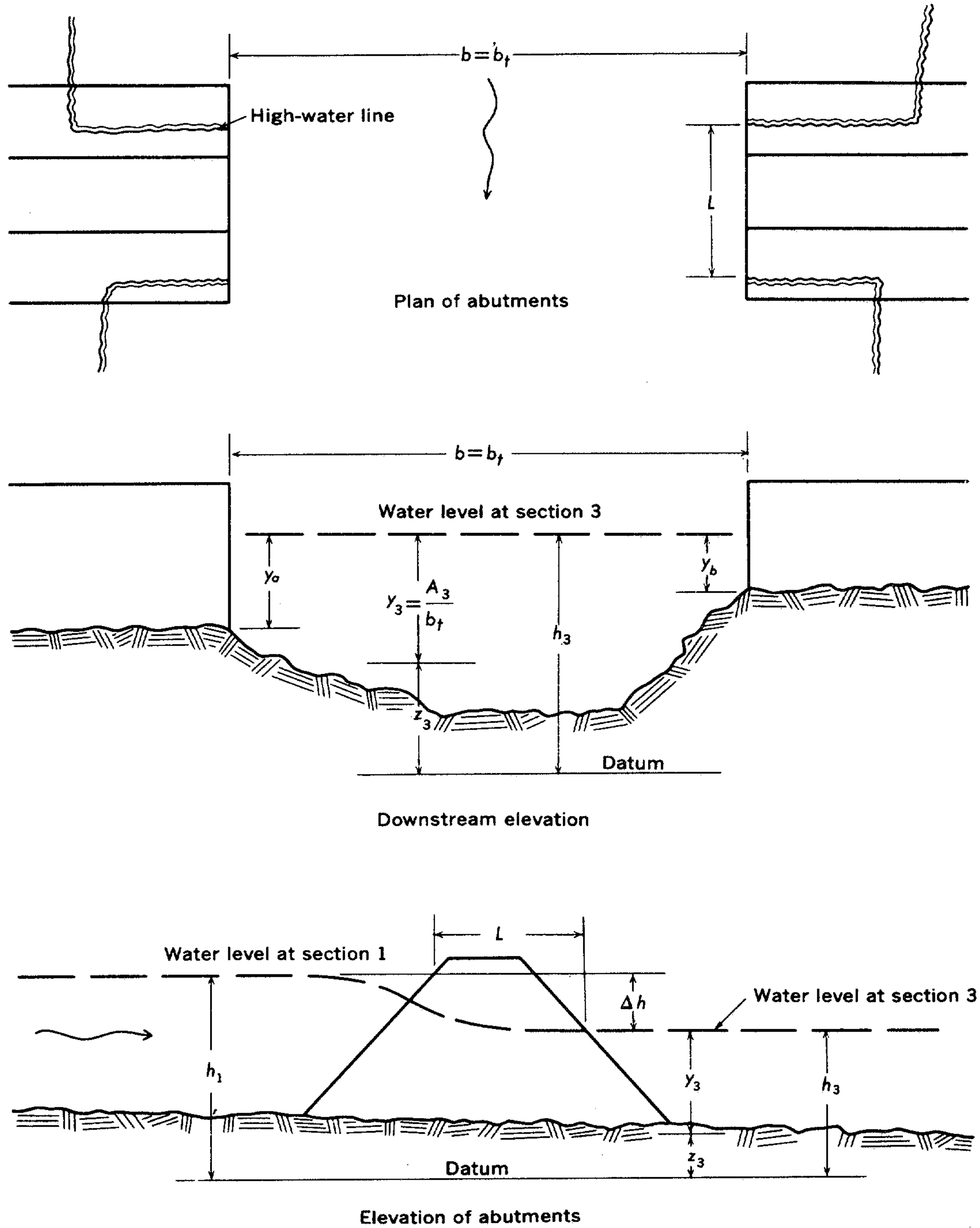

Figure 21. Definition sketch of type 2 opening, sloping embankments without wingwalls (after Matthai).

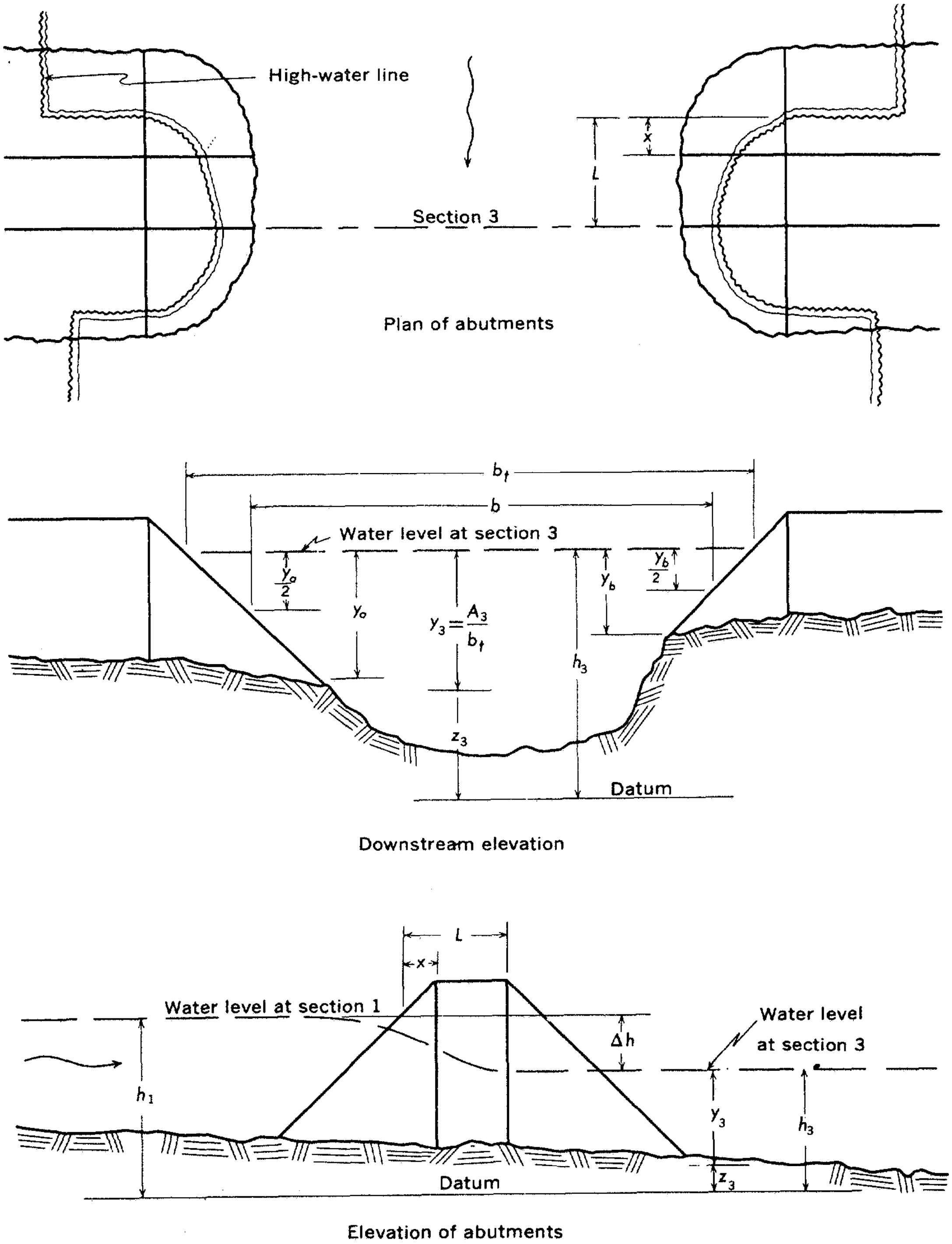

Figure 22. Definition sketch of type 3 opening, sloping embankments and sloping abutments (spillthrough) (after Matthai).

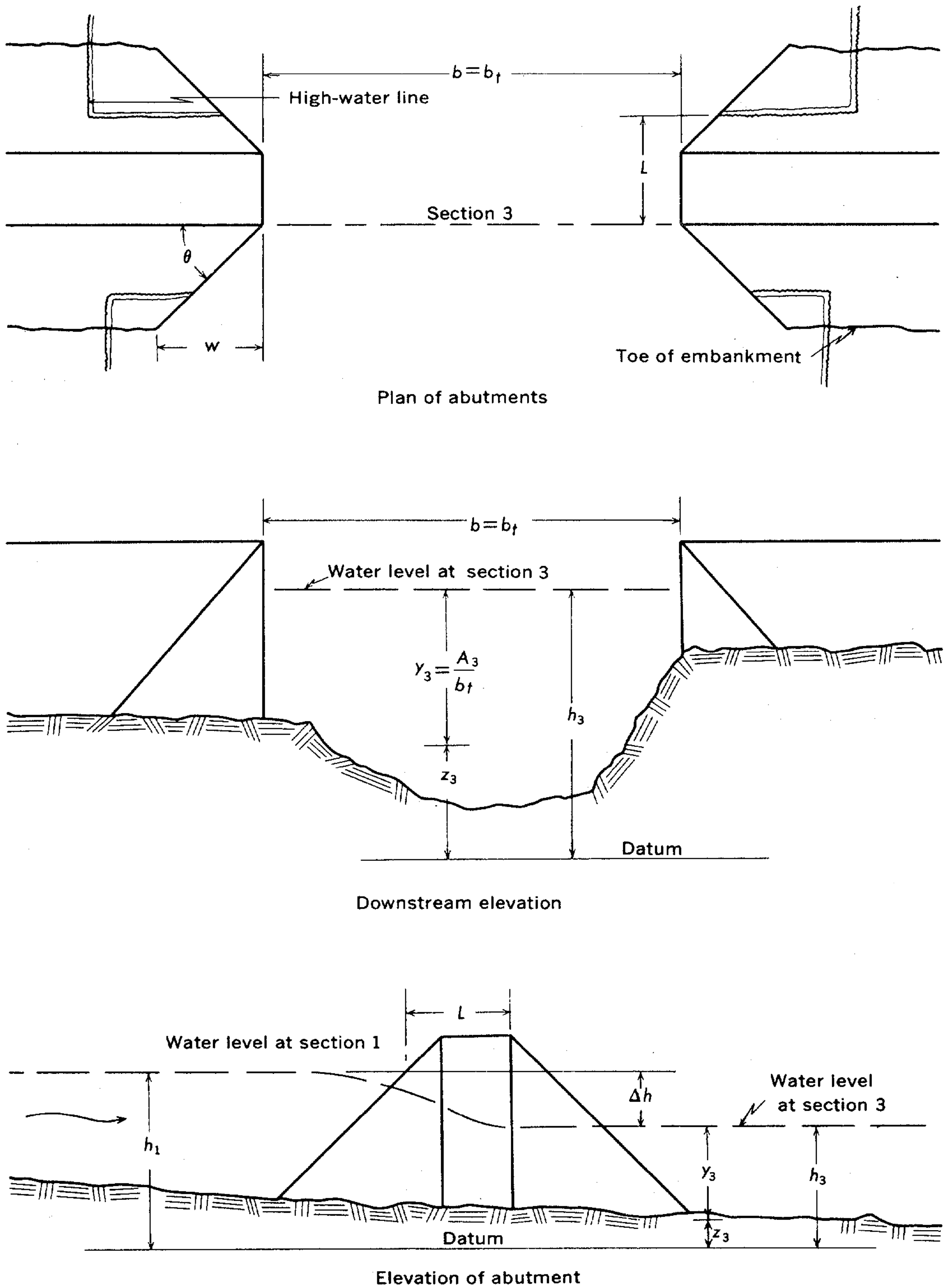

Figure 23. Definition sketch of type 4 opening, sloping embankments and vertical abutments with wingwalls (after Matthai).

Table 8. Cross-reference of figures and tables pertaining to the base coefficient of discharge.

Type Opening	Embankment Slope	Figure No.	Table No.
1		24	10
2	1 to 1 2 to 1	26 27	13 15
3	1 to 1 1 1/2 to 1 2 to 1	28 29 30	17 19 21
4	1 to 1 2 to 1	31 32	22 24

Table 9. Cross-reference of figures and tables pertaining to adjustment factors.

Type Opening	Embankment Slope	Adjustment Factor For:	Figure No.	Table No.
1		Entrance Rounding Wingwalls Froude Number	24 25 Eq.	11 12 Eq.
2	1 to 1 2 to 1	Average Depth	26 27	14 16
3	1 to 1 1 1/2 to 1 2 to 1	Entrance geometry	28 29 Eq.	18 20 Eq.
4	1 to 1 2 to 1	Wingwalls	31 32	23 25
All		Piers or piles Spur dikes	33 34	26, 27 28

Eq. indicates that an equation is used.

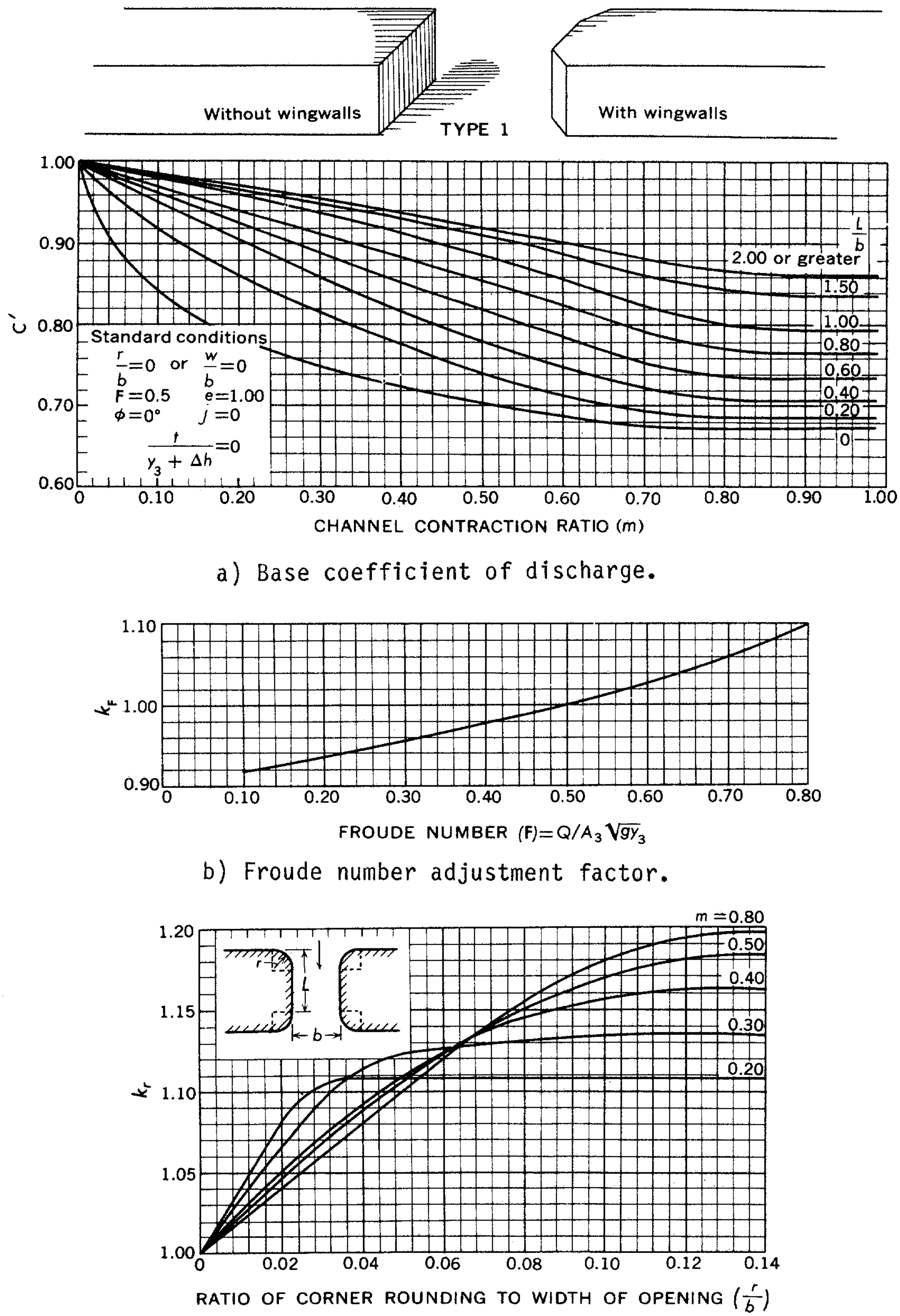

a) Base coefficient of discharge.

b) Froude number adjustment factor.

c) Corner rounding adjustment factor.

Figure 24. Coefficients for type 1 openings (after Matthai).

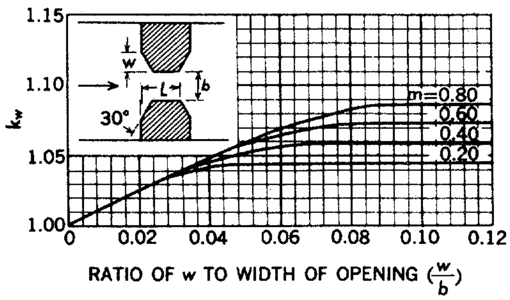

a) 30° wingwalls.

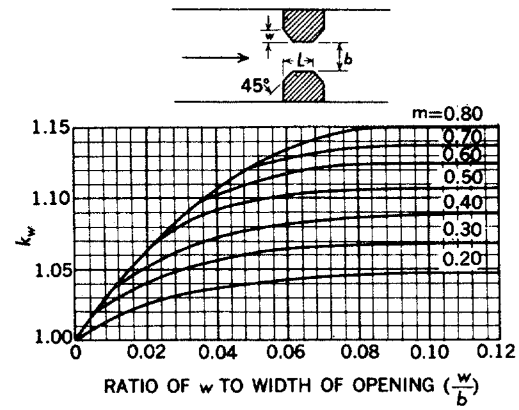

b) 45° wingwalls.

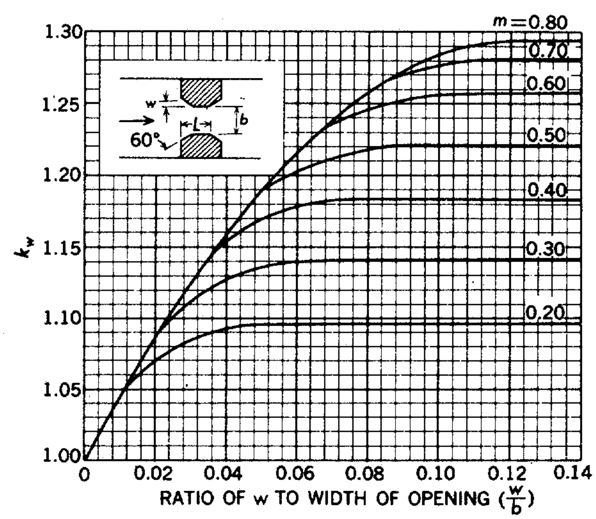

c) 60° wingwalls.

Figure 25. Wingwall adjustment factors for type 1 openings (after Matthai).

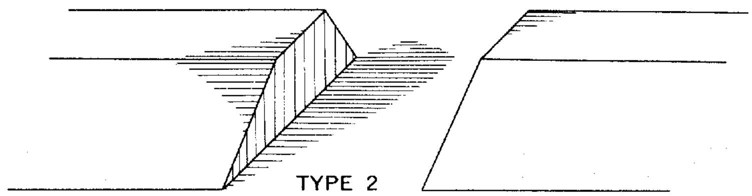

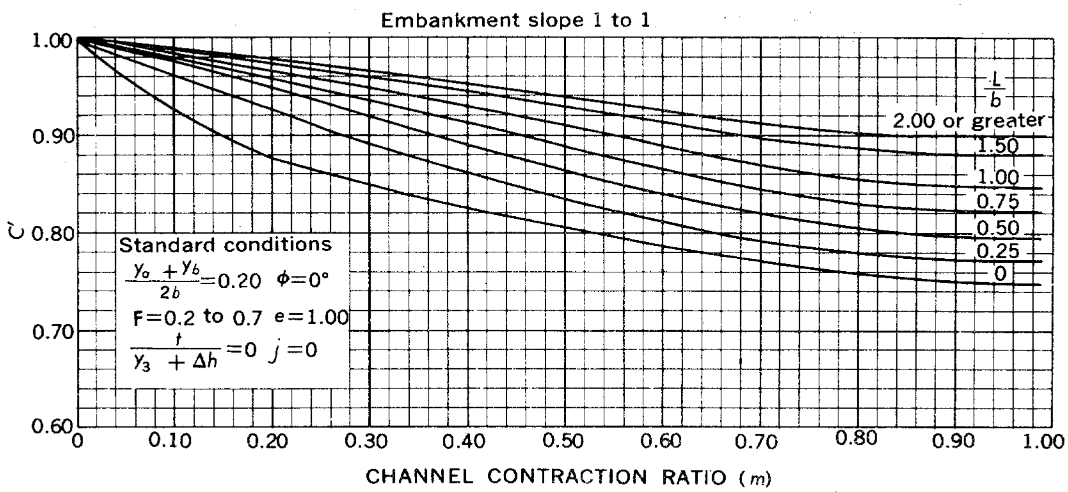

a) Base coefficient of discharge.

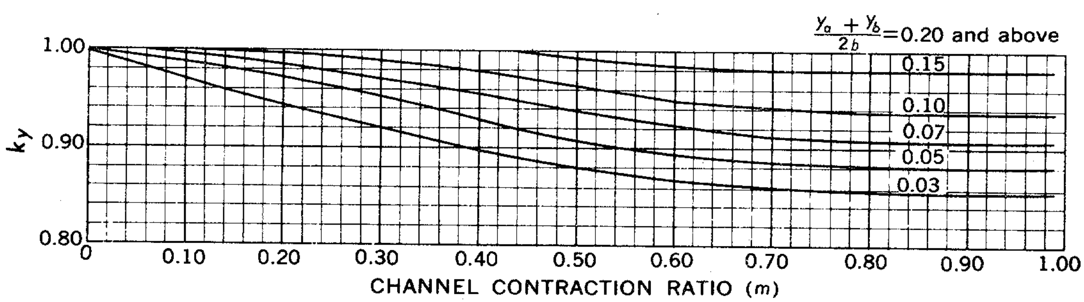

b) Average depth adjustment factor.

Figure 26. Coefficients for type 2 openings, embankment slope 1 to 1 (after Matthai).

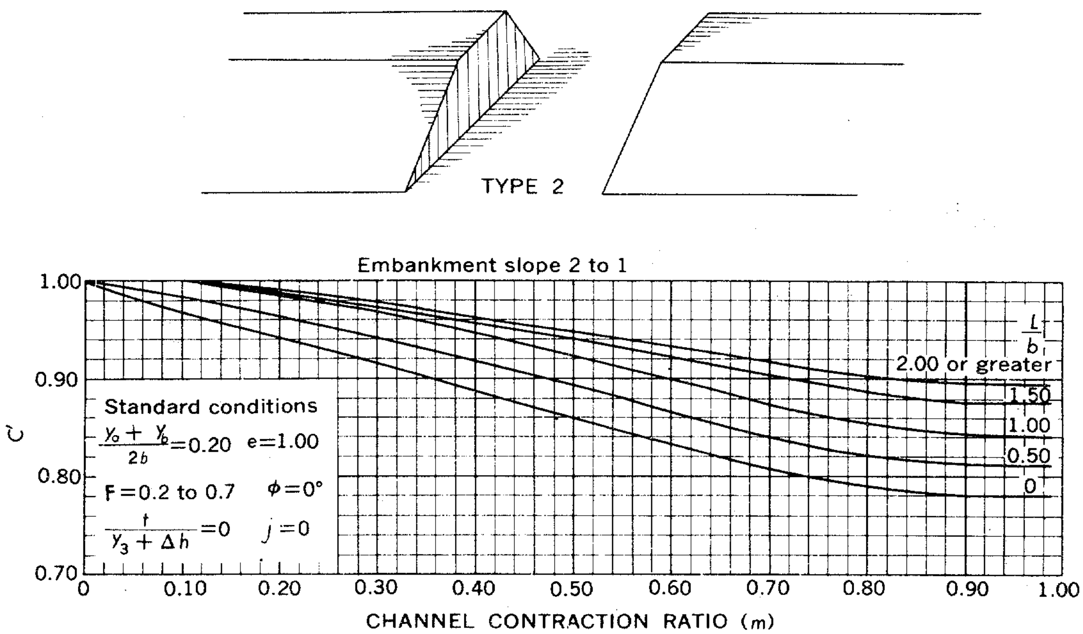

a) Base coefficient of discharge.

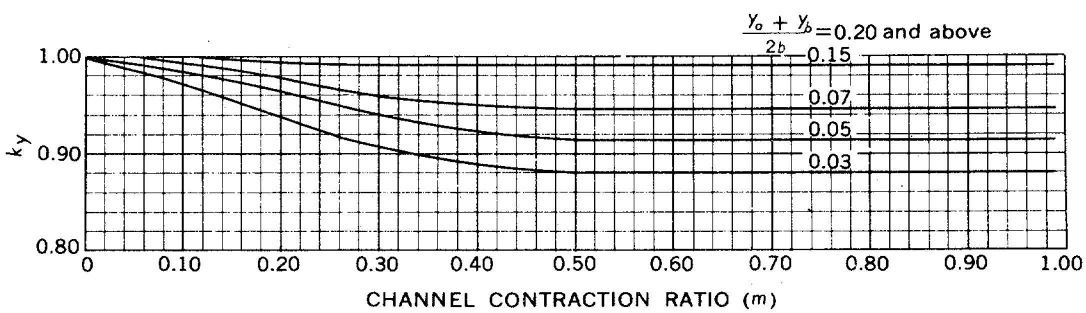

b) Average depth adjustment factor.

Figure 27. Coefficients for type 2 openings, embankment slope 2 to 1 (after Matthai).

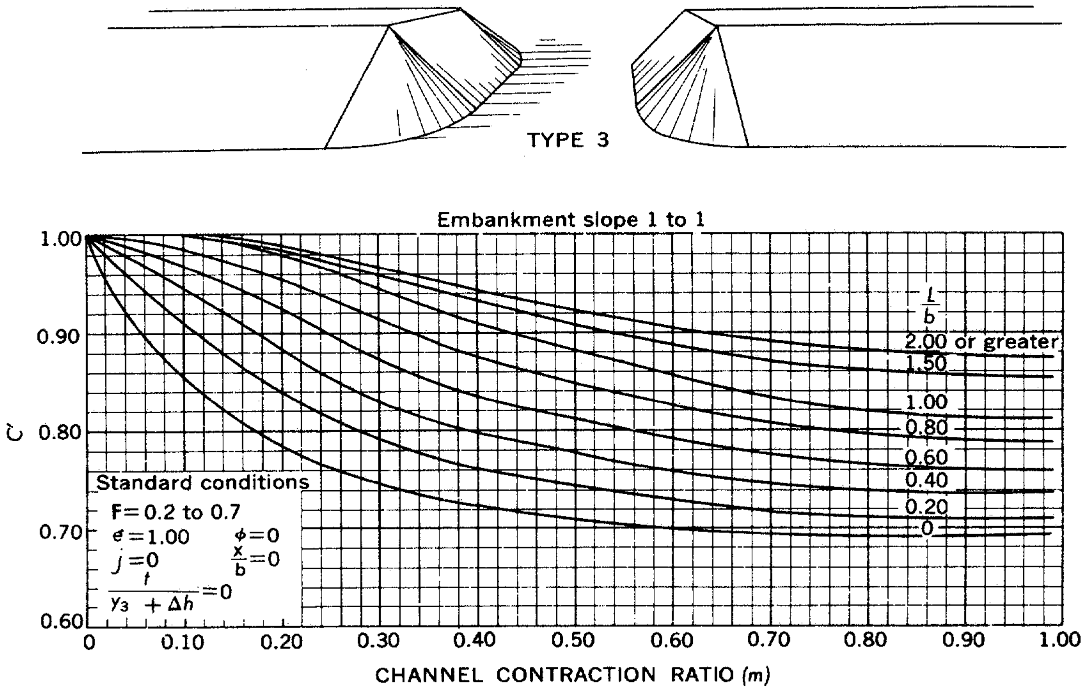

a) Base coefficient of discharge.

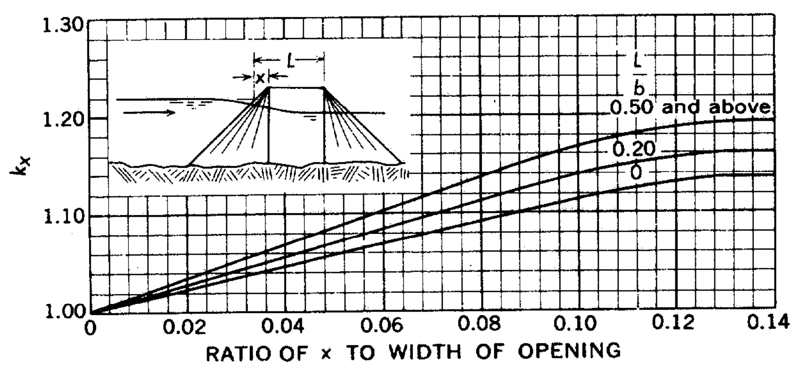

b) Unwetted abutment adjustment factor.

Figure 28. Coefficients for type 3 openings, embankment slope 1 to 1 (after Matthai).

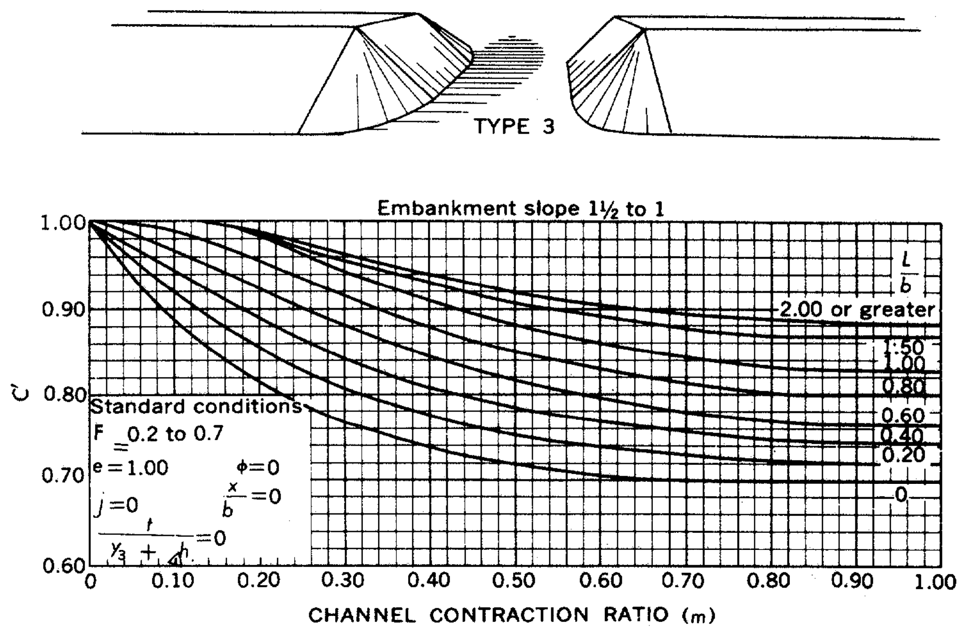

a) Base coefficient of discharge.

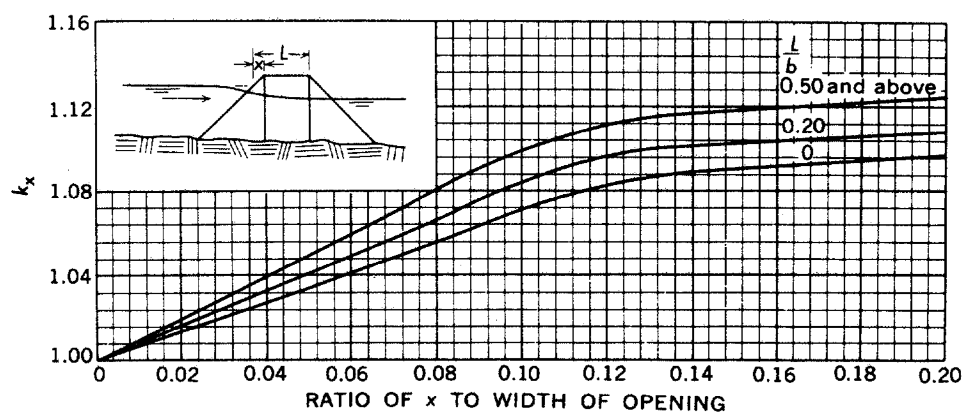

b) Unwetted abutment adjustment factor.

Figure 29. Coefficients for type 3 openings, embankment slope 1 1/2 to 1 (after Matthai).

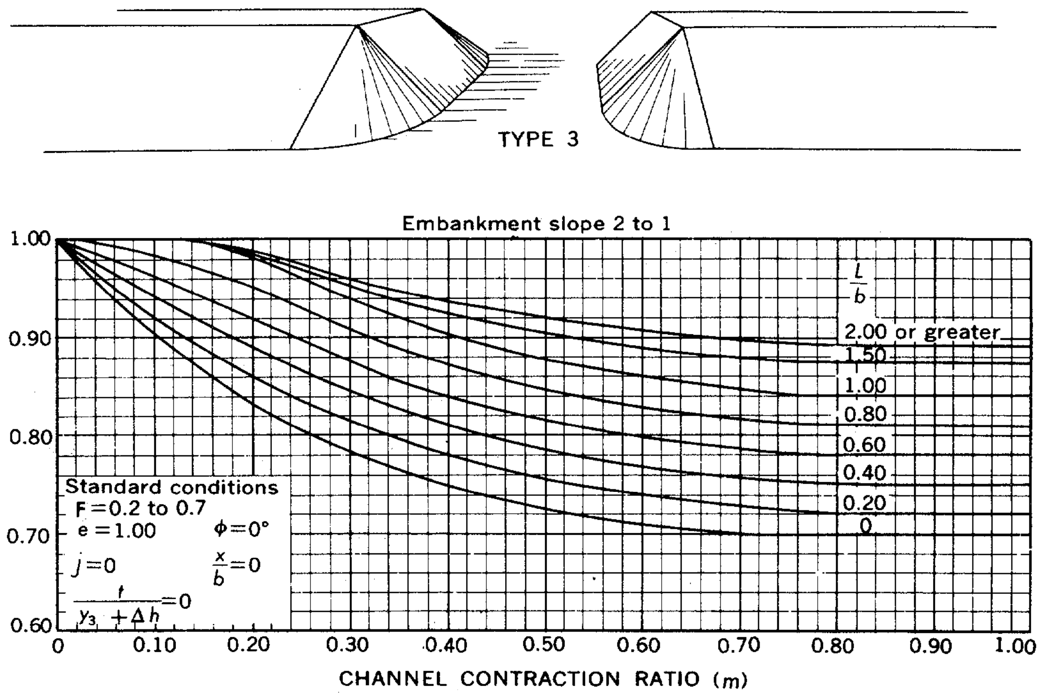

a) Base coefficient of discharge.

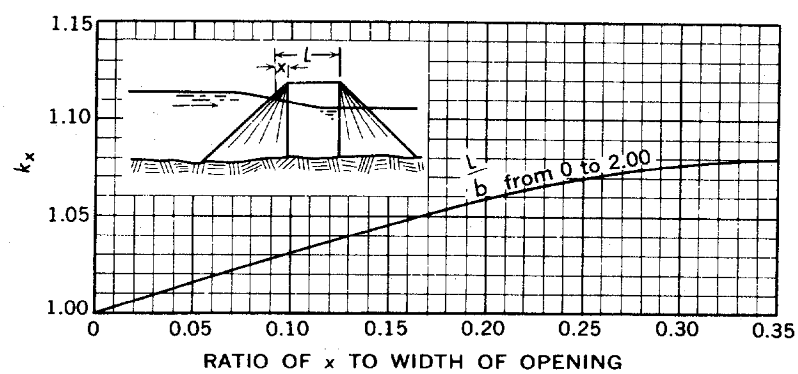

b) Unwetted abutment adjustment factor.

Figure 30. Coefficients for type 3 openings, embankment slope 2 to 1 (after Matthai).

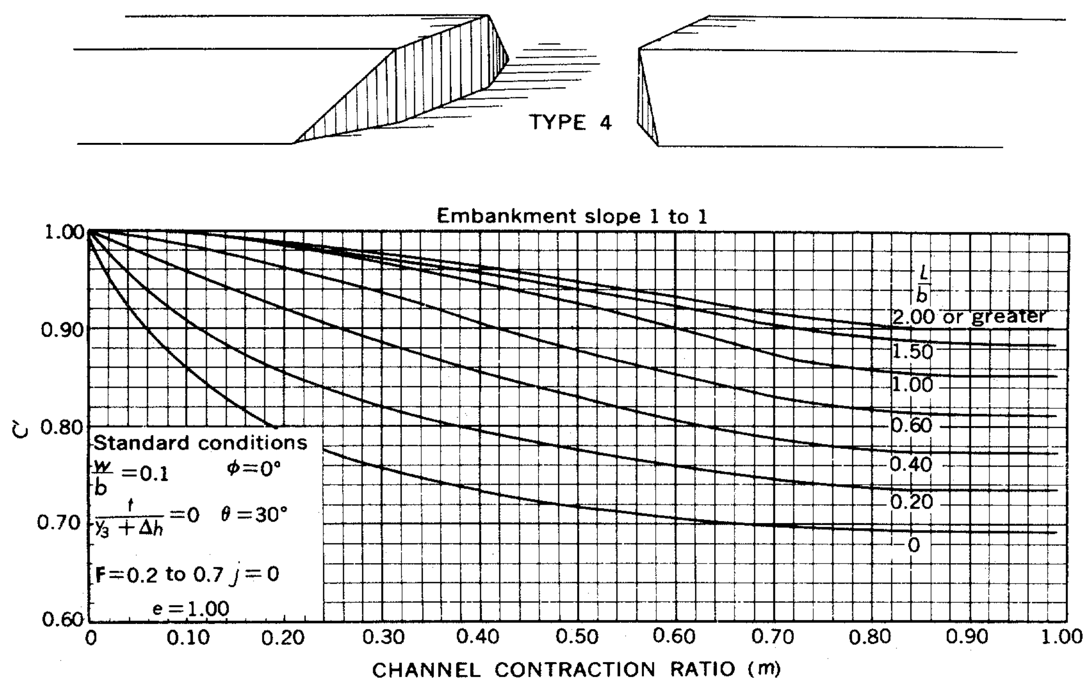

a) Base coefficient of discharge.

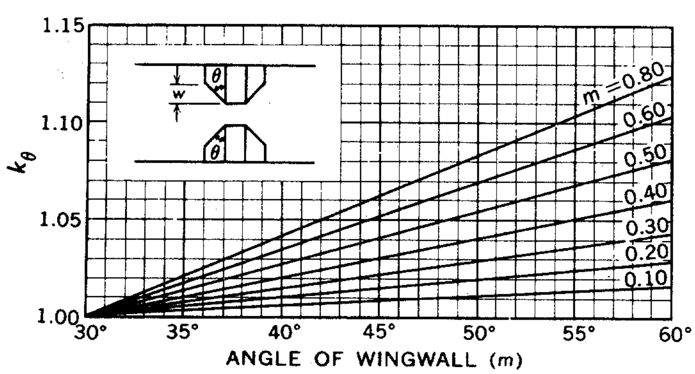

b) Wingwall adjustment factor.

Figure 31. Coefficients for type 4 openings, embankment slope 1 to 1 (after Matthai).

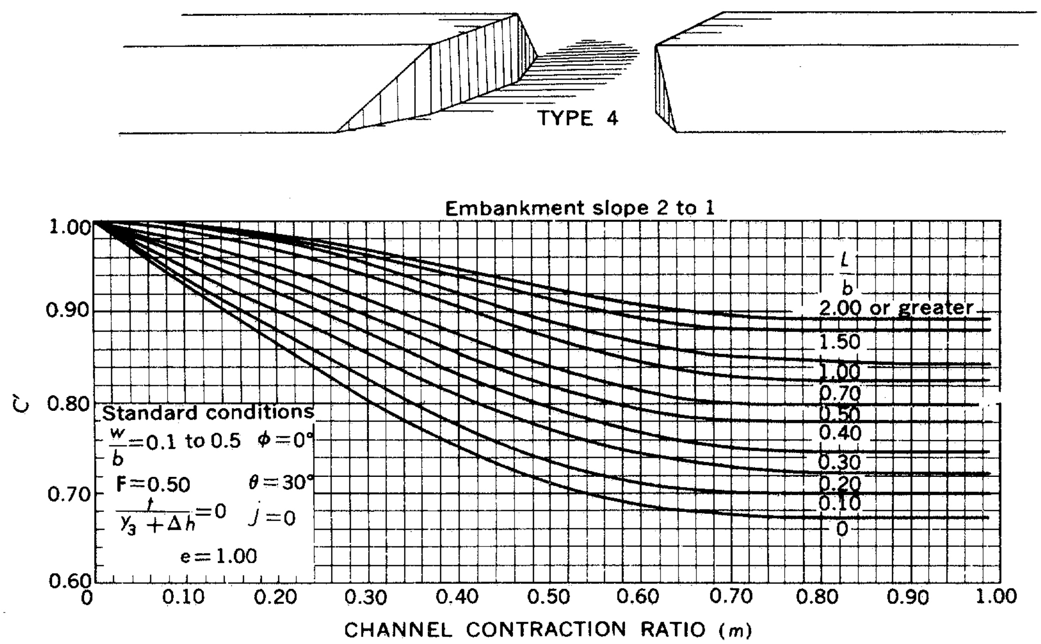

a) Base coefficient of discharge.

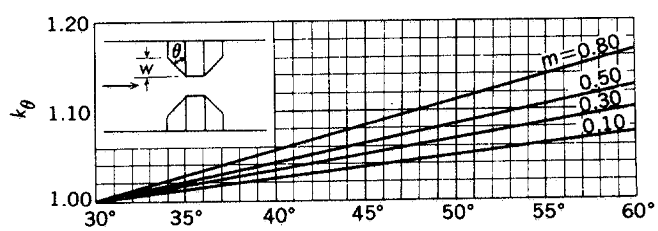

b) Wingwall adjustment factor.

Figure 32. Coefficients for type 4 openings, embankment slope 2 to 1 (after Matthai).

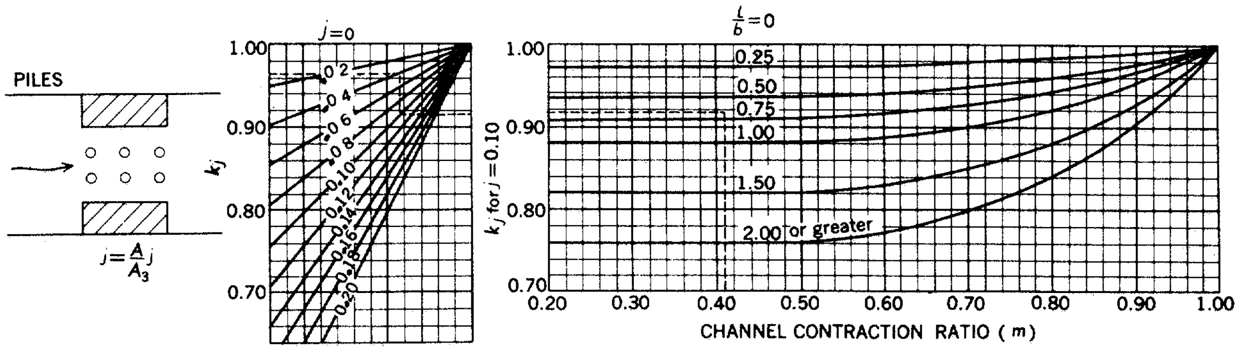

a) Adjustment factor for piles.

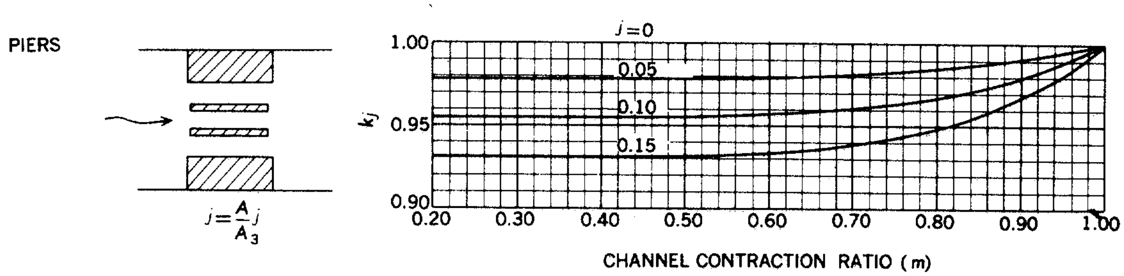

b) Adjustment factor for piers.

Figure 33. Adjustment factors for piers or piles (after Matthai).

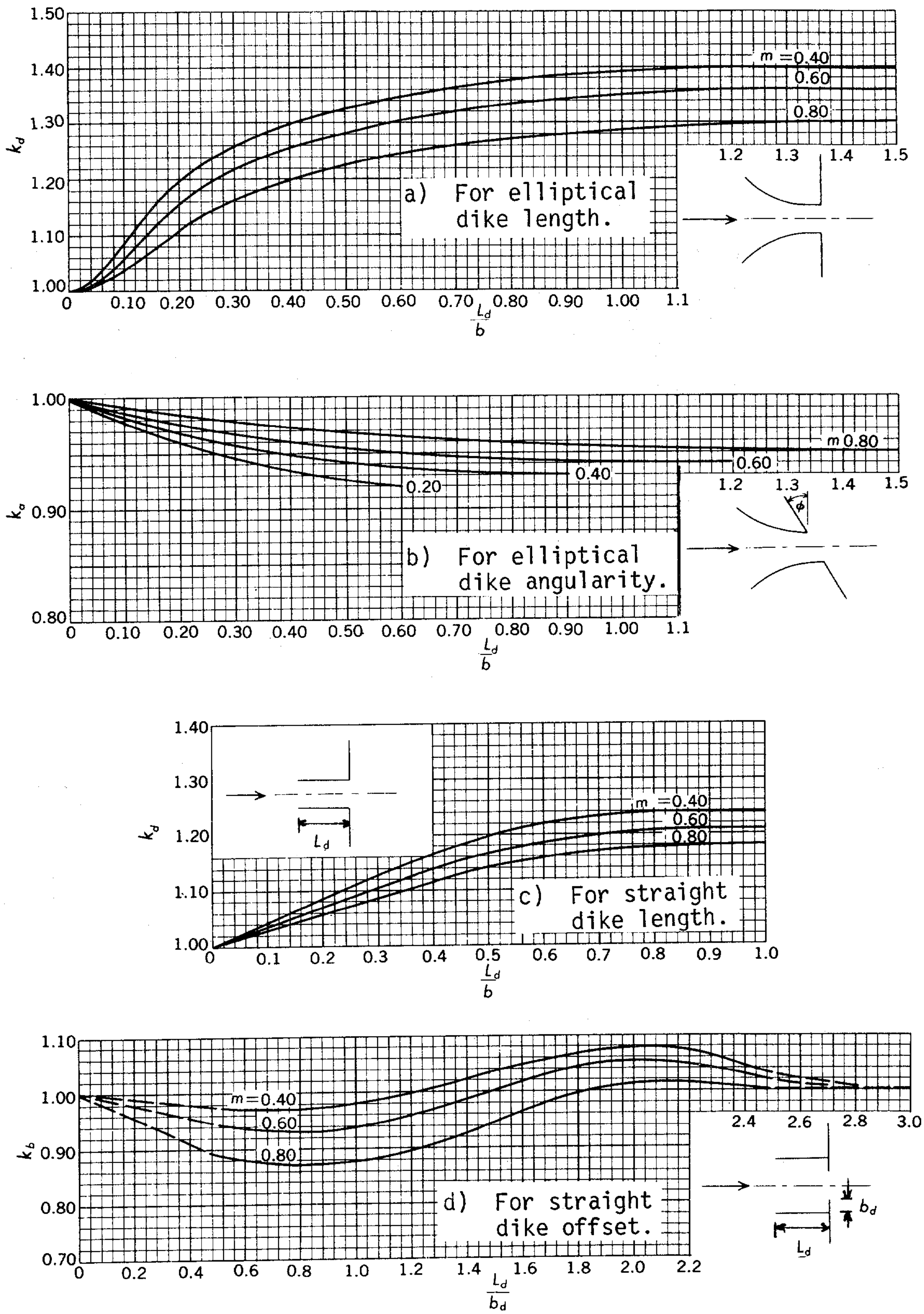

Figure 34. Adjustment factors for spur dikes (after Matthai).

Table 10. Base coefficient of discharge, C′, for type 1 opening, with or without wingwalls (see fig. 24).

		m					
		0.0	0.1	0.3	0.5	0.8	1.0
	0.0	1.00	0.83	0.745	0.70	0.67	0.67
	0.2	1.00	0.92	0.81	0.74	0.685	0.685
	0.4	1.00	0.95	0.86	0.775	0.71	0.71
L/b	0.6	1.00	0.965	0.89	0.82	0.735	0.735
	0.8	1.00	0.97	0.91	0.855	0.77	0.765
	1.0	1.00	0.98	0.935	0.885	0.80	0.795
	1.5	1.00	0.985	0.95	0.91	0.845	0.835
	2.0	1.00	0.99	0.955	0.92	0.87	0.86

m is the channel contraction ratio.

L/b is the ratio of flow length to bridge-opening length.

Table 11. Variation of adjustment factor, k_r, for type 1 opening with entrance rounding (see fig. 24).

		r/b						
		0.01	0.02	0.04	0.06	0.08	0.10	0.14
	0.1	1.06	1.07	1.07	1.07	1.07	1.07	1.07
	0.2	1.04	1.08	1.11	1.11	1.11	1.11	1.11
m	0.4	1.03	1.05	1.09	1.12	1.14	1.15	1.16
	0.6	1.02	1.04	1.08	1.12	1.15	1.17	1.18
	0.8	1.02	1.04	1.08	1.12	1.16	1.18	1.20
	1.0	1.02	1.04	1.08	1.12	1.16	1.18	1.22

r/b is the ratio of entrance rounding to bridge-opening length.

m is the channel contraction ratio.

Table 12. Variation of adjustment factor, k_θ, for type 1 opening with wingwalls (see fig. 25).

w/b

	m	0.01	0.02	0.04	0.06	0.08	0.10	0.14
	0.1	1.01	1.02	1.02	1.02	1.02	1.02	1.02
	0.2	1.01	1.025	1.04	1.04	1.04	1.04	1.04
m	0.4	1.01	1.025	1.04	1.06	1.06	1.06	1.06
	0.6	1.01	1.025	1.05	1.06	1.07	1.07	1.07
	0.8	1.01	1.025	1.05	1.07	1.08	1.09	1.09
	1.0	1.01	1.025	1.05	1.07	1.08	1.09	1.10

(a) 30° wingwalls

	m	0.01	0.02	0.04	0.06	0.08	0.10	0.14
	0.1	1.00	1.01	1.01	1.02	1.02	1.02	1.02
	0.2	1.01	1.02	1.04	1.04	1.05	1.05	1.05
m	0.4	1.03	1.05	1.07	1.08	1.09	1.09	1.09
	0.6	1.03	1.06	1.10	1.11	1.12	1.12	1.12
	0.8	1.03	1.06	1.11	1.13	1.15	1.15	1.15
	1.0	1.03	1.06	1.11	1.13	1.15	1.16	1.17

(b) 45° wingwalls

	0.01	0.02	0.04	0.06	0.08	0.10	0.14
0.1	1.02	1.04	1.05	1.05	1.05	1.05	1.05
0.2	1.04	1.07	1.09	1.10	1.10	1.10	1.10
0.4	1.04	1.09	1.15	1.18	1.18	1.18	1.18
0.6	1.04	1.09	1.15	1.21	1.24	1.25	1.26
0.8	1.04	1.09	1.15	1.22	1.26	1.28	1.29
1.0	1.04	1.09	1.15	1.22	1.26	1.28	1.32

(c) 60° wingwalls

w/b is ratio of wingwall width to bridge-opening length.

m is the channel contraction ratio.

Table 13. Base coefficient of discharge, C′, for type 2 opening, embankment slope 1 to 1 (see fig. 26).

		m					
		0.0	0.1	0.3	0.5	0.8	1.0
	0.0	1.00	0.92	0.845	0.805	0.755	0.745
	0.2	1.00	0.955	0.88	0.83	0.775	0.765
	0.4	1.00	0.97	0.91	0.85	0.795	0.79
L/b	0.6	1.00	0.975	0.925	0.87	0.81	0.805
	0.8	1.00	0.98	0.94	0.895	0.835	0.825
	1.0	1.00	0.985	0.95	0.91	0.855	0.845
	1.5	1.00	0.988	0.96	0.93	0.885	0.88
	2.0	1.00	0.99	0.965	0.94	0.905	0.90

m is the channel contraction ratio.

L/b is the ratio of flow length to bridge-opening length.

Table 14. Variation of adjustment factor, k_y, for type 2 opening, embankment slope 1 to 1 (see fig. 26).

		m				
		0.0	0.2	0.4	0.7	1.0
	0.03	1.00	0.94	0.895	0.86	0.86
	0.05	1.00	0.97	0.93	0.88	0.88
$\frac{y_a + y_b}{2b}$	0.07	1.00	0.985	0.955	0.91	0.91
	0.10	1.00	0.995	0.98	0.94	0.94
	0.15	1.00	1.00	1.00	0.98	0.98

m is the channel contraction ratio.

$\frac{y_a + y_b}{2b}$ is ratio of average depth at the abutments to bridge-opening length.

Table 15. Base coefficient of discharge, C′, for type 2 opening, embankment slope 2 to 1 (see fig. 27).

	m					
	0.0	0.1	0.3	0.5	0.8	1.0
L/b 0.0	1.00	0.965	0.915	0.86	0.79	0.78
0.2	1.00	0.97	0.925	0.87	0.80	0.79
0.4	1.00	0.98	0.935	0.89	0.81	0.80
0.6	1.00	0.99	0.95	0.90	0.83	0.82
0.8	1.00	0.995	0.96	0.91	0.845	0.83
1.0	1.00	1.00	0.97	0.925	0.855	0.84
1.5	1.00	1.00	0.975	0.94	0.89	0.875
2.0	1.00	1.00	0.98	0.95	0.905	0.895

m is the channel contraction ratio.

L/b is the ratio of flow length to bridge-opening length.

Table 16. Variation of adjustment factor, k_y, for type 2 opening, embankment slope 2 to 1 (see fig. 27).

	m				
	0.0	0.2	0.4	0.7	1.0
$\frac{y_a + y_b}{2b}$ 0.03	1.00	0.935	0.89	0.88	0.88
0.05	1.00	0.965	0.925	0.91	0.91
0.07	1.00	0.975	0.95	0.945	0.945
0.10	1.00	0.985	0.97	0.97	0.97
0.15	1.00	0.99	0.99	0.99	0.99

m is the channel contraction ratio.

$\frac{y_a + y_b}{2b}$ is the ratio of average depth at the abutments to bridge-opening length.

Table 17. Base coefficient of discharge, C′, for type 3 opening, embankment slope 1 to 1 (see fig. 28).

	m					
	0.0	0.1	0.3	0.5	0.8	1.0
L/b 0.0	1.00	0.85	0.74	0.71	0.69	0.69
0.2	1.00	0.91	0.79	0.745	0.71	0.71
0.4	1.00	0.945	0.83	0.775	0.74	0.735
0.6	1.00	0.97	0.87	0.81	0.765	0.76
0.8	1.00	0.985	0.91	0.85	0.795	0.79
1.0	1.00	0.995	0.945	0.88	0.82	0.81
1.5	1.00	1.00	0.96	0.91	0.86	0.85
2.0	1.00	1.00	0.97	0.925	0.88	0.875

m is the channel contraction ratio.

L/b is the ratio of flow length to bridge-opening length.

Table 18. Variation of adjustment factor, k_x, for type 3 opening, embankment slope 1 to 1 (see fig. 28).

	x/b					
	0.00	0.08	0.12	0.16	0.20	0.25
L/b 0.0	1.00	1.09	1.13	1.14	1.14	1.14
0.2	1.00	1.11	1.155	1.16	1.16	1.16
0.5	1.00	1.135	1.19	1.20	1.20	1.20

x/b is the ratio of "unwetted" abutment length to bridge-opening length.

L/b is the ratio of flow length to bridge-opening length.

Table 19. Base coefficient of discharge, C′, for type 3 opening, embankment slope 1 1/2 to 1 (see fig. 29).

	m					
	0.0	0.1	0.3	0.5	0.8	1.0
L/b 0.0	1.00	0.885	0.76	0.715	0.70	0.70
0.2	1.00	0.92	0.80	0.75	0.725	0.72
0.4	1.00	0.945	0.84	0.78	0.75	0.745
0.6	1.00	0.97	0.88	0.815	0.77	0.765
0.8	1.00	0.99	0.915	0.85	0.805	0.80
1.0	1.00	1.00	0.945	0.88	0.83	0.825
1.5	1.00	1.00	0.955	0.905	0.87	0.87
2.0	1.00	1.00	0.965	0.92	0.885	0.885

m is the channel contraction ratio.

L/b is the ratio of flow length to bridge-opening length.

Table 20. Variation of adjustment factor, k_x, for type 3 opening, embankment slope 1 1/2 to 1 (see fig. 29).

	x/b					
	0.00	0.08	0.12	0.16	0.20	0.25
L/b 0.0	1.00	1.055	1.085	1.09	1.095	1.10
0.2	1.00	1.065	1.10	1.105	1.11	1.115
0.5	1.00	1.08	1.11	1.12	1.125	1.13

x/b is the ratio of "unwetted" abutment length to bridge-opening length.

L/b is the ratio of flow length to bridge-opening length.

Table 21. Base coefficient of discharge, C′, for type 3 opening, embankment slope 2 to 1 (see fig. 30).

		m					
		0.0	0.1	0.3	0.5	0.8	1.0
	0.0	1.00	0.90	0.78	0.72	0.70	0.70
	0.2	1.00	0.92	0.81	0.755	0.72	0.72
	0.4	1.00	0.94	0.845	0.785	0.75	0.75
L/b	0.6	1.00	0.96	0.875	0.81	0.78	0.78
	0.8	1.00	0.985	0.91	0.845	0.81	0.81
	1.0	1.00	1.00	0.94	0.87	0.845	0.84
	1.5	1.00	1.00	0.95	0.905	0.875	0.87
	2.0	1.00	1.00	0.96	0.92	0.895	0.89

m is the channel contraction ratio.

L/b is the ratio of flow length to bridge-opening length.

Table 22. Base coefficient of discharge, C′, for type 4 opening, embankment slope 1 to 1 (see fig. 31).

		m					
		0.0	0.1	0.3	0.5	0.8	1.0
	0.0	0.99	0.85	0.755	0.715	0.695	0.69
	0.2	1.00	0.90	0.815	0.775	0.735	0.73
	0.4	1.00	0.955	0.885	0.83	0.775	0.77
L/b	0.6	1.00	0.985	0.935	0.875	0.815	0.81
	0.8	1.00	0.99	0.955	0.91	0.84	0.835
	1.0	1.00	1.00	0.965	0.925	0.855	0.85
	1.5	1.00	1.00	0.97	0.94	0.89	0.885
	2.0	1.00	1.00	0.975	0.95	0.905	0.90

m is the channel contraction ratio.

L/b is the ratio of flow length to bridge-opening length.

Table 23. Slopes of family of curves for determining adjustment factor, k_θ, for wingwall angle for type 4 openings, embankment slope 1 to 1 (see fig. 31).

m	Sk_θ
0.1	0.00057
0.2	0.001
0.4	0.002
0.6	0.00343
0.8	0.00413
1.0	0.00483

Table 24. Base coefficient of discharge, C′, for type 4 opening, embankment slope 2 to 1 (see fig. 32).

		m					
		0.0	0.1	0.3	0.5	0.8	1.0
L/b	0.0	1.00	0.93	0.80	0.705	0.67	0.67
	0.2	1.00	0.95	0.855	0.765	0.725	0.725
	0.4	1.00	0.97	0.895	0.815	0.78	0.78
	0.6	1.00	0.985	0.925	0.845	0.805	0.805
	0.8	1.00	0.99	0.94	0.87	0.825	0.825
	1.0	1.00	0.995	0.95	0.89	0.85	0.85
	1.5	1.00	0.995	0.965	0.91	0.88	0.88
	2.0	1.00	1.00	0.97	0.925	0.89	0.89

m is the channel contraction ratio.

L/b is the ratio of flow length to bridge-opening length.

Table 25. Slopes of family of curves for determining adjustment factor, k_θ, for wingwall angle for type 4 openings, embankment slope 2 to 1 (see fig. 32).

m	Sk_θ
0.1	0.00243
0.2	0.00283
0.4	0.00373
0.6	0.00467
0.8	0.00557
1.0	0.00667

Table 26. Adjustment factor, k_j, for piers (see fig. 33).

		m				
		0.40	0.60	0.80	0.90	1.00
j	0.00	1.00	1.00	1.00	1.00	1.00
	0.05	0.978	0.979	0.985	0.991	1.00
	0.10	0.955	0.957	0.967	0.98	1.00
	0.15	0.93	0.933	0.948	0.968	1.00
	0.20	0.903	0.907	0.928	0.956	1.00

Table 27. Adjustment factor, k_j, for piles (see fig. 33).

		m				
		0.40	0.60	0.80	0.90	1.00
L/b	0.00	1.00	1.00	1.00	1.00	1.00
	0.25	0.973	0.973	0.984	0.99	1.00
	0.50	0.933	0.94	0.96	0.976	1.00
	1.00	0.88	0.888	0.92	0.953	1.00
	2.00	0.76	0.772	0.84	0.905	1.00

(a) k_j for piles when $j = 0.10$

		j					
		0.00	0.04	0.08	0.12	0.16	0.20
k_j for $j = 0.10$	0.76	1.00	0.902	0.81	0.71	0.615	0.52
	0.80	1.00	0.92	0.841	0.761	0.684	0.605
	0.90	1.00	0.961	0.921	0.88	0.842	0.802
	1.00	1.00	1.00	1.00	1.00	1.00	1.00

(b) k_j for piles when $j \neq 0.10$

Table 28. Adjustment factors for spur dikes (see fig. 34).

		L_d/b					
		0.0	0.2	0.4	0.6	1.0	1.5
m	0.2	1.00	1.23	1.32	1.37	1.41	1.42
	0.4	1.00	1.20	1.30	1.35	1.39	1.40
	0.6	1.00	1.16	1.25	1.30	1.35	1.36
	0.8	1.00	1.11	1.20	1.25	1.29	1.30

(a) k_d for elliptical dike length

		L_d/b					
		0.0	0.2	0.4	0.6	1.0	1.5
m	0.2	1.00	0.96	0.935	0.92	0.91	0.905
	0.4	1.00	0.968	0.95	0.935	0.93	0.925
	0.6	1.00	0.976	0.96	0.95	0.94	0.935
	0.8	1.00	0.984	0.973	0.965	0.955	0.95

(b) k_a for elliptical dike angularity

		L_d/b					
		0.0	0.2	0.4	0.6	1.0	1.5
m	0.2	1.00	1.09	1.18	1.25	1.27	1.27
	0.4	1.00	1.08	1.16	1.22	1.24	1.24
	0.6	1.00	1.07	1.14	1.18	1.21	1.21
	0.8	1.00	1.06	1.12	1.16	1.18	1.18

(c) k_d for straight dike length

		L_d/b_d					
		0.0	0.5	1.0	1.5	2.0	2.8
m	0.2	1.00	0.99	1.00	1.06	1.10	1.00
	0.4	1.00	0.97	0.98	1.04	1.08	1.00
	0.6	1.00	0.94	0.94	1.00	1.05	1.00
	0.8	1.00	0.89	0.88	0.945	1.01	1.00

(d) k_b for straight dike offset

REFERENCES

1. Arcement, G. J., Colson, B. E., and Ming, C. O., 1979, Backwater at bridges and densely wooded flood plains, Cypress Creek near Downsville, Louisiana: U.S. Geological Survey Hydrologic Investigations Atlas HA-603, 3 sheets.
2. Benson, M. S., and Dalrymple, T., 1967, General field and office procedures for indirect discharge measurements: U.S. Geological Survey Techniques of Water-Resources Investigations, book 3, chap. A1, 30pp.
3. Bradley, J. N., 1970, Hydraulics of bridge waterways: Federal Highway Administration, Hydraulic Design Series No. 1, 111pp.
4. Chow, V. T., 1959, Open-channel hydraulics: New York, McGraw-Hill, Inc., 680 pp.
5. Colson, B. E., Arcement, G. J., and Ming, C. O., 1978, Backwater at bridges and densely wooded flood plains, Okatama Creek East of Magee, Mississippi: U.S. Geological Survey Hydrologic Investigations Atlas HA-595, 3 sheets.
6. Colson, B. E., Ming, C. O., and Arcement, G. J., 1978, Backwater at bridges and densely wooded flood plains, Okatoma Creek near Magee, Mississippi: U.S. Geological Survey Hydrologic Investigations Atlas HA-596, 3 sheets.
7. Colson, B. E., and Schneider, V. R., 1983, Backwater and discharge at highway crossings with multiple bridges: U.S. Geological Survey Open-File Report 83-4065, 39pp.
8. Cragwall, J. S., Jr., 1958, Computation of backwater at open-channel constrictions: U.S. Geological Survey Open-File Report, 23 pp.
9. Davidian, Jacob, 1984, Computation of water-surface profiles in open channels: U.S. Geological Survey Techniques of Water-Resources Investigations, book 3, chap. A15, 48pp.
10. Davidian, Jacob, Carrigan, P. H., and Shen, John, 1962, Flow through openings in width constrictions: U.S. Geological Survey Water-Supply Paper 1369-D, pp. 108-112.

11. Henderson, F. M., 1966, Open channel flow: New York, The MacMillan Co., 522 pp.

12. Hulsing, H., 1967, Measurement of peak discharge at dams by indirect methods: U.S. Geological Survey Techniques of Water-Resources Investigations, book 3, chap. A5, 29 pp.

13. Lee, F. N., 1976, Field verification of method for distributing flow through multiple-bridge openings: Journal of Research of the U.S. Geological Survey, Vol. 4, No. 5, September-October 1976, pp. 539-543.

14. Liu, H. K., Bradley, J. N., and Plate, E. J., 1957, Backwater effects of piers and abutments: Civil Engineering Department, Colorado State University Report CER57HKL10, 364 pp.

15. Matthai, H. F., 1967, Measurement of peak discharge at width contractions by indirect methods: U.S. Geol. Survey Techniques of Water-Resources Investigations, book 3, chap. A4, 44pp.

16. Ming, C. O., Colson, B. E., and Arcement, G. J., 1979, Backwater at bridges and densely wooded flood plains, Buckhorn Creek near Shiloh, Alabama: U.S. Geological Survey Hydrologic Investigations Atlas HA-607, 3 sheets.

17. Ming, C. O., Colson, B. E., and Arcement, G. J., 1978, Backwater at bridges and densely wooded flood plains, Poley Creek near Sanford, Alabama: U.S. Geological Survey Hydrologic Investigations Atlas HA-609, 3 sheets.

18. Schneider, V. R., Board, J. W., Colson, B. E., Lee, F. N., and Druffel, L. A., 1977, Computation of backwater and discharge at width constrictions of heavily vegetated flood plains: U.S. Geological Survey Water-Resources Investigations 76-129, 64pp.

19. Shearman, J. O., 1976, Computer applications for step-backwater and floodway analysis: U.S. Geological Survey Open-File Report 76-499, 103 pp.

20. U.S. Army Corps of Engineers, 1981, Water Surface Profiles: Hydrologic Engineering Center, Davis, California, HEC-2, 242 pp.

21. U.S. Federal Highway Administration, 1982, Hydraulic analysis of pipe-arch and elliptical shape culverts using programable calculators: Calculator Design Series No. 4, 74 pp.

22. U.S. Federal Highway Administration, 1981, The design of encroachments on flood plains using risk analysis: Hydraulic Engineering Circular No. 17, 173 pp.

23. U.S. Federal Highway Administration, 1980, Hydraulic charts for the selection of highway culverts: Hydraulic Engineering Circular No. 5, 54 pp.

24. U.S. Federal Highway Administration, 1979, HY-6 -- Electronic computer program for hydraulic analysis of culverts: 107 pp.

25. U.S. Federal Highway Administration, 1969, HY-4 -- Electronic computer program for hydraulic analysis of bridge waterways: 89 pp.

FEDERALLY COORDINATED PROGRAM (FCP) OF HIGHWAY RESEARCH, DEVELOPMENT, AND TECHNOLOGY

The Offices of Research, Development, and Technology (RD&T) of the Federal Highway Administration (FHWA) are responsible for a broad research, development, and technology transfer program. This program is accomplished using numerous methods of funding and management. The efforts include work done in-house by RD&T staff, contracts using administrative funds, and a Federal-aid program conducted by or through State highway or transportation agencies, which include the Highway Planning and Research (HP&R) program, the National Cooperative Highway Research Program (NCHRP) managed by the Transportation Research Board, and the one-half of one percent training program conducted by the National Highway Institute.

The FCP is a carefully selected group of projects, separated into broad categories, formulated to use research, development, and technology transfer resources to obtain solutions to urgent national highway problems.

The diagonal double stripe on the cover of this report represents a highway. It is color-coded to identify the FCP category to which the report's subject pertains. A red stripe indicates category 1, dark blue for category 2, light blue for category 3, brown for category 4, gray for category 5, and green for category 9.

FCP Category Descriptions

1. **Highway Design and Operation for Safety**
   Safety RD&T addresses problems associated with the responsibilities of the FHWA under the Highway Safety Act. It includes investigation of appropriate design standards, roadside hardware, traffic control devices, and collection or analysis of physical and scientific data for the formulation of improved safety regulations to better protect all motorists, bicycles, and pedestrians.

2. **Traffic Control and Management**
   Traffic RD&T is concerned with increasing the operational efficiency of existing highways by advancing technology and balancing the demand-capacity relationship through traffic management techniques such as bus and carpool preferential treatment, coordinated signal timing, motorist information, and rerouting of traffic.

3. **Highway Operations**
   This category addresses preserving the Nation's highways, natural resources, and community attributes. It includes activities in physical maintenance, traffic services for maintenance zoning, management of human resources and equipment, and identification of highway elements that affect the quality of the human environment. The goals of projects within this category are to maximize operational efficiency and safety to the traveling public while conserving resources and reducing adverse highway and traffic impacts through protections and enhancement of environmental features.

4. **Pavement Design, Construction, and Management**
   Pavement RD&T is concerned with pavement design and rehabilititation methods and procedures, construction technology, recycled highway materials, improved pavement binders, and improved pavement management. The goals will emphasize improvements to highway performance over the network's life cycle, thus extending maintenance-free operation and maximizing benefits. Specific areas of effort will include material characterizations, pavement damage predictions, methods to minimize local pavement defects, quality control specifications, long-term pavement monitoring, and life cycle cost analyses.

5. **Structural Design and Hydraulics**
   Structural RD&T is concerned with furthering the latest technological advances in structural and hydraulic designs, fabrication processes, and construction techniques to provide safe, efficient highway structures at reasonable costs. This category deals with bridge superstructures, earth structures, foundations, culverts, river mechanics, and hydraulics. In addition, it includes material aspects of structures (metal and concrete) along with their protection from corrosive or degrading environments.

9. **RD&T Management and Coordination**
   Activities in this category include fundamental work for new concepts and system characterization before the investigation reaches a point where it is incorporated within other categories of the FCP. Concepts on the feasibility of new technology for highway safety are included in this category. RD&T reports not within other FCP projects will be published as Category 9 projects.